COMPREHENSIVE DESCRIPTION OF A SKELETON OF *ENDOTHIODON BATHYSTOMA* (ANOMODONTIA, THERAPSIDA), A DICYNODONT FROM THE LATE PERMIAN OF THE KAROO BASIN OF SOUTH AFRICA

by

IYRA ESMEN MAEVE MAHARAJ

(MHRIYR001)

Department of Biological Sciences

University of Cape Town

DISSERTATION

Presented for the degree of Master of Sciences in the Department of Biological Sciences,

University of Cape Town

2018

SUPERVISOR: Prof. Anusuya Chinsamy-Turan

Department of Biological Sciences, University of Cape Town

CO-SUPERVISOR: Prof. Roger M. H. Smith

Evolutionary Studies Institute, University of the Witwatersrand

Iziko Museums of South Africa

UNIVERSITY OF CAPE TOWN

IYUNIVESITHI YASEKAPA • UNIVERSITEIT VAN KAAPSTAD

National Research Foundation

PLAGIARISM DECLARATION

I know the meaning of plagiarism and declare that all of the work in the dissertation, save for that which is properly acknowledged, is my own.

Signed by candidate

Iyra E. M. Maharaj

5 February 2018

TABLE OF CONTENTS

LIST OF FIGURES

LIST OF TABLES

ACKNOWLEDGEMENTS

I would like to sincerely thank the following people for the successful completion of this dissertation:

- The National Research Foundation for funding this project.
- My supervisor Prof. Anusuya Chinsamy-Turan for welcoming me into her research group; for her incredible enthusiasm, guidance, patience and feedback throughout the duration of this work; and for always inspiring me to become a better scientist.
- Prof. Roger Smith for his supervision, support and excellent feedback; and to his field and lab team for giving me the opportunity to work on such a beautiful fossil.
- Zaituna Erasmus and the staff of Karoo Palaeontology at the Iziko Museum of Cape Town for access to specimens, including Sibusisu Mtungata for finding and excavating the specimen, Georgina Farrell for preparing the skeleton, and Nigel Pamplin for assistance with photographs.
- The following individuals for their kind permission to access collections: Dr Bernhard Zipfel and Sifelani Jirah at the Evolutionary Studies Institute at the University of Witwatersrand, Johannesburg; Nonhlanhla Mchunu at the Council for Geosciences, Pretoria; and Dr Rose Prevec at the Albany Museum, Grahamstown.
- Dr Ken Angielczyk and Dr Christian Kammerer for their feedback and encouragement.
- The students and postdocs of the UCT Palaeobiology Research Group for their friendship, encouragement and support.
- Vileska Benjamin, Tamlyn Gangiah and Andy Walker for their kindness and motivation.
- Finally, and most importantly, my family (Clara, Pravinand and Zaineta Maharaj) for doing more for me than I could ever imagine or describe.

ABSTRACT

The dicynodonts are an extinct group of herbivorous non-mammalian synapsids that were fairly abundant in Gondwanan deposits of the middle Permian to the Early Triassic periods. The extinct genus *Endothiodon* was first described by Sir Richard Owen in 1876, and is well known from the late Permian deposits of the Karoo Basin of South Africa. It is characterized by rows of internal teeth on the premaxilla and dentary arranged in replacement waves called *Zahnreihen*; longitudinal ridges running from the premaxilla to the pineal crest; and a prominent pineal boss with a pineal foramen. *Endothiodon* is well-represented by cranial and postcranial material in the Karoo vertebrate collections at various museums in South Africa. The repeated taxonomic revision of this genus over the years has led to much confusion about what constitutes the type species, *E. bathystoma*. Recently, an almost complete skeleton of *Endothiodon* (SAM-PK-K011271) was recovered from the uppermost *Pristerognathus* Assemblage Zone of the Karoo Supergroup. The fossil comprises the skull and most of its postcranial elements preserved in articulation. The current study provides a comprehensive description of the anatomy of this specimen, which permitted its identification as *E. bathystoma.* Furthermore, by comparison with other South African *Endothiodon* specimens this study determined that this specimen is the second largest *E. bathystoma* specimen known to date. The well-preserved skull and postcranial skeleton of SAM-PK-K011271 makes it an ideal reference specimen for *E. bathystoma* and has permitted a good assessment of its overall anatomy. The findings of this study provide a perfect stepping-stone for future studies to further address *E. bathystoma*'s skeletal reconstruction and biomechanical functions, as well as other aspects of the palaeobiology of this animal.

ABBREVIATIONS

Institutions

AM – Albany Museum (Grahamstown, South Africa)

CGS - Council for Geosciences (Pretoria, South Africa)

ESI - Evolutionary Studies Institute (University of the Witwatersrand, Johannesburg, South Africa)

ISI – Indian Statistical Institute (Kolkata, India)

NHMUK – Natural History Museum (London, UK)

SAM – Iziko Museums of South Africa (Cape Town, South Africa)

Anatomy

ang	angular	*l*	lacrimal
ant	anterior portion	*Ls*	M. levator scapulae
art	articular	*M*	metacarpal
ast	astragalus	*mf*	mandibular fenestra
ax	axis	*Mid*	middle
br	M. brachialis	*Mt*	metatarsal
c	centrale	*n*	nasal
ca	calcaneum	*nc*	neural canal
cb	M. coracobrachialis	*ns*	neural spine
cbl	M. coracobrachialis longus	*orb*	orbital
d	dentary	*P*	phalanx
del	M. deltoideus	*pb*	pineal boss
Dist	distal	*pec*	M. pectoralis
DV	dorsal vertebra	*pf*	pineal foramen
dors. mid.	dorsal midline	*pm*	premaxilla
ent	entepidcondyle	*po*	postorbital
ent f	entepicondylar foramen	*poz*	postzygapophysis
Ent. For.	entepicondylar foramen	*Prox*	proximal
f	frontal	*Pu*	pubis
Il	ilium	*q*	quadrate
Is	ischium	*r con*	radial condyle
j	jugal	*ref. l*	reflected lamina

sas	M. serratus anterior superficialis	*sup*	supinator
scs	M. subcoracoscapularis	*SW*	skull width
sha	M. scapulohumeralis anterior	*tp*	transverse process
SL	skull length	*tr*	trochlea
spc	M. supracoracoideus	*tri*	M. triceps
sq	squamosal		

Other

Comp.	lateral compression
H	height
L	length
Ma	million years ago
R	right
W	width

CHAPTER 1

INTRODUCTION

1.1 OVERVIEW: DICYNODONTS

Dicynodonts are an extinct clade of non-mammalian synapsids that range in age from the middle Permian to Late Triassic periods (Boos *et al*., 2013; Frobisch, 2009; Kemp 2012). Belonging to Anomodontia, an abundant group that radiated around the middle Permian, they were the dominant herbivorous tetrapods of the late Permian. Dicynodonts owed their success to the evolution of a unique skull and masticatory morphology, as well as high growth rates (Boos *et al.*, 2016; Botha-Brink and Angielczyk, 2010; Chinsamy and Rubidge, 1993; Kammerer *et al.*, 2011; Ray, 2000). Dicynodont fossils are known from South Africa, Brazil, India, Madagascar, Mozambique, Tanzania and Zambia (Ray, 2006), as well as Scotland, Russia, China and Laos (Angielczyk and Kurkin, 2003; Angielczyk and Sullivan, 2008; Cruickshank *et al*., 2005; Lucas and Ziegler, 2005). They are well represented in the Beaufort Group of the Karoo Basin of South Africa, being the most abundant fossil group from the *Eodicynodon* Assemblage Zone (Wordian) all the way to the *Cynognathus* Assemblage Zone (Anisian). Between these two assemblage zones, approximately 32 dicynodont genera are represented (Smith *et al*., 2012). A dramatic reduction to 2–3 genera of dicynodont fossils in the earliest Triassic was the result of the End-Permian mass extinction. *Lystrosaurus curvatus* was the only species to cross the Permo-Triassic boundary as indicated by fossils collected from below and above the Permo-Triassic boundary, while the rare kingoriidd *Kombuisia* from Antarctica, its relative *Myosaurus* from South Africa and Antarctica appeared in the Triassic (Botha and Smith, 2007).

Over 100 species of dicynodonts are known from deposits of the middle Permian to Late Triassic (Castanhinha *et al*., 2013). This abundance of skeletal elements in the terrestrial vertebrate fossil record allows detailed deductions to be made about their anatomy, morphology, population ecology, diet and to some extent, their behaviour. The anatomical complexity of their cranial features has prompted studies of functional anatomy (Jasinoski *et al.*, 2009; King, 1 990; Ray, 2006), while postcranial remains of certain forms suggest a variety of locomotory adaptations, including burrowing lifestyles seen in *Diictodon*, *Cistecephalus* and *Lystrosaurus* (Botha-Brink, 2017; Cluver 1978; Kemp, 2012; Nasterlack, *et al*., 2012; Smith, 1987). Palaeobiological studies of dicynodonts have accelerated in the last few decades: particularly anatomical studies of jaw musculature and dentition, which have provided ample evidence of jaw function and herbivory (Cox, 1964; Jasinoski *et al.*, 2009; Ray, 2006). Furthermore, the possibility that dicynodonts displayed gregarious behaviour was suggested by

analyses of coprolite accumulations attributed as communal latrines of dicynodonts (Fiorelli *et al*., 2013). Other studies of putative dicynodont coprolites suggest that longer food retention periods were an adaptation that helped dicynodonts achieve their large body size towards the end of their existence (Bajdek *et al*., 2014).

1.1.1 General cranial morphology

Characteristic cranial features of dicynodonts include a "turtle-like" keratinous beak covering the masticatory region in place of incisors; and in some species, the presence of maxillary canine tusks in place of incisors, which are suggested to be used for grubbing (Ray, 2006). A W-shaped quadrate-articular joint for palinal mastication, a flared zygomatic arch and large temporal openings for jaw muscle support are also present (Botha-Brink and Angielczyk, 2010; Hotton, 1984). It has been deduced from cranial anatomy that dicynodonts were specialized plant browsers and foraged leaves, roots, other hard plant matter and/or small invertebrates (Jasinoski *et al.*, 2009; King, 1993; Ray, 2006). A review of the cranial organisation of dicynodonts by King (1990) specifically notes the absence of maxillary teeth (except for two canine tusks in some taxa, after which the suborder Dicynodontia is named) — a shortening of the preorbital, a wide squamosal bone expanded laterally and the anteriorly positioned orbit displaced by a more elongated temporal fenestra.

1.1.2 Diversity

Cranial diversity

The skull size of dicynodonts varies among genera, and include the very small Mozambican *Niassodon*: skull length (snout to basioccipital) = 63 mm; the medium-sized *Oudenodon*: skull length = 100–300 mm; and the medium to large *Endothiodon*: skull length 220–511 mm (Botha, 2003; Castanhinha *et al*., 2013). Certain genera also display distinct skull shapes adapted for specialised functions such as feeding, e.g. *Lystrosaurus* displayed an elongated snout as well as a deeper, shorter cranium, implying it searched for food that was present on or below the substrate, such as low stems, roots or rhizomes; while *Oudenodon* had a more horizontal skull for foraging above the substrate (Jasinoski *et al*., 2009). A study by Nasterlack *et al*. (2012) showed that the shortened, broad skull of *Cistecephalus* suggested a bite force concentrated at the snout tip, ideal for feeding on hard plant matter, and perhaps even invertebrate exoskeletons.

The presence or absence of tusks among dicynodont species differs. The tusks were likely used for grubbing of plant matter, as indicated by lateral wear facets present on *Lystrosaurus* tusks (Jasinoski *et al*., 2009). It has also been suggested that the presence or absence of tusks may represent sexual dimorphism in *Diictodon* (Sullivan *et al*., 2002). Tusks are absent in skull remains of *Endothiodon* species, with the exception of the Tanzanian *E. tolani* which has small tusks on either side of the skull (Cox and Angielczyk *et al*., 2015).

Postcranial diversity

Postcranial material has been extremely useful in analysing the locomotory and biomechanical adaptations of several dicynodonts (Bandyopadhyay, 1988; Ray, 2006). For example, the complete articulated skeletons of *Diictodon* preserved in burrows have permitted in depth studies of their postcranial morphology and fossorial adaptations (Ray and Chinsamy, 2003; Smith, 1987). A study of *Cistecephalus* showed that their limb bones supported the digging lifestyle of this animal, as indicated by compact bones, thicker bone walls and a mole-like forelimb consisting of a robust humerus and claws (Cluver, 1978; Cox, 1972; Kemp, 2012; Nasterlack *et al*., 2012).

1.2 OVERVIEW: *ENDOTHIODON*

One of the first dicynodont genera to be described from the Karoo Basin of South Africa is the large form *Endothiodon* (Therapsida: Anomodontia, Dicynodontia, Endothiodontidae) (Owen, 1876). For the last few decades, this genus was considered to consist of five species, *viz*. *E. bathystoma*, *E. uniseries*, *E. mahalanobisi*, *E. whaitsi* and *E. tolani*; however, discussions of *Endothiodon* taxonomy in recent work suggests that *E. uniseries* and *E. whaitsi* are synonymous with *E. bathystoma* (Cox and Angielczyk, 2015). This suggests that only *E. bathystoma* (known from South Africa), *E. mahalanobisi* (from India) and *E. tolani* (from Tanzania) are valid species.

Endothiodon has unique dentition consisting of the presence of rows of internal teeth, called *Zahnreihen,* on the premaxilla, maxilla and dentary which likely aided in specialized herbivory (King, 1990). In early studies of *Endothiodon,* the presence of *Zahnreihen* were noted and described as a series of consecutive replacement waves of teeth, as shown in Figure 1 (b) and (c) (Cox, 1964; Latimer *et al*., 1995). In each *Zahnreihe* or tooth row, it appears that teeth grew sequentially from front to back. The roots of the teeth are circular in cross section, often with the presence of fine serrations along the posterior edges of the crowns. This replacement process seemed to have been ongoing throughout the animal's life (Latimer *et al*., 1995). *Endothiodon* is unique among dicynodonts in possessing these *Zahnreihen*, and no other anomodont genus displays different modes of tooth replacement in both upper and lower jaws (Latimer *et al*., 1995). Other cranial features that characterise *Endothiodon* include a narrow intertemporal bar, often with a pineal foramen situated on a raised, robust pineal boss, which is formed by the preparietal and parietal bones; a deeply vaulted secondary palate of the premaxilla; toothless anterior portion of lower jaw extending upward into a curved beak (fitting into the vaulted palate); prominent swelling on anterolateral sides of the dentary; and a laterally expanded squamosal bone (Boos *et al*., 2013; Cox, 1964; Cox and Angielczyk, 2015; King, 1990; Latimer *et al*., 1995).

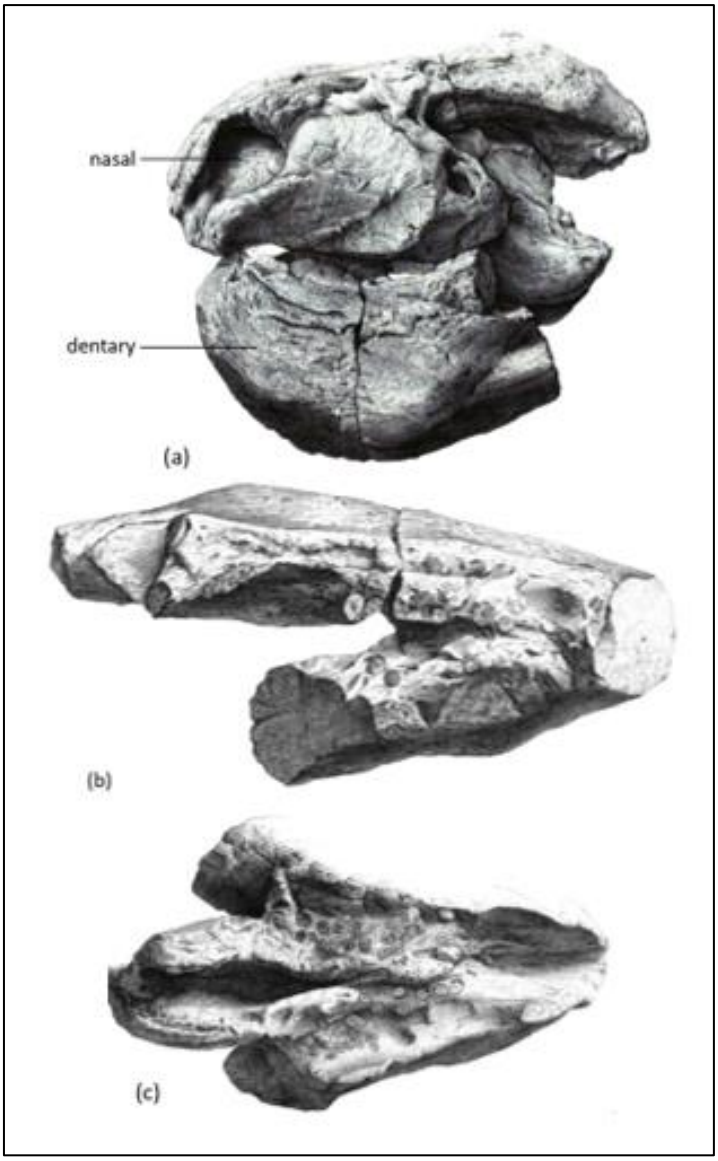

Figure 1. Anterior portion of the skull of the type specimen *E. bathystoma* in (a) left lateral view, (b) the anterior portion of the lower jaw and teeth in dorsal view and (c) the anterior portion of the upper jaw and teeth in palatal view. Images from Owen (1876).

1.2.1 Distribution

The rocks of the Karoo Basin of South Africa represent the period from the Late Carboniferous to the Early Jurassic, i.e. 300 Ma to 190 Ma, and although therapsid fossils have been found throughout the world, the Karoo Basin in particular has revealed an abundance of these specimens, so much so that these fossils have been used for biostratigraphic subdivision of the Beaufort Group (Day, 2013; Hancox and Rubidge, 1997; Smith *et al*., 2012). *Endothiodon* had a Gondwana-wide distribution, with species known from South Africa (*E. bathystoma*), Zambia, Tanzania (*E. tolani*), Brazil, Malawi,

Mozambique and India (*E. mahalanobisi*) (Boos *et al*., 2013) ranging from the *Pristerognathus* Assemblage Zone to the upper *Cistecephalus* Assemblage Zone (Latimer *et al*., 1995; Smith *et al*., 2012). *Endothiodon* was initially used as an index fossil due to its limited biostratigraphic range (Cox and Angielczyk, 2015; Day, 2013; Kitching 1977; Latimer *et al*., 1995). Today, with more collecting, *Endothiodon* remains are known from the *Pristerognathus* Assemblage Zone through the *Tropidostoma* and into the basal *Cistecephalus* Assemblage Zone of the Beaufort Group, although some specimens including those described by Broom (1905) are said to come from the *Tapinocephalus* Assemblage Zone (Iziko Museum Collections, 2016). To date six *Endothiodon* specimens are reported from the *Pristerognathus* Assemblage Zone, 72 from the *Tropidostoma* Assemblage Zone, and 13 from the *Cistecephalus* Assemblage Zone (Smith *et al*., 2012).

1.2.2 *Endothiodon* taxonomy

The genus *Endothiodon* was first described by Sir Richard Owen in 1876 following the discovery of an anterior portion of the skull and a corresponding mandible from the Sneewberg Range (Gouph District) of the Beaufort Group in South Africa (Owen, 1876). This material is currently housed at the Natural History Museum, UK (pers. comm., S. D. Chapman, 2017). *Endothiodon bathystoma*, the type species, was one of the first dicynodonts to be described (Owen, 1876). "*Endothiodon"* means "tooth within" in Greek and describes one of its key diagnostic features: many rows of internal upper and lower teeth, in contrast to marginal teeth as seen in many other amniotes (Boos *et al.*, 2013). Owen (1879) later described another mandible as belonging to *E. bathystoma*. In the same publication, he described an anterior half of a skull similar to the original skull portion that was used to first describe *Endothiodon*. He described this element as belonging to *E. uniseries*, which shared the same beak-shaped premaxillary and vault-like palatal of *E. bathystoma*. The antero-posterior shape of the nostril in *E. uniseries* was observed to be different to that of *E. bathystoma*. However, the same type of suture between the nasal and maxillary bones was noted (Owen, 1879). In 1905, Broom assigned a partial skeleton to the same species. This material is now housed in the Karoo fossil collections at the Iziko Museum in Cape Town. Broom's study of *E. bathystoma* included a description of cranial as well as some of the postcranial elements.

The cranial features that characterise the order Anomodontia were identified by Owen (1879) in *Endothiodon*, namely premaxillae that formed a toothless beak-shaped bone; nasal bones divided by nasal process on the premaxilla; vomer consisting of a pair of vertical lamella. In both *E. bathystoma* and *E. uniseries* the nostrils were compared with *Oudenodon* and were observed to have a similar forwardly placed nasal bone; and in *E. bathystoma* and *E. uniseries* the premaxilla and maxilla are part of the caniniform process. The dental system of dicynodonts is reduced to a pair of upper canines,

which are absent in some genera such as *Oudenodon* but seen in others such as *Diictodon*, where they are present in only some members of the adult population, suggesting that they might represent a sexually dimorphic character (Sullivan *et al*., 2002). The development of internal teeth, the *Zahnreihen*, was regarded as "a character of family value in the Order". Owen (1879) suggested that the dental characteristics of *Endothiodon* indicated a crushing action to break up vegetation.

Since its discovery, the taxonomy of *Endothiodon* has seen much confusion. The family Endothiodontidae, proposed by Lydekker (1890) contained a split in genera and species *viz*. *Endothiodon bathystoma*, *Endothiodon seeleyi*; *Esoterodon uniseries*, *Esoterodon whaitsi*, *Esoterodon paucidens*, *Esoterodon angusticeps*; *Emydochampsa platyceps*, *Emydochampsa oweni*; *Endogomphodon crassus* and *Endogomphodon minor* based on morphological features such as the degree of flattening of the skull, the pointedness of the snout and the number of rows of upper teeth. Later, a taxonomic review by Cox (1964) regarded some of these features to be artefacts of fossilization and thus not valid for distinguishing the various species. A review of the taxonomy by Cox (1964) identified *Endothiodon* as the only valid genus with three species, *E. uniseries*, *E. bathystoma* and *E. whaitsi*, on the basis of the palate and dentition. Another species was discovered in the Kundaram Formation in India and was described by Ray (2000) as *E. mahalanobisi*, which has a skull size significantly smaller than that of *E. bathystoma*, *E. uniseries* and *E. whaitsi* (Ray, 2000).

The taxonomy of *Endothiodon* had not been thoroughly revised since Cox (1964), and appears to be quite problematic: when describing the *Endothiodon* specimen from Brazil, Boos *et al*. (2013) explained the difficulty of species diagnosis in this genus, since the morphological characters used to distinguish the different species were not entirely clear. Boos *et al*. (2013) noted that the robustness and size of the dentary symphysis, which is often considered in diagnosing species, was quite an unreliable feature, since it was dependent on ontogenetic age. More recently, Cox and Angielczyk (2015), suggested that many of the characteristics use to differentiate between the different species could have resulted from deformation or ontogenetic variation. For example, the small skull size of the Indian *E. mahalanobisi* and the reduced ornamentation on many parts of the skull could simply represent juvenile features of *Endothiodon* (Cox and Angielczyk, 2015). However, bone histology features of *E. mahalanobisi* appeared to be consistent with those of subadult *E. bathystoma* specimens (Botha-Brink and Angielczyk, 2010). Additionally, Ray (2000) inferred that the small size of the specimens does not necessarily indicate juvenile status, since the teeth were well-developed and sutural contact between bones was highly interdigitated (p 394). Cox and Angielczyk (2015) tentatively accepted *E. mahalanobisi* as a separate species, although they mention the possibility of *E. mahalanobisi* specimens being juvenile *E. bathystoma* individuals; however, they suggested that further confirmation is required as to whether the *E. mahalanobisi* specimens were predominantly subadult *E. bathystoma* individuals, or whether *E. mahalanobisi* was a distinct species.

Cox (1964) considered *Pachytegos stockleyi* (Haughton, 1932), from the Usili Formation of the Ruhuhu Basin, Tanzania, as a separate genus from *Endothiodon*. However, Cox and Angielczyk (2015) suggested that the taxonomic value of the diagnostic features of *P. stockleyi* was questionable since *E. bathystoma* is known from the same locality as *P. stockleyi* (Usili Formation), and furthermore, the specimen was badly weathered, and a pineal boss was probably originally present, as indicated by thickened bones around the pineal foramen. Cox and Angielczyk (2015) concluded that there was no reason to recognize *P. stockleyi* as a valid taxon, since there were no characteristics that significantly differentiated it from *E. bathystoma*. Thus, these researchers concluded that only three *Endothiodon* species are valid, *viz*. *E. bathystoma, E. tolani* and possibly *E. mahalanobisi* (Cox and Angielczyk, 2015).

1.2.3 Cranial anatomy of *Endothiodon* species

Some of the cranial features considered diagnostic of species have contributed to disputes about *Endothiodon* taxonomy, as many are deemed unreliable or inconsistent. However, the two species that are morphologically distinct from the others (including the type species *E. bathystoma*) are the small Indian form *E. mahalanobisi* and *E. tolani* from Tanzania, described below.

Material from the Kundaram Formation in India was described in detail by Ray (2000) as belonging to a new species, *E. mahalanobisi*, being significantly smaller in size than the other species of *Endothiodon*. Ray (2000) differentiated it from *E. bathystoma*, *E. uniseries* and *E. whaitsi* on the basis of the small size of the skull, the number of ridges along the snout (*E. mahalanobisi* only has one broad ridge), the slender dentary symphysis, as well as the elliptical shape of the pineal foramen. Boos *et al*. (2013) state that it is the only species of *Endothiodon* that can be confidently distinguished from the others, owing to its small skull size, slender dentary symphysis, single longitudinal ridge on snout, absence of swelling on the prefrontal bone, and the pineal foramen located on a low boss.

Cox and Angielczyk (2015) described cranial material from the Ruhuhu Basin of Tanzania as a new *Endothiodon* species called *E. tolani*. Its two autapomorphies include the presence of caniniform tusks, as well as a slightly elevated and thin collar of bone surrounding the pineal foramen. This is remarkably the only species of *Endothiodon* to show the presence of tusks, despite tusks being a common feature of many other dicynodont genera (Cox and Angielczyk, 2015).

Boos *et al*. (2013) reported the first dicynodont from the Permian of South America and described fragmentary cranial material from the Rio do Rasto Formation in Brazil as belonging to *Endothiodon*. An extensive description of this material was given; however, it could not be identified to a species level, due to the fragmentary nature of the material which lacked species-diagnosing features.

However, they concluded that the Brazilian specimen is more similar to *E. bathystoma*, *E. uniseries* and/or *E. whaitsi*, than to *E. mahalanobisi* based on its size, as well as the prefrontal and pineal boss (Boos *et al*., 2013). Angielczyk *et al*. (2014) recently described material originally collected from the Luangwa Basin of Zambia in the 1920s as belonging to *Endothiodon*. The material consisted mainly of fragmentary jaws and palates, with the diagnostic tooth rows being present. However, it also could not be identified as a particular species.

1.2.4 Other work on *Endothiodon* palaeobiology

Since the first description of *Endothiodon* in 1876, different studies of *Endothiodon* specimens have provided insights regarding its dentition and feeding system, as well as deductions about their palaeoenvironment. The work done by Cox (1964) resulted in an essential taxonomic revision, which became the basis for several other consequent studies of *Endothiodon*. A study by Latimer *et al*. (1995) of fragmentary skull material from Mozambique highlighted some important features of the palate and dentition, and used this to understand its unique masticatory system. The major observations made in this study were that the teeth of *Endothiodon* were organised in replacement waves called *Zahnreihen*, whereby the anterior teeth are the oldest and the posterior ones are the youngest; and that the lower and upper jaws displayed different patterns of tooth replacement. Some palaeobiological suggestions were made based on the presence of a groove at the external surface of the premaxilla, *viz*. it allowed exhaled water vapour to be recycled; it may have contained a pheromone-depositing gland for scent-marking; or it could have been the duct of a salt gland, with the animal rubbing away accumulated salt as it feeds. Latimer *et al.* (1995) stated that a keratinous beak did not suit these possible functions.

Latimer *et al*. (1995) also suggested that *Endothiodon* lived in the dense, flourishing vegetation along the riverbanks of alluvial plains that was described by Smith (1993) in a review of vertebrate taphonomy in the Karoo Basin of South Africa. Since the niche that *Endothiodon* occupied may not have been suited to smaller, more terrestrial dicynodonts, Latimer *et al*. (1995) predicted that when searching for *Endothiodon* fossils, more articulated skeletons would probably be found near the river channels. Latimer *et al*. (1995) also determined that this animal was a specialised browser, in contrast to feeding by grubbing vegetable matter from mud swamps, as claimed by Cox (1964). This is due to features that favour specialised browsing, such as the forceps-like muzzle being present, which is ideal for selective cropping of individual leaves (Latimer *et al*., 1995). Ray (2000) suggested that the masticatory processes of *Endothiodon* involved slicing of plant material by a slight lateral movement of the animal's lower jaw. A more recent study on the feeding system of *E. tolani* by Cox and Angielczyk (2015) suggested that the animal displayed unilateral chewing due to the diverging tooth

rows. They estimated that obtaining food was made possible by the anterior parts of the jaws for initial cropping of plant matter. The teeth towards the back of the mouth and the lateral keratin-covered areas of the jaws would have allowed the processing of food. The lower teeth have serrations on their posterolateral edges for cutting. Furthermore, they suggested that the well-developed palatine pads seen in all *Endothiodon* species may have prevented food from moving up dorsally and that the food bolus was pressed against them by the tongue in order to be held in place (Cox and Angielczyk, 2015).

Only a few histological studies have been done on *Endothiodon* specimens, but similar results were reported, i.e. rapid growth indicated by fibrolamellar bone, and the presence of growth rings on the humerus (Chinsamy and Rubidge, 1993; Ray *et al*., 2009). Although the histology of *Endothiodon* has not yet been studied in great detail, there are many studies of other dicynodonts that examine histology. Botha (2003) concluded that the cyclical growth of *Oudenodon* was shown by the organisation of bone tissue in limb bones, *viz*. rapidly deposited fibro-lamellar bone and slowly deposited lamellar bone. Jasinoski and Chinsamy-Turan (2012) described the cranial histology of *Oudenodon* and *Lystrosaurus*, allowing the cranial functions of these dicynodonts to be understood. The growth patterns of several other dicynodonts have been noted in previous histological work, including the Indian *Endothiodon* species *E. mahalanobisi*, *Lystrosaurus murrayi* and *Wadiasarus* (Ray *et al*., 2009; Ray *et al*., 2012).

1.3 RATIONALE OF CURRENT STUDY

Many studies have focused on the dentition and cranial elements of *Endothiodon*, but there is little information regarding the rest of the skeleton, because postcranial remains were not as common as skull remains. It is widely accepted that a detailed anatomical description of the postcranial elements of *Endothiodon* is long overdue. This stems from the fact that until recently, most *Endothiodon* specimens discovered were only fragmentary skull remains with many of them having post-mortem damage, and thus few deductions could be made about the posture and post-cranial biomechanics (Latimer *et al*., 1995). However, in 2013, a very well-preserved, articulated specimen identified as *Endothiodon bathystoma* was recovered from the uppermost *Pristerognathus* Assemblage Zone (Adelaide Subgroup, Beaufort Group) of the Karoo Supergroup on an expedition organised by palaeontologist, Roger Smith of Iziko SA Museum. When the new *Endothiodon* specimen was prepared it soon became apparent that it was possibly the most complete *Endothiodon* specimen discovered thus far, with both cranial and postcranial elements including forelimbs and hindlimbs in full articulation. The specimen is preserved lying on its side with the right side of the skeleton uppermost.

The new specimen presented a unique opportunity to analyse both *Endothiodon* skull and postcrania. This specimen, SAM-PK-K011271 is the focus of the current study. Having the most complete skull allowed it to be studied and positioned in an ontogenetic series of all *Endothiodon* specimens. The importance of assessing ontogeny stems from the uncertainty that still exists regarding the distinction between certain *Endothiodon* species. For example, *E. mahalanobisi* is notably smaller in skull size than any other *Endothiodon* species, and although Ray (2000) described it as a distinct species, there is still a possibility that these specimens represent juvenile forms of *E. bathystoma* (Cox and Angielczyk, 2015). Such a consideration has been made for *Endothiodon* specimens that were accepted as *Pachytegos stockleyi* (Haughton, 1932), until very recently when Cox and Angielczyk (2015) synonymised *P. stockleyi* with *E. bathystoma*, arguing that the features used to diagnose the species were not taxonomically significant. A thorough analysis of the large *Endothiodon* skeleton followed by comparison with other previously-described South African specimens was therefore expected to contribute significantly to the clarification of some of the confusion that exists with regard to its systematics, and taxonomy and ontogenetic status.

The entire skeleton is approximately 2 m long, with the skull length (i.e. distance from anterior tip of maxilla to posterior surface of basi-occipital condyle) measuring 433 mm. The proportion and shape of skull size, pineal foramen on a raised boss, intertemporal bar, and robust dentary with an upturned beak-like structure are characteristics that suggest that it is referable to *Endothiodon*.

1.3.1 Hypotheses for this study

a. **SAM-PK-K011271 from the late Permian of the Karoo Basin of South Africa is *Endothiodon bathystoma*.**

The recent discovery of an articulated dicynodont (possibly *Endothiodon*) including skull and postcranial skeleton (SAM-PK-K011271) presents a unique opportunity to understand various aspects of dicynodont palaeobiology. A detailed anatomical study of the skull and postcrania will be conducted to ascertain whether the specimen is indeed *Endothiodon*, and more specifically if it has the cranial autapomorphies that characterise *E. bathystoma*. This analysis will permit a re-assessment of the of *Endothiodon bathystoma*, and will allow deductions concerning whether all the "*Endothiodon*" material in South African collections do indeed belong to *E. bathystoma* or any of the other valid species. If this hypothesis is correct, then the new specimen should show the autapomorphies associated with the diagnoses of *E. bathystoma*.

b. **SAM-PK-K011271 is the largest known individual of *E. bathystoma* thus far described, and is the most complete skeleton of this taxon found worldwide to date it.**

If this specimen is indeed, *E. bathystoma*, a thorough analysis of all the *Endothiodon bathystoma* specimens in collections around South Africa will be made to determine how it compares with others in the collections, in terms of size and completeness. In so doing, the relative ontogenetic status of the individual will be determined. Since this is an articulated specimen, it will also allow deductions about the relative sizes of other isolated skull and postcranial elements ascribed to *E. bathystoma*. If this hypothesis is correct, the skull length of SAM-PK-K011271 should be the largest known, and the proportions of the postcrania should be larger than any of the previously described *E. bathystoma* specimens.

1.3.2 Aims of the study

This study aimed to comprehensively describe the anatomy of the skull and postcrania of SAM-PK-K011271 in order to:

(1) Confirm whether the specimen belongs to the species *E. bathystoma*.

(2) Deduce the ontogenetic context of the new *E. bathystoma* specimen through comparison of anatomical features with those of other known South African specimens.

(3) To comment on the currently accepted taxonomy of *Endothiodon* i.e. can skull specimens attributed to *E. bathystoma* be distinguished from *E. whaitsi* and *E. uniseries*?

CHAPTER 2

MATERIALS AND METHODS

2.1 SPECIMENS AND DATA COLLECTION

2.1.1 SAM-PK-K011271

In November 2013, the specimen SAM-PK-K011271 was discovered by Sibusiso Mtungata on a field trip led by Prof. Roger Smith (both of Iziko SA Museum in Cape Town) as part of a 3-year NRF/AOP-funded project investigating the terrestrial ecosystem recovery from the End-Guadalupian mass extinction. It was identified upon excavation as a large, articulated skeleton of a dicynodont, most likely *Endothiodon*. The specimen was retrieved some 80 m above the mid/late Permian boundary near Fraserburg (Northern Cape) in the uppermost *Pristerognathus* Assemblage Zone (Adelaide Subgroup, Beaufort Group) of the Karoo Supergroup. Dicynodonts represent 87.5% of therapsid fossils found in the *Pristerognathus* Assemblage Zone, six of which were reported to be *Endothiodon* specimens (Smith *et al*., 2012). Specimen SAM-PK-K011271 was mechanically prepared at Iziko SA Museum in Cape Town by Georgina Farrell using a pneumatic scribe to expose an extremely well-preserved complete skull and postcranial skeleton in articulation.

The skeleton is lying on its left side, exposing all elements on the right side (Figure 2). The skeleton has not experienced any major deformation but is somewhat laterally compressed in several areas including the left side of the skull, the squamosals, the pelvic girdle and left hind limb. Compression has also displaced a few isolated vertebrae and rib fragments near the skeleton. Several parts of the skull including the prominent pineal boss had broken off and were found by systematically searching the debris beneath the in-situ skeleton. These were all carefully re-attached during preparation (S. Mtungata, 2016, pers. comm.). The entire exposed anatomy of the skeleton is described in this study to shed light on the skull and postcranial anatomy of *Endothiodon* which until now was poorly known.

Figure 2. Plan view of SAM-PK-K011271, the *E. bathystoma* skeleton. Scale bar represents 100 mm.

2.1.2 South African Collections of *Endothiodon*

In order to determine whether SAM-PK-K011271 is *Endothiodon bathystoma*, and its ontogenetic status, the specimen was compared to previously described elements of *Endothiodon.* All of the South African *Endothiodon* specimens were studied in the following museum collections, and several visits to the following institutions were made: The Evolutionary Studies Institute, University of the Witwatersrand (Johannesburg, Gauteng); The Council for Geosciences (Pretoria, Gauteng); The Albany Museum (Grahamstown, Eastern Cape); and Iziko Museum of SA (Cape Town, Western Cape). All *Endothiodon* elements were documented by taking precise measurements and photographs, and anatomical descriptions were made. The type specimen of *E. bathystoma*, consisting of an anterior portion of skull and lower jaw (Figure 1) was moved from South Africa to the Natural History Museum (UK), and therefore could not be directly compared to SAM-PK-K011271 but anatomical details available in the publication was utilised in this study. Excluding SAM-PK-K011271, across all the South African museums, a total of 51 catalogued specimens consisting of 92 separate elements were studied (see Appendix, Tables A and B for a complete list of all the specimens examined). Out of 92 elements identified in the collections as *E. bathystoma*, 45 were cranial and 47 were postcranial elements. It was not possible to determine exactly how many *Endothiodon* individuals these elements belonged to.

2.2 ANATOMICAL DESCRIPTION

The skull and postcranial skeleton of SAM-PK-K011271 were visually inspected, measured and described as far as possible. Thereafter photogrammetry was applied.

2.2.1 Photogrammetry

Photogrammetry is a versatile method that can be used to obtain accurate measurements of digital three-dimensional models of solid objects. Photogrammetric software uses multiple high-resolution photographs of the object from different angles and collates them to produce a digital three-dimensional model which can be manipulated and analysed easily. It has successfully been used to aid body mass estimations in extinct mammals (Basu *et al*., 2015) and is an effective way of precisely studying vertebrate bone anatomy. The size of SAM-PK-K011271 proved it too large to be CT-scanned, and thus the elements of its left side could not be examined in this study, as these were still embedded in the surrounding matrix, and the museum were reluctant to give permission to completely prepare out the bones. Although photogrammetry can only be used on exposed surfaces, it assisted in the ease and accuracy of the anatomical description of the skeleton. For example, it permitted accurate measurements that were not possible to measure physically with callipers, such as for example, the height of a partially exposed neural spine covered by other elements.

High-resolution photographs of all visible cranial and postcranial elements of SAM-PK-K011271 were taken using a Nikon D990 camera. Virtual 3D models of skeletal elements were produced using photogrammetric software, *viz*. Autodesk ReMake version 17.24.3.14 and Agisoft PhotoScan Professional version 1.2.6 build 2834. Three-D models were made of the skull, an isolated vertebra and of the entire skeleton. Both abovementioned programs were able to give an accurate scale measurement, which was tested against physical measurements made using digital callipers on the specimen. Basic figures were drawn (not to scale) of all elements in study to assist in the descriptions. Annotated figures of certain elements were made to aid the descriptions.

2.2.2 Morphology and measurements

As far as possible, all cranial and postcranial elements were measured to describe the anatomy of SAM-PK-K011271 and to identify the species it belongs to (Figures 3 and 4). Physical measurements (mm) were taken using Mitutoyo Absolute Digimatic callipers, while digital measurements were

taken on the virtual 3D models via photogrammetric software. It is imperative that the skull morphology of *Endothiodon* is carefully considered when determining species, however, there is a consensus that a thorough taxonomical review of the genus *Endothiodon* is long overdue. This was taken into account when determining which cranial characters are diagnostic of particular species. A detailed description of the skull morphology of SAM-PK-K011271 was done used previous descriptions of *Endothiodon* crania as a guide (Boos *et al.*, 2013; Broom, 1905; Cox and Angielczyk, 2015; Owen, 1876; Ray, 2000). The postcrania of SAM-PK-K011271 was described following that of other anatomical studies of dicynodonts (Angielczyk and Rubidge, 2013; Bandyopadhyay, 1988; Govender and Yates, 2009; Ray, 2006; Ray and Chinsamy, 2003). Tables 1 and 2 depicts the elements measured and described in this study. Note that precise measurements could not be taken for some elements (e.g. occiput) due to compression in these regions. For these only visual/anatomical descriptions have been made.

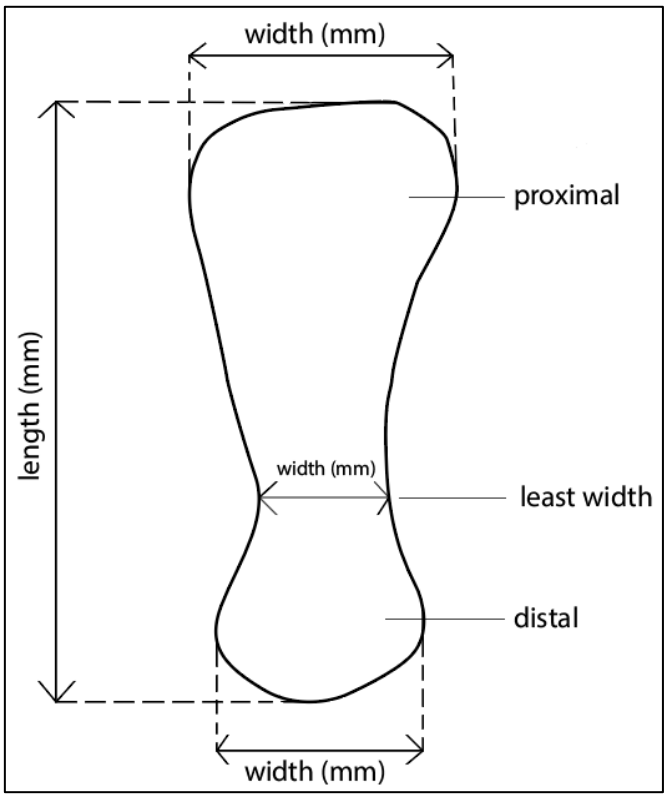

Figure 3. Diagram depicting measurements taken from long bones *viz*. humerus, ulna, radius, femur, tibia and fibula; as well as both scapulae.

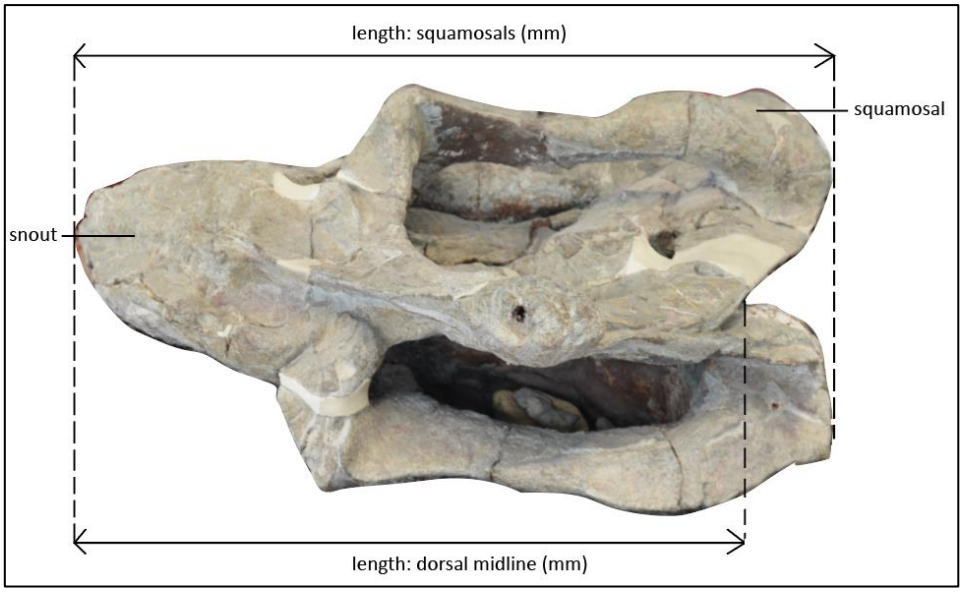

Figure 4. Skull length measurements taken from all South African *Endothiodon* skulls. Measurements taken from tip of anterior snout to squamosals (top) and tip of anterior snout across dorsal midline (bottom). Skull of SAM-PK-K011271 shown in dorsal view.

Table 1. SAM-PK-K011271 cranial elements examined. Note "Visual" refers to a visual description of the element (described in text), while "Numerical" refers to physical measurements taken.

Element	Measurements taken (mm)	Description method
Skull	L (anterior tip of snout to posterior surface of basi-occipital condyle); W	Numerical
	L (anterior tip of snout to squamosal wings); W	Numerical
Pineal boss	L	Visual, numerical
Pineal foramen	L; W	Visual, numerical
Dentary	L	Visual, numerical
Mandibular fenestra	L; W	Visual, numerical
Snout and premaxilla	-	Visual
Nasal bone	-	Visual
Parietal bone	-	Visual
Orbital	Comp.	Visual
Occipital region	Comp.	Visual
Intertemporal bar	-	Visual
Squamosals	Comp.	Visual

Table 2. SAM-PK-K011271 postcranial elements examined. Note "Visual" refers to a visual description of the element (described in text), while "Numerical" refers to physical measurements taken.

Element	Measurement taken (mm)	Description method
Clavicle	L; W	Visual, numerical
Scapula (left)	L; Width (Prox, Mid, Dist)	Visual, numerical
Scapula (right)	L; Width (Prox, Mid, Dist)	Visual, numerical
Coracoid	-	Visual, numerical
Humerus	L; W (Prox, Mid, Dist)	Visual, numerical
Radius	L; W (Prox, Mid, Dist)	Visual, numerical
Ulna	L; (Prox, Mid, Dist)	Visual, numerical
Ilium	L; W	Visual, numerical
Ischium and pubis	L; W	Visual, numerical
Femur	L; W (Prox, Mid, Dist)	Visual, numerical
Tibia	L; W (Prox, Mid, Dist)	Visual, numerical
Fibula	L; W (Prox, Mid, Dist)	Visual, numerical
Manus	-	Visual
Pes	-	Visual
Atlas-axis vertebrae	Comp.	Visual
Vertebrae	H; L; W	Visual, numerical
Ribs	W	Visual, numerical

2.3 SPECIES IDENTIFICATION

Species-diagnostic features of the skull were determined from previous work on *Endothiodon* crania (Cox and Angielczyk, 2015; Ray, 2000). The following cranial features are described in the literature as diagnostic of *E. bathystoma*: narrow intertemporal bar, pineal foramen situated on a robust pineal boss which is formed by the preparietal and parietal bones, a deeply vaulted secondary palate of the premaxilla, toothless anterior portion of lower jaw extending upward into a curved beak (fitting into the vaulted palate), prominent swelling on anterolateral sides of the dentary, dentary teeth arranged in replacement waves termed *Zahnreihen*. In addition, a description of the Indian species *E. mahalanobisi* (Ray, 2000) noted that *E. bathystoma* could be identified by three longitudinal ridges on its snout, a wide interorbital region, swollen prefrontals, a narrow intertemporal bar, a raised parietal crest and a circular pineal foramen situated on a robust boss that is positioner on the anterior side of the intertemporal bar. Where applicable, these features were identified and described on whichever specimens among the collection material possessed them. Unfortunately, there were not enough postcranial elements to compare the rest of SAM-PK-K011271 with, as they were all too fragmented.

One of the most unique features of the *Endothiodon* genus is the dentition arranged in replacement waves. It is possible that the pattern of these tooth rows could be different across the species. However, the upper and lower jaws of SAM-PK-K011271 are closed, thus the teeth were not examined nor compared with other skulls for species diagnosis. Although skull size was said to be indicative of species (Ray, 2000) and was noted in this study, the degree of compression affecting physical measurements of length and width should be noted.

CHAPTER 3

RESULTS

3.1 FULL DESCRIPTION OF SAM-PK-K011271

The following is a description of the preserved cranial and postcranial elements of specimen SAM-PK-K011271. From the tip of the snout to the tip of the tail, the skeleton has a straight length of approximately 1.5 m. The following preserved elements are present on the exposed (right) side of the skeleton: complete skull; 18 ribs in articulation; scapula; humerus; ulna; radius; carpals, manus (missing part of digit III and all of digits IV and V); displaced coracoid process; pelvis, hindlimb and pes. The following elements of the articulated vertebral column are preserved: five cervical, 17 dorsal, five sacral, 10 caudal, and about three disarticulated isolated dorsal vertebrae, as well as three partial ribs disarticulated from the skeleton. Tables 3 and 4 contain measurements of the elements examined. The skeleton is lying on its left side. leaving the right side fully exposed and the left side partially exposed. Most elements from the left side are still embedded in rock, but some are partially visible. One cervical rib from the left side is partially exposed, and is lying beneath the cervical vertebrae. The entire left scapula is present in medial view and will be included in the description, as the exposed right scapula can only be studied in lateral view. Furthermore, on the left side, ribs, the left hindlimb (exposed in ventral view), and the left forelimb are partially exposed.

Table 3. Measurements of cranial elements of *E. bathystoma*, SAM-PK-K011271.

Element	**Width (mm)**	**Length (mm)**
Skull	-	433.69
	-	447
Pineal boss	-	67
Pineal foramen	14	14
Dentary	-	326.36
Mandibular fenestra	15.60	59.12

Table 4. Measurements of postcranial elements of *E. bathystoma*, SAM-PK-K011271.

Element	Width (mm)			Length (mm)
	Prox	**Mid**	**Dist**	
Clavicle	39.07	-	21.58	186.90
Scapula (left)	125.61	63.88	58.36	277.65
Scapula (right)	115.73	64.02	-	273.12
Coracoid	72.97	-	75.11	109.27
Humerus	124.30	56.87	100.82	217.22
Radius	37.71	-	43.9	163.6
Ulna	76.99	44.11	-	185.67
Ilium	155.77	-	86.29	180.05
Ischium and pubis	104.96	-	27.76	117.34
Femur	103	52.54	-	229.81
Tibia	66.35	32.92	-	151.62
Fibula	-	18.3	43.99	137.86
Manus	See Table 5			
Pes	See Table 6			
Vertebrae	See section 3.1.2.5 (b)			
Ribs	See Table 7			

3.1.1 Crania

The overall shape of the skull is depicted correctly in the 3D model generated with Autodesk Remake (discontinued in 2017, now Autodesk Recap Pro), which has been used as a primary reference for this description, while being frequently cross-checked against physical observations and measurements taken on the actual skeleton (Tables 3 and 4). The only discrepancy is that the squamosal wings are thinner and slightly more outwardly flared than depicted in the model, which may be due to discrepancies (image quality, number of photographs) in the photographs taken of this area, which were used to produce the model. However, the physical measurements have been noted from the skeleton itself.

3.1.1.1 The skull of SAM-PK-K011271

The skull of this dicynodont is large, with a length of approximately 433.69 mm and this is comparable to cranial lengths of referred specimens of *E. bathystoma* and *E. whaitsi* (suggested to now be synonymized with *E. bathystoma*) that have been previously described. Although the skull is quite laterally compressed, it is still widest across the squamosal wings (Figures 5 and 6). There is a prominent sagittal ridge that runs along the parietals towards a large, bulbous pineal boss with a pineal foramen. The pineal boss has an anterior/posterior length of 67 mm and a width of 41 mm; while the pineal foramen within has a length and width of 14 mm. The postorbital is relatively robust and has resisted compaction thus distorting the orbit which is positioned anterolaterally, with an anterior/posterior orbit length of 72 mm across the lateral side. The anterior tip of the premaxilla (snout) has an inverted V-shaped notch and its surface is rugose. This may have been an area for a keratinous attachment in life. The dentary is robust, and has a maximum width of 97 mm and a length of 326.36 mm. The anterior portion of the dentary tapers upward and seems to fit tightly into the vaulted palate.

3.1.1.2 Snout and skull roof

Suture lines defining the bones of the snout and skull roof are not distinct and are thus approximated in Figure 7; and the location of these bones are estimated based on interpretive skull diagrams of other *Endothiodon* species described by Broili and Schroeder (1936), Cox (1964), Cox and Angielczyk (2015) and Ray (2000) (see Figure 5). The compression of the skull has caused the already robust bones of the snout to appear raised above the level of the orbital cavities. On the upper jaw, the border of the premaxilla is toothless, and its anteriormost portion has a “deep notch”, which appears slightly weathered, but corresponds with Ray’s (2000) description of a “v-shaped notch” and seems to accommodate the “upturned beak”-like shape of the anteriormost part of the dentary. The surface of the premaxilla has a significant amount of rugosity indicating the possible presence of a keratinous structure covering the “beak” to assist in obtaining and mastication of food matter. This rugosity seems to be more pronounced inside the “V-shaped” notch in the premaxilla.

Posterior to the nasals is a line 41.42 mm in length that is likely a suture above the premaxilla, although it is a straight, horizontal line on the dorsal surface with not much interdigitation between the bones (Figure 7). The nasal cavities are positioned anterolaterally, within which septomaxillae structures are seen. Posterior to the nasals lie broad frontals that are slightly compressed but come together to form a small, raised area on the median surface that looks irregular due to the compression, but seems to mark the beginning of the sagittal ridge. Despite the large amount of lateral

compression, a medially positioned longitudinal ridge appears on the frontals and continues posteriorly towards the parietals. The ridge is more well-defined in dorsal view (Figure 6). There also seems to be much lower longitudinal depressions on either side of the medial ridge, however, these are uneven and the left depression lies towards the bones that have been distorted by compression. There are three longitudinal elevations of ridge-like structures on the snout, but they are not as prominent as seen in other specimens of *E. bathystoma* (see Chapter 4, Section 4.4.1). A comparison of *Endothiodon* species in Ray (2000) notes that the Indian form *E. mahalanobisi* was the only species to have a single medial ridge, while all other species including *E. bathystoma* had three ridges.

The angle of inclination of the medial ridge from the frontals to the pineal boss is significantly larger than that of *E. mahalanobisi* from India (Ray, 2000) such that the entire pineal "crest" is very prominent in lateral view. In dorsal view, the postorbital bone is robust and seems to protrude laterally (raised anterodorsally above the level of the orbit in anterior view). This may not be a result of compression, as most of the compression seems to be lateral and not dorsal. The lacrimal bone is small and not clearly defined from the prefrontal. The jugal seems to form most of the orbital rim in lateral view and meets the postorbital bone in a small but significant protruding boss. The preparietal originates from the abovementioned longitudinal ridge and widens towards the pineal boss.

The pineal boss is a prominent feature on the skull and distinctly bulbous such that it does not appear to have been affected by lateral compression. The robustness of the pineal boss is considered a diagnostic feature (Ray, 2000). Within the pineal boss, in dorsal view is a small pineal foramen. The preparietal continues to the front margin of the boss. Posterior to the pineal boss are the relatively short parietal bones which surround the boss and continue in a longitudinal ridge and diverge towards the squamosals. It is not entirely possible to differentiate the parietal bones from the interior-posterior ends of the postorbitals. The squamosals are wing-like and are at the posteriormost end of the skull in dorsal view have also experienced a degree of lateral compression, as they do not flare outwards as much as seen in other descriptions of *Endothiodon* skulls, and show brittle fractures where the compaction stresses were released (Figure 7).

3.1.1.3 Lower jaw

Since the upper and lower jaws could not be separated for this study, the palate and dentition of this specimen cannot be examined; however, features of the lower jaw will be described as far as possible.

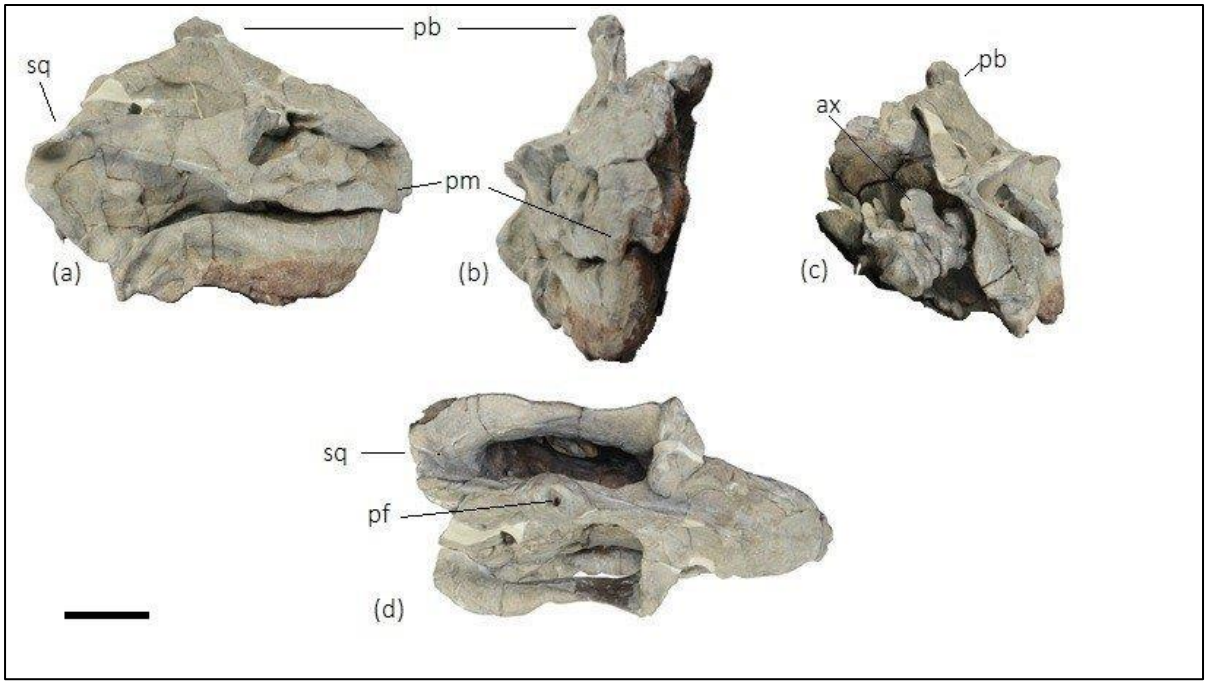

Figure 5. Skull of SAM-PK-K011271 in (a) right lateral; (b) anterior; (c) postero-lateral and (d) dorsal views. Images from 3D model of skull (Autodesk ReMake). Scale bar represents 100 mm.

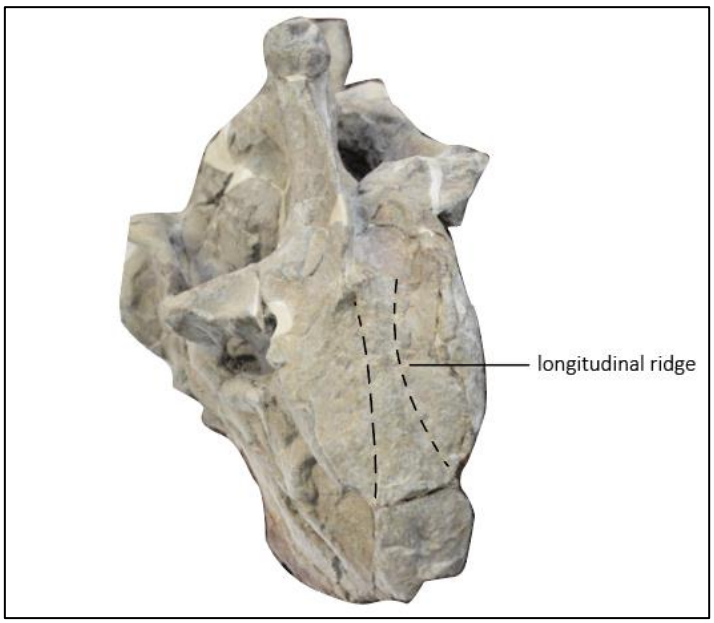

Figure 6. Skull of SAM-PK-K011271 in dorsal view showing raised longitudinal ridge represented by broken lines.

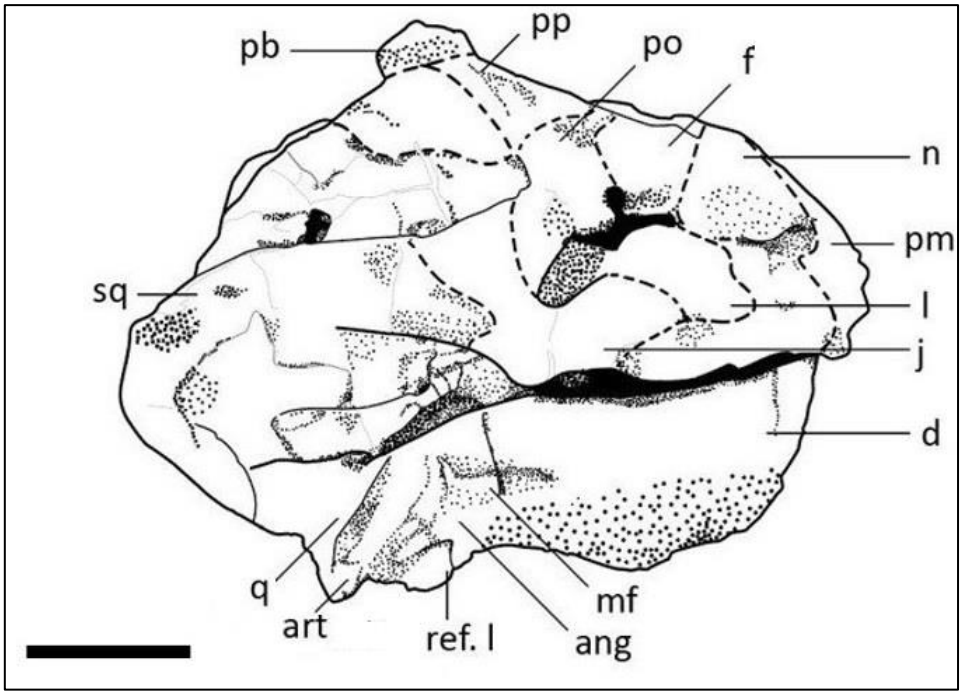

Figure 7. Schematic drawing of *E. bathystoma*, SAM-PK-K011271 skull in right lateral view. Broken lines indicate approximate suture lines. Scale bar represents 100 mm.

The dentary of SAM-PK-K011271 is significantly robust compared to that of other *Endothiodon* species (Figures 5 and 6). Its length is 326.36 mm from the anteriormost snout tip to the posterior margin of the articular. Its anterior portion is tapered upwards, to fit into the deep notch observed in the premaxilla. The anterior surface is rugose and contains surface impressions of possible foramina, possibly indicative of the attachment sites of the keratinous beak. The dorsolateral margin towards the middle of the dentary above the mandibular fenestra is significantly more bulbous than at the anterior end, and this area is likely the lateral dentary shelf. A very small part of the most exterior margin of the lower jaw (buccal side) can be seen in dorsal view, and its surface appears uneven, rugose and contains thin longitudinal grooves continuing with the length of the dentary. The teeth are not visible.

In lateral view, across the fracture line is a relatively deep mandibular fenestra, the deepest part of which is 59.12 mm long and 15.60 mm wide (Figure 7). Towards the posterior end of the dentary, the angular process is relatively bulbous and lies just above the reflected lamina, posterior to the mandibular fenestra in lateral view. Its posterior margin borders the deeply depressed angular cleft, which is anterior to the articular process. The reflected lamina is more flattened and its border lies on the ventral surface of the jaw.

The articular is a thin, long process supported by the robust angular. The posterior end of its lateral condyle is posteroventrally directed and forms part of the retroarticular process, whereas the anterior end tapers dorsally and meets with the surangular. The ventral surface of the lower jaw in general is quite rough and not entirely separated from the sediment of the rock base. It is unclear whether the rugosity on the anteriormost portion of the mandible in ventral view is a continuation of the attachment sites for keratin.

3.1.2 Postcrania

3.1.2.1 Pectoral girdle

i. *Left scapula*

Even though some of the left half of the skeleton has been laterally compressed, and/or has not been prepared out of the sediment, the left scapula is quite clearly visible and stands out as a well preserved, complete element (see Figure 8). It has shifted out of articulation, but the fusion of a few rib heads to the ventral region of the scapula could indicate that its angle relative to the vertebral (horizontal) axis is the same as it would have been in life, which is reinforced by the fact that it has the same orientation as the right scapula. It is approximately 277.65 mm in length. The scapula can only be seen in medial view, as it has not been lifted to expose its lateral side (see right scapula for a description of the lateral view). The following features are visible in medial view: a pattern of longitudinal ridges from the dorsal edge of the scapula blade converging towards the centre of the blade, which may be an attachment area for M. subcoracoscapularis (Ray, 2006); a shallow, rounded depression mediolaterally (towards where the acromion process would be on the lateral side); a narrow groove ventrally, towards the site for coracoid articulation. The scapular blade is widest at its dorsal edge, which is relatively straight with slightly convex lateral edges. The blade narrows ventrally and expands slightly at the level of the acromion process, thereafter narrowing again towards the level of coracoid articulation. The scapula is not attached to its associated coracoid process, although the coracoid attachment site is estimated to be at the raised right-lateral border on the most ventral part of the scapula. The entire scapula is gently curved, with the posterolateral border being concave and the anterolateral border being slightly convex.

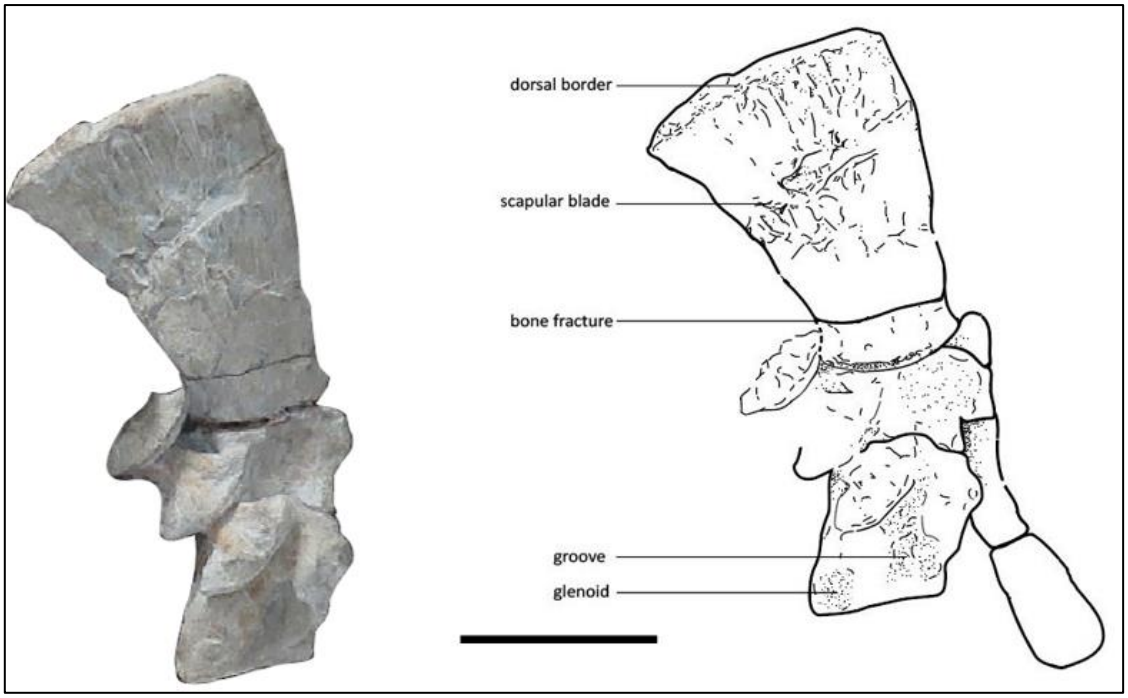

Figure 8. Left scapula of *E. bathystoma*, SAM-PK-K011271 in medial view. Scale bar represents 100 mm.

ii. *Right scapula*

The right scapula is also well-preserved, and it is positioned at approximately the same angle as the left scapula, which is at a 45° angle from the horizontal axis (formed by eight vertebrae along the column). It has not been lifted from the rest of the skeleton during preparation, therefore, it is described here in lateral view only (Figure 9). The following features are visible in lateral view: acromion process; coracoid process; glenoid fossa articulation site; coracoid attachment site. A longitudinal spine is often seen in dicynodonts (Kammerer *et al*., 2013) however, such a spine is not visible on this scapula. The absence of the spine may be a feature of *E. bathystoma* scapulae. The acromion process is small and gently triangular.

Besides the left and right scapulae, a few other elements are preserved in the general region of the scapulae (Figure 2) which may belong to the pectoral girdle. There is a long, thin element beneath the left scapula which could either be a displaced rib fragment or a part of the clavicle.

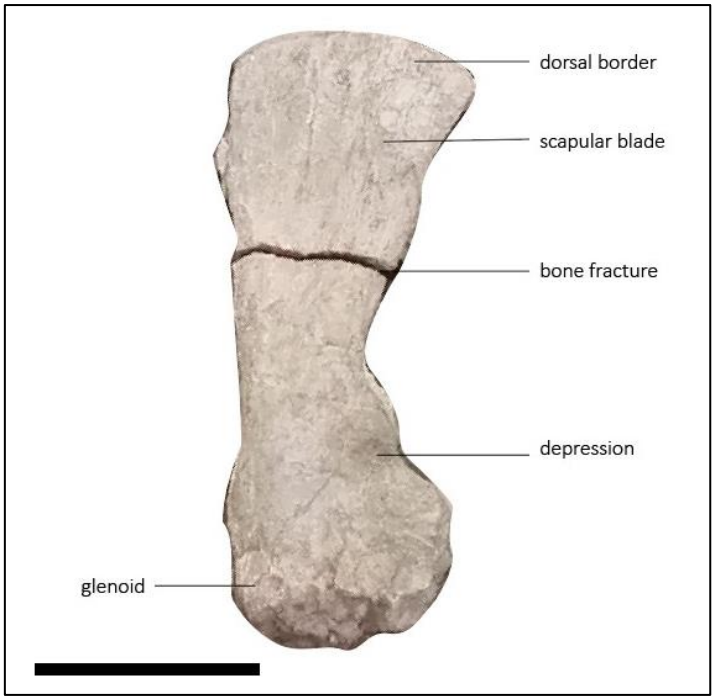

Figure 9. Right scapula of *E. bathystoma*, SAM-PK-K011271 in lateral view. Scale bar represents 100 mm.

3.1.2.2 Right forelimb

i. *Right humerus*

SAM-PK-K011271 has a robust right humerus which is entirely preserved. In lateral view, most of the humerus is well-exposed. Although separated from the scapula, the humerus lies in approximate articulated position and is still articulated with the ulna and radius at its distal end. The proximal and distal ends of the humerus are widely expanded in comparison to the shaft, which is quite narrow (Figure 10). The proximal end has a width of 124.3 mm across the deltopectoral crest. Since the head is not clearly defined, there is also no defined anatomical neck. Its smallest width is 56.87 mm (across the mid shaft) and the humerus has a length of 217.22 mm. The humeral head is porous in texture and covered in small foramina, most likely for the attachment of cartilage in life (Govender and Yates, 2009). The following features are visible: proximal articulation; deltopectoral crest; pectoralis insertion; olecranon fossa; ectepicondyle; entepicondyle; capitellum; and trochlea. In right lateral view, the proximal humerus is wide and becomes gradually thicker anteriorly along the dorsal border towards the deltopectoral crest (Figure 10 a). Along the dorsal border anteriorly, there is a shallow depression followed by the peak of the deltopectoral crest which is gently rounded. The deltopectoral crest can be seen anteriorly on the proximal humerus. In lateral view, the crest is broad and occupies just over a third of the length of the humerus and is approximately double the width of the humeral shaft. A prominent fossa medial to the deltopectoral crest is likely the site for pectoralis insertion. Due

to the position of the humerus, the posterior end of the dorsal border is still embedded in the sediment, however it is likely that the attachment site for M. subcoracoscapularis is located here.

The distal end of the humerus is expanded to a width of 100.82 mm. The radius and ulna are positioned in articulation with the distal humerus. The capitellum of the humerus (on which the radius rotates) is not visible, due to the position of the humerus. A shallow radial fossa is seen dorsoventrally along the distal humerus. An ectepicondylar foramen is not visible on the ectepicondyle. In dorsal view, the distal humerus shows a clear triangular-shaped olecranon fossa which is widest ventrally between the epicondyles, narrowing medially (Figure 10 c). There are shallow, small and irregular depressions on the ectepicondyle and the entepicondyle. Most of the rugosity on the humerus is seen along the dorsal border (in lateral view) towards the deltopectoral crest, and on the dorsal surface of the entepicondyle. The trochlea on the ventral surface is not clearly defined, but is however indicated by a shallow depression ventrally.

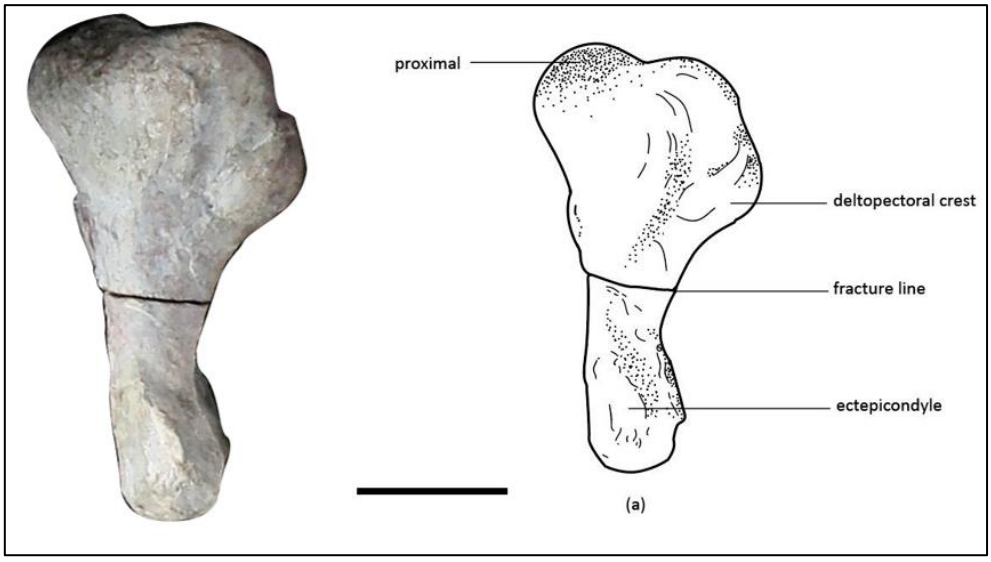

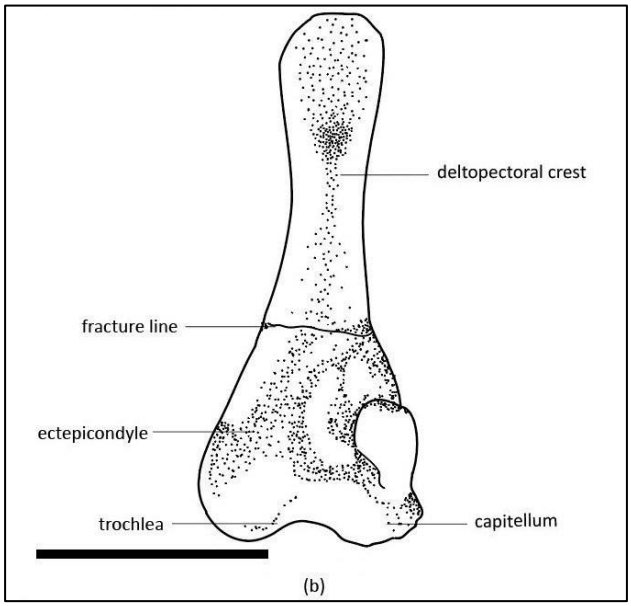

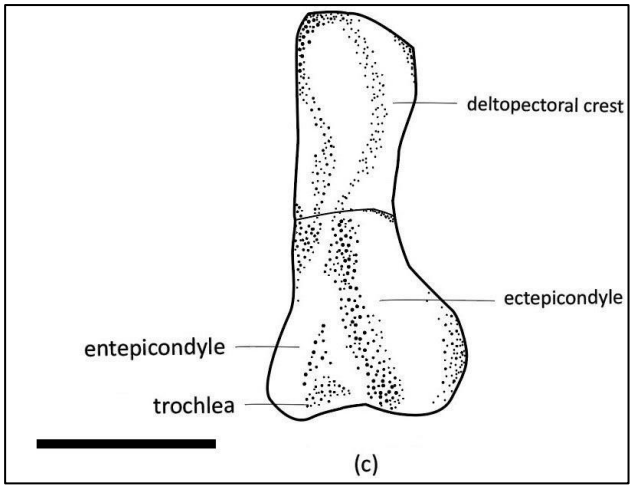

Figure 10. Right humerus of *E. bathystoma*, SAM-PK-K011271 (a) lateral view, (b) ventral view and (c) dorsal view. Scale bars represent 100 mm.

ii. *Ulna*

The right ulna is preserved entirely and most of the lateral surface area is exposed (Figure 11). It has a length of 185.67 mm, and is positioned in articulation with the distal humerus, and its proximal and distal ends abut that of the radius. The ulna is slightly more robust than the radius and expands across its proximal end, becoming narrower towards the distal end. Its greatest width, across the proximal end is 76.99 mm. The distal end has a width of 44.11 mm. The distal end of the ulna is slightly more laterally compressed in comparison to the proximal end. On the proximal left corner of the lateral surface is a shallow fossa. The proximal right corner has a rugose surface, and distal to that is the radial articulation site. In lateral view, the shaft has a short, shallow groove on its surface towards the right. Directly distal to the groove is a small area of rugosity or possibly foramina for muscle attachment on its lateral surface. No distinct ridges seem to be present on the bone surface. There is contact between the distal articular surface and the proximal carpals of the hand, and the articular surface of the ulna seems to be slightly distorted. The proximal ends of both the radius and ulna are much more rugose than that of the other long bones of the skeleton.

iii. *Radius*

The right radius of SAM-PK-K011271 is well-preserved and exposed in lateral view (Figure 11). It is slightly more slender than the right ulna, and shorter with a length of 163.6 mm, and a width of 37.71 mm across the shaft, which is relatively narrow and straight. The proximal and distal ends are

expanded, having widths of 58.78 mm and 64.46 mm respectively. The radial articulation site of the ulna is fused to the lateral edge of the proximal radius. The lateral edge of the distal radius and the medial corner of the distal ulna are also fused. The distal end of the radius is aligned (but not in contact) with the proximal end of the radiale of the manus. The proximal end of the radius is slightly fractured.

iv. *Manus*

The right manus is the most poorly represented of the entire (exposed) skeleton, since not all carpus and phalangeal elements are present (Figure 11). Based on the positions of the elements relative to the distal ulna and radius, the following 14 elements are present: three proximal carpals (radiale, a potential intermedium and ulnare); one distal carpal; one lateral centrale; three metacarpals (II, III and IV); the proximal phalanx of metacarpal II (R.Prox.P.MII); the right middle phalanx of metacarpal II (R.Mid.P.MII); the distal phalanx of metacarpal II (R.Dist.P.MII); the proximal phalanx of metacarpal III (R.Prox.P.MIII); the middle phalanx of metacarpal III (R.Mid.P.MIII); and the distal phalanx of metacarpal III (R.Dist.P.MIII). The abovementioned elements are very well preserved individually and can be clearly described. See Table 5 for measurements of right manual elements. The manus is exposed in dorsal view. The manus is approximately as long as the ulna. The missing digits I and V make it difficult to determine the phalangeal formula of this specimen. However, the left manus is very likely to be fully preserved as it is lying protected beneath the skull. If permission to prepare the specimen more fully is obtained, future work will enable us to confirm the manual phalangeal formula for *E. bathystoma*.

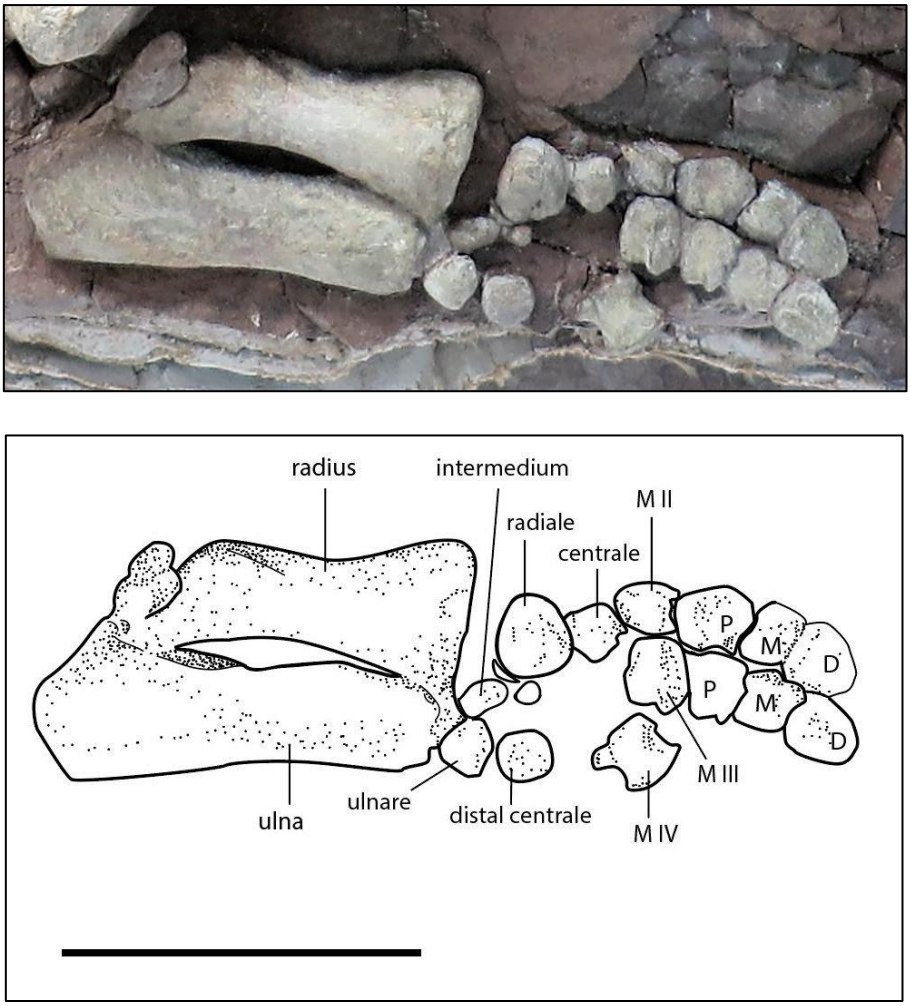

Figure 11. Right radius, ulna and manus with metacarpals M II–IV in lateral view. NB. D, M and P indicate distal, middle and proximal phalanges, respectively. Scale bar represents 100 mm.

Table 5. Measurements of the right manual elements of *E. bathystoma*, SAM-PK-K011271 (mm).

Element	Width (Prox)	Width (Dist)	Length
radiale	33.26	25.55	35.49
intermedium	12.83	11.37	36.05
ulnare	26.19	22.5	23.26
distal carpal	23.46	20.98	26.03
MII	15.95	18.07	19.31
MIII	31.95	28.67	27.32
MIV	36.25	26.93	35.27
R.Prox.P.MII	22.25	22.80	37.25
R.Mid.P.MII	28.66	27.06	22.27
R.Dist.P.MII	30.26	24.99	22.78

R.Prox.P.MIII	29.14	27.92	21.92
R.Mid.P.MIII	23.85	23.67	23.93
R.Dist.P.MIII	22.50	19.07	15.74

Carpals

The **radiale** is distinctly robust and convex, and it is larger than the other bones of the carpus. Since it is more three-dimensional than the other carpal bones, it can be described from a lateral and dorsal view. Its surface in lateral view is a slightly rounded trapezoid shape. The distal edge of the radiale is narrower than the proximal edge. The bone is raised on its medial edge, and thinner on its lateral edge. There is a shallow groove running from the lateral edge towards the medial edge, ending about midway on the surface of the bone in lateral view. In dorsal view the bone surface becomes more robust towards its proximal articulation. It is uncertain if this can be attributed to deformation. The **distal carpal** is well exposed and completely preserved. It is located directly distal to ulnare. All edges of the carpal are rounded, with the proximal edge being slightly narrower than the distal, medial and lateral edges. There is a shallow concavity of the dorsal surface of the bone. It is about the same size as, if not larger than the ulnare, and is distinctly more rounded than the other preserved carpus bones. A **lateral centrale** is preserved completely and is found distal and very slightly medial to the radiale. It has relatively straight distal and proximal edges. The medial edge is slightly concave anteriorly, while the lateral edge is rounded and convex. The exposed dorsal surface is relatively smooth and convex. The centrale is smaller than the radiale but retains a slight trapezoidal shape.

The **intermedium** is identified based on its position directly medial to the ulnare, while being lateral and slightly proximal to the radiale. Its proximal end contacts the distal-medial corner of the ulna. The exposed (dorsal) portion of the intermedium is elongated and widest at the proximal end. However, it is possible that the fragment had shifted on its lateral side, as the surface of the bone in its lateral view is wide and smooth and could represent its true dorsal surface, which would mean that the medial edge is exposed upwards. Assuming this is the case, it can be said that the intermedium has relatively straight medial, proximal and distal edges, with the medial edge being slightly raised distally. It is also in contact with a smaller unknown fragment of one of the associated carpals, since it also laterally contacts the lateral edge of the radiale.

It is still possible that the intermedium is incomplete. Assuming the intermedium shifted onto its lateral side, the dorsal surface exposed can be described as smooth and flat, while the medial edge bears a deep longitudinal groove that could be attributed to the bone being damaged or broken on that end. It is far smaller in size than the other carpus bones since it is potentially only a fragment of the intermedium. The **ulnare** seems to be entirely well-preserved. It is positioned directly distal to the

articulating distal end of the ulna. The two elements are not fused but are in close contact, with increased rugosity on the articulating surfaces of both. The proximal and distal edges are relatively straight, while the medial and lateral edges are rounded. The lateral edge appears to be the widest. Apart from the slight rugosity on articulating ends of the ulnare, the bone surface is relatively smooth and convex. It is a fairly rounded bone, similar in size to the carpal distal to it.

Metacarpals

Three bones present in the right manus can be identified as metacarpals II, III and IV based on their position and their similarities in morphology to the hourglass-shaped metacarpals of other dicynodonts (Angielczyk and Rubidge, 2013). All three metacarpals are relatively broad and blocky compared to the carpals. The metacarpals seem to become longer and larger from metacarpal II to IV. It is uncertain whether the orientation of metacarpal II is aligned correctly for articulation with the other carpals and phalanges. **Metacarpal II** is less robust and more rounded than III and IV. A large portion of it is still embedded in the rock and possibly distorted. It lies distal and slightly lateral to the lateral centrale and is directly proximal to the three phalanges of digit II. Its lateral edge is directly medial to (and almost in contact with) metacarpal III, and its dorsal and medial sides have broad, shallow grooves toward the distal end. **Metacarpal III** is a robust bone lateral to metacarpal II, medial to metacarpal IV and directly proximal to the phalanges of digit III. It seems to have been slightly displaced such that its distal end is protruding upwards. There is a small, deep groove on the medial corner of the distal edge, as well as from the proximal end until about halfway along the medial edge. It has a wide, blocky shape, with a concave lateral edge, and convex medial and proximal edges. The distal end seems to be wider than the proximal end.

Metacarpal IV appears to be the most robust of the metacarpals. It is positioned distal to the distal centrale and directly lateral to metacarpal III. There are no corresponding phalanges of digit IV present in the manus. Metacarpal IV is distinctly more hourglass-shaped than the other metacarpals. Its proximal and distal edges are wide and convex, while its medial and lateral ends concavely curve outwards. Across its proximal-distal plane, it appears to be longest of the metacarpals.

Phalanges

The phalanges of the right hand are present in digits II and III only, and are completely preserved. The right proximal phalanx of metacarpal II (**R.Prox.P.MII)** is the largest phalanx in digit II, located directly distal to metacarpal II, medial and slightly distal to metacarpal III and proximal to R.Mid.P.MII. The medial edge can be described in two parts: 1) a straight edge running distally from the proximal end, protruding at about a 30° angle from the longitudinal plane, until about halfway

down the phalanx; and 2) a straight edge running proximally from the distal end, protruding at a smaller angle from the longitudinal plane, until about halfway up the phalanx. The two straight edges meet to form a "corner" about halfway across the phalanx which protrudes outward to give the phalanx its greatest width. The lateral edge is relatively straight. The proximal and distal ends are much narrower than the medial and lateral edges. The bone surface appears to have a shallow, rounded depression.

R.Mid.P.MII is positioned distal to R.Prox.P.MII and medial to R.Mid.P.MIII; and it is proximal to and fused with R.Dist.PMII. This phalanx is rectangular and has a block-like width similar to that of R.Prox.P.MII, but is only about two thirds the length. Its lateral and medial edges are much narrower than its proximal and distal edges. It has relatively straight proximal, distal, medial and lateral edges, although the proximal edge appears slightly more concave than the others. The bone surface has a shallow concavity across the width of the phalanx. **R.Dist.P.MII** is the terminal phalanx of digit II and is located distal to R.Mid.P.MII — to which it is also fused. This fusion is likely an artefact of preservation. It is a slightly wide, rounded phalanx, and distally becomes more dorsoventrally flattened. The proximal edge is straight, and the medial and lateral edges are convex. The rounded distal end is far less claw-like than the terminal phalanges of the right pes.

The proximal phalanx of digit III, **R.Prox.P.MIII**, is distal to metacarpal III, proximal to R.Mid.P.MIII, and lateral to R.Prox.P.MII. Its general shape is rectangular and it is smaller than metacarpal III. It has wide distal and proximal ends, and narrow medial and lateral ends, but its lateral edge is slightly concave and it has a slightly convex distal edge. Its proximal edge is rugose and its distal end is fused to the proximal end of the middle phalanx of digit III. The dorsal bone surface of the phalanx also has a shallow concavity as seen in the proximal and middle phalanges of digit II.

R.Mid.P.MIII is located distal to R.Prox.P.MIII, proximal to R.Dist.P.MIII and lateral to R.Mid.PMII & R.Dist.P.MII. The proximal end of the phalanx is fused to the distal end of R.Prox.P.MIII (where there is an area of rugosity on the bone surface) and its distal end is fused to the proximal end of R.Dist.P.MIII. It is similar in size to but more square-shaped than the other phalanges. All edges are relatively straight. The bone surface is uneven with a few small, shallow fossae.

R.Dist.P.MIII is a slightly more slender terminal phalanx than that of digit II. It is located distal to R.Mid.P.MIII, to which it is fused. Its proximal end is relatively straight. Both medial and lateral edges are wide and curve convexly to a rounded point on the distal end. It is much flatter dorsoventrally compared to the terminal phalanx of digit II. Two shallow fossae are seen on the surface towards the proximal end.

3.1.2.3 Pelvic girdle

The left and right elements of the pelvic girdle are preserved, although dorsoventral compression around the acetabulum is evident, and the left ischium and pubis are compressed under the left ilium (Figure 12). The sacrum has shifted slightly to the right and articulates with the left side of the right ilium. There is contact between the ilium, ischium, pubis and femur. The left and right elements of the pelvic girdle are preserved entirely, although some areas have been dorsoventrally compressed. The right ilium, ischium and pubis are exposed in lateral view. The outermost wing of the left ilium is exposed in medial view, however, the severe dorsoventral compression on the left side makes the ischium and pubis difficult to identify and describe.

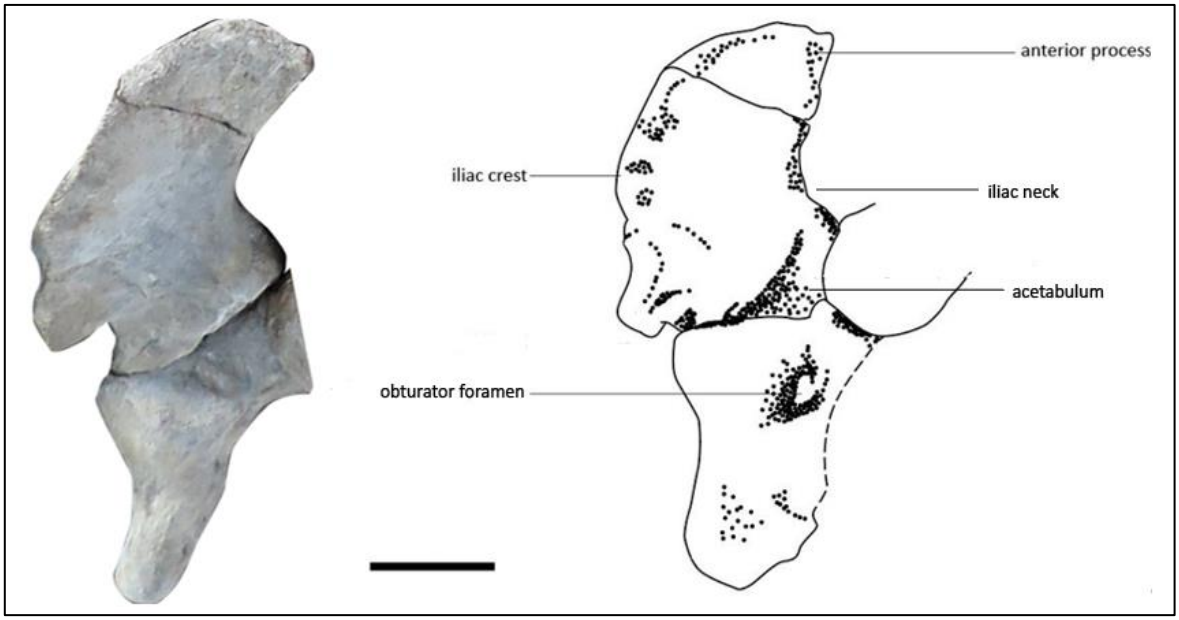

Figure 12. Right pelvis of *E. bathystoma*, SAM-PK-K011271 in lateral view. Scale bar represents 100 mm.

i. *Ilium*

The ilium is exposed in lateral view. It is widest anteroposteriorly along its dorsal border and narrowest anteroposteriorly between the iliac neck and the anterior corner of the distal process. The dorsal edge of the iliac blade is fan shaped and gently curved, running from the posterior process (followed by a small convexity on the edge), along the iliac crest, towards the anterior processes; with rugosity along the surface of the border. Behind the blade is the articulation site for the right sacral vertebrae, five of which are preserved in this skeleton. The posterior process is a short, robust edge Its lateral surface is slightly concave and rugose (Figure 12). The anterior process is wide and robust and seems to be about a third of the length of the blade.

The distal end of the ilium is slightly bulbous and contributes to the dorsal border of the acetabulum. Although the bones have been compressed, the anteriormost corner of the distal ilium is robust and prominent and contacts the proximal articulation of the femur. There seems to be sutural contact between the posterior corner of the distal ilium and the dorsal edge of the ischium. The compression of the acetabulum makes it difficult to determine whether it was circular in life, as seen in other dicynodonts (Govender and Yates, 2009). The lateral surface of the iliac blade is gently concave with a large breakage line between most of the anterior process and the rest of the blade. The bone surface contains longitudinal striations concentrated near the dorsal border, which could be sites for muscle attachment.

ii. *Ischium and Pubis*

The right ischium and pubis are fused together and exposed in lateral view, and can be described together as the right pubo-ischiadic plate, which is roughly triangular-shaped in lateral view. It is widest across from proximal to distal end. The dorsal border forms a gentle concave curve running from the posterior end of the ischium to the proximal articulation (where the pubic tubercle would be). The dorsal surface of the ischium is convex across the greatest width but becomes deeply concave towards a prominent, medium-sized oval-shaped obturator foramen which lies between the ischium and pubic bone (Romer, 1956). Beneath the distal end of the ischium are three or four caudal vertebrae which appear to have broken off the posterior sacrum and have curved laterally. There is strong rugosity on the posterior end of the ischium which is likely a muscle attachment site. The head of the femur is resting on the anterior end of the pubis. Extending dorsally, the proximal edge of the pubo-ischiadic plate contributes to the distal border of the acetabulum in a gently concaved, almost semi-circular shape. The dorsal-most corner of the ischium contacts the posterior corner of the distal

ilium, forming an isosceles-triangle-shaped dorsal border of the acetabulum. The ischium has a larger proximal articulation surface than the pubis.

3.1.2.4 Right Hindlimb

i. *Femur*

The right femur is well-preserved and exposed in dorsal view, and has a length of 229.81 mm, which is slightly longer than the right humerus, which is 217.22 mm in length. The greatest width across the femoral head is 103 mm, and the smallest width is 52.54 mm across the mid shaft. The ventral side of the femur is embedded in rock and not visible. The femur is a fairly robust bone that expands proximally across the femoral head, and the distal articulation is narrower than the proximal (Figure 13). The dorsal border is thick and curves convexly with rugosity on the surface. The more medial corner of the dorsal border is the site for proximal articulation which is in contact with the acetabulum. The medial border is also quite thick and rugose, and is gently concave beneath the proximal articulation. The lateral edge of the bone (towards the proximal end) is relatively straight and is slightly expanded laterally, and this is possibly the swollen tuberosity of the trochanter major.

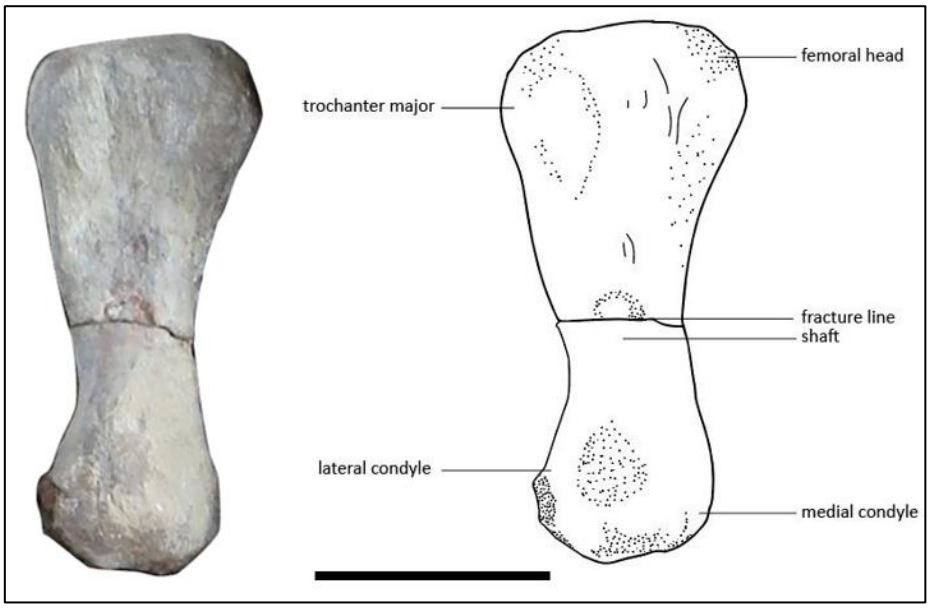

Figure 13. Right femur of *E. bathystoma,* SAM-PK-K011271 in dorsal view. Scale bar represents 100 mm.

There is rugosity along the lateral edge of the shaft, which is slightly concave before slightly flaring outwards at the distal articulation. An area of damage/breakage is clearly seen on the lateral-most corner of the distal femur, at the site for articulation of the fibula. The distal border also has some rugosity on its surface. On the distal end laterally is the prominent, raised posterior (lateral) condyle; and next to it is the anterior (medial) condyle which is much less robust. The dorsal surface of the femur is relatively uneven. There is a prominent swelling on the dorsal surface (close to the proximal end and towards the medial edge) which is likely the site for attachment of the ischiotrochantericus muscle. Medial to that is a longitudinal concavity running towards the middle of the shaft. This area is possibly an attachment site for the puboischiofemoralis internus muscle. Medial to the concavity is a shallow depression on the dorsal surface of the femoral head.

ii. *Tibia*

The complete right tibia is well-preserved and exposed in anterior view. It has a length of 151.62 mm. Its proximal and distal ends articulate with that of the right fibula. The proximal surface is wide, uneven and rugose, with slightly concave areas towards the lateral corner, where the distal femur articulates (Figure 14). The tibia is stout and widely expanded towards its proximal end, which is approximately 66.35 mm. It is narrowest at the midpoint of the shaft (32.92 mm), around which there is a break in the bone. It is unclear whether the shaft would be circular in cross-section as seen in *Diictodon* and *Wadiasaurus* (Bandyopadhyay, 1988) due to the slight dorsoventral flattening of the hindlimb. On the anterior surface proximally there is a prominent, slightly triangular protrusion which is the cnemial crest. It narrows distally and has a small circular foramen on its surface. Medial to the cnemial crest is a wide, shallow concavity. Due to the articulation of the fibula on the lateral side of the tibia it is not clear whether the lateral side of the cnemial crest also has a depression. However, there is a deep, oval-shaped groove on the lateral edge, proximally. The tibia expands towards the distal end, which is fairly oval shaped in distal view. The medial corner of the distal tibia articulates with the astragalus of the pes and is slightly convex, while the lateral corner is more concave. The anterior surface of the tibia is rugose proximally but becomes relatively smooth and slightly concave at the shaft. The posterior surface of the tibia is not visible.

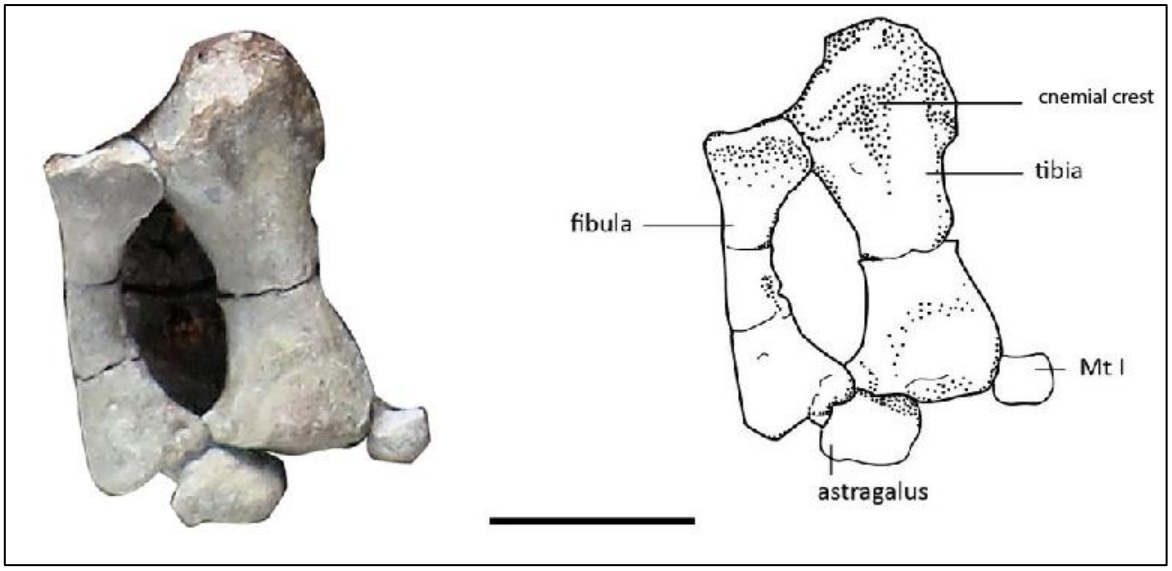

Figure 14. Right fibula and tibia of *E. bathystoma* SAM-PK-K011271 in lateral view. Scale bar represents 100 mm.

iii. *Fibula*

The right fibula is well preserved and is in direct contact with the tibia. It is distinctly more slender than the tibia and is 137.86 mm long. In anterior view, the shaft of the fibula curves strongly away from the tibia, while the proximal and distal ends are more expanded (Figure 14). The smallest width is just below the expanded proximal end, about one third of the way down the shaft and is 18.3 mm wide. The midpoint of the shaft is slightly anteroposteriorly flattened. The distal end is 43.99 mm wide and is more expanded than the proximal end. The proximal end protrudes medially towards the tibia and has a slight golf club-head shape. The proximal articulating surface has an oval outline, and is uneven and rugose with slight breakage on the superficial bone surface. On the anterior surface, there is a slightly elongated groove on the more medial edge, proximally; and there is a very shallow concave area towards the distal end. The medial corner of the distal end articulates with the tibia and is very rugose. The lateral edge of the fibula is fairly smooth but becomes more rugose distally. The surface of the distal expansion has a rounded articulation on the medial corner (for articulation with the calcaneum).

iv. *Pes*

The right tarsus is fairly well preserved and exposed in dorsal view (Figure 15). Elements of the first four digits are present, while some bones of the fourth digit are missing, and no bones of the fifth digit are present. The following tarsus elements are exposed in dorsal view: three proximal tarsals (calcaneum, astragalus, centrale) and an unidentified tarsal element; one fragment of "distal tarsal 4"; four metacarpals (I, II, III and IV); right proximal, middle and distal phalanges of digits II and III; right proximal phalanx of digit IV; unidentified second phalanx of digit IV. Most bones of the pes seem to be in articulation, apart from the calcaneum which has disarticulated from the fibula; and the second phalanx of digit IV. See Table 6 for all right pedal measurements.

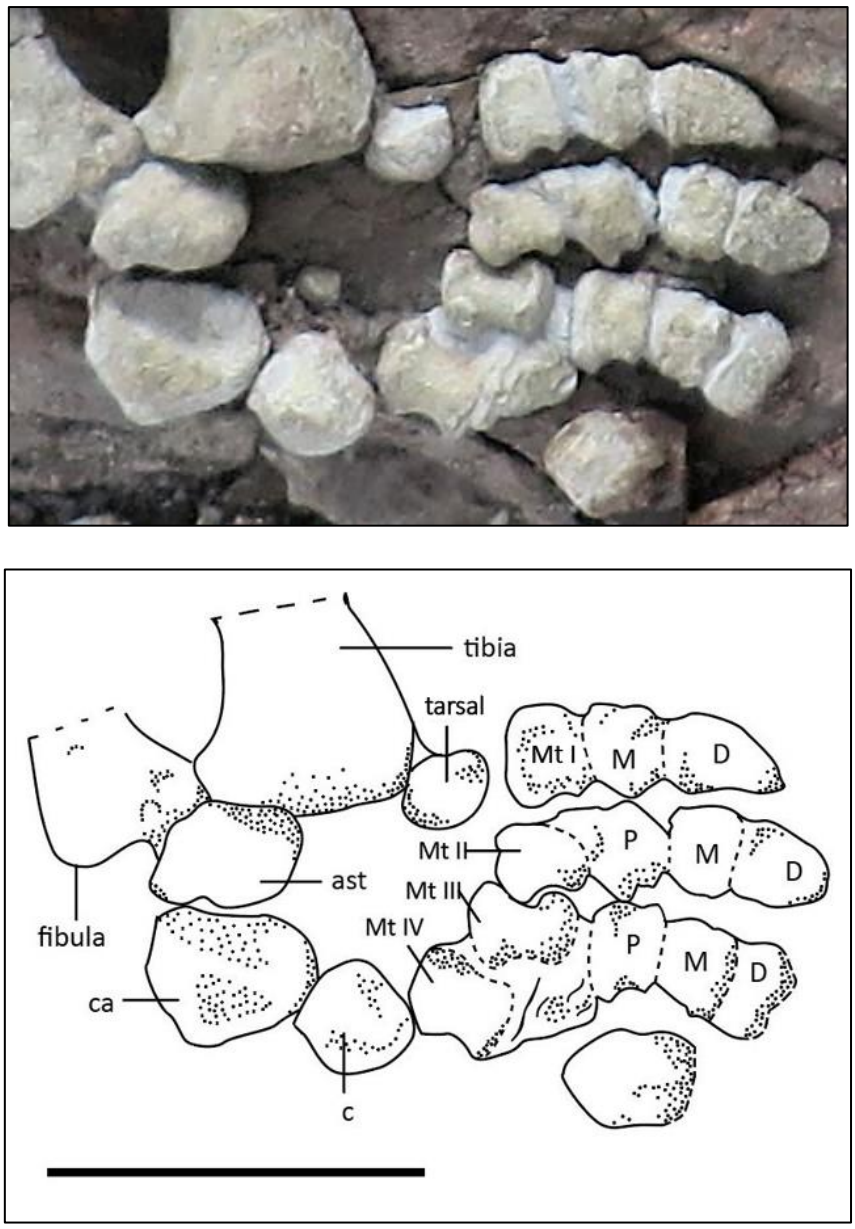

Figure 15. Right pes of *E. bathystoma*, SAM-PK-K011271 in dorsal view showing the claw-shaped terminal phalanx of digit I. I–IV indicate digits. Scale bar represents 100 mm.

Table 6. Measurements of right pedal elements of *E. bathystoma*, SAM-PK-K011271 (mm).

Element	Width (Prox)	Width (Dist)	Length
Calcaneum	35.26	25.70	48.414
Astragalus	28.7	20.7	45.92
Centrale	21.22	19.05	39.72
Distal tarsal 4	-	-	13.8
Tarsal ?	22.01	16.35	29.69
MtI	18.67	21.54	25.55
MtII	17.08	20.67	28.26
MtIII	20.31	17.94	33.86
MtIV	27.8	18.69	37.39
R.Mid.P.MtI	21.78	18.33	21.09
R.Dist.P.MtI	22.19	-	33.51
R.ProxP.MtII	21.87	15.52	20.03
R.Mid.P.MtII	21.22	22.3	20.39
R.Dist.P.MtII	23.32	19.09	28.56
R.Prox.P.MtIII	26.21	23.8	30.78
R.Mid.P.MtIII	24.63	21.78	20.03
R.Dist.P.MtIII	23.64	24.96	18.1
P.MtIV	14.93	16.47	27.52

Tarsals

The **astragalus** is well-preserved and is positioned between the distal ends of the tibia and fibula. It is a fairly thick bone with rounded rectangular shape in dorsal view, with an uneven, slightly concave distal border. Its proximal edge is relatively straight, and it is widest at its lateral border, which is also fairly straight. The bone becomes slightly narrower towards its rounded medial border. The dorsal bone surface appears to be smooth and even.

The **calcaneum** is distinctly larger than the astragalus and is positioned distal to the astragalus and proximal to the centrale. Its distal end articulates with the proximal centrale and is roundly trapezoidal in dorsal view, narrowing towards the distal end. There is a triangular process protruding on the dorsal surface tapering towards the distal end of the bone. In proximal view, the calcaneum is spool-like in that its proximal surface is concave all the way down to its lateral surface.

The proximal **centrale** is smaller than the other two proximal tarsals, and is slightly rounded, with a pointed medial edge. It is proximo-distally wide and has a narrower, concave proximal edge. On the

dorsal surface, the centre of the bone is a longitudinal concave groove formed by thick lateral, distal and medial margins. Its distal edge is smoothly convex. Medial to the centrale is a very small, almost spherical fragment of bone embedded in the rock which is disarticulated from the rest of the tarsus (not illustrated in Figure 15). Based on its position, it might belong to "distal tarsal 4". Another unidentified tarsal element is preserved. It has a slightly convex lateral edge and a concave medial edge, which appears straight in dorsal view. It does not directly contact any of the other bones, but is in position to articulate with the right proximal phalanx of digit I. Its proximal end is also positioned close to the medial corner of the distal tibia. The distal end of this element is relatively straight and its dorsal surface is smooth.

Metatarsals

Most of the metatarsals present maintain the general hour-glass shape. Metatarsal I is a stout, trapezoidal bone. It is not in direct contact with metatarsal I but is positioned distal to it. Its distal end is fused to the proximal end of R.Mid.P.MtI. The lateral edge of the metatarsal is strongly curved and the proximal surface is wide and rugose. The medial edge is quite convex. The dorsal surface of the bone is smooth and concave, bordered by the slightly raised lateral, medial, distal and proximal edges. **Metatarsal II** is longer and its distal and proximal edges expand to produce a more prominent hour-glass shape than that of metatarsal I. Its distal end is completely fused to the proximal end of the right proximal phalanx of metatarsal II. It has strongly concave medial and lateral ends and is proximo-distally elongated. It has a very slightly robust expansion of the distal border, and its dorsal surface is smooth and slightly concave. **Metatarsal III** is lateral to metatarsal II, medial to metatarsal III and proximal to the right proximal phalanx of metatarsal III. It is a bit more proximo-distally elongated than metatarsal II. Its proximal end is robustly expanded with a small groove on the dorsal surface, proximally. Its medial and lateral sides are gently concave and its lateral side is entirely fused to the right proximal phalanx of metatarsal IV. This fusion is possibly an artefact of preservation, as it does not show any room for separation of the third and fourth digits at the metatarsals. The distal end of metatarsal III is gently convex. Directly distal to the centrale is **metatarsal IV.** It seems to have skewed slightly and its entire medial side and part of its distal edge is fused to the right proximal phalanx of metatarsal IV. This bone also has a robust proximal expansion which seems to articulate with the distal part of the centrale. The lateral edge is concave, and even though the medial edge is fused to another bone, a strong degree of concavity can be seen. The fusion of part of the distal end makes it difficult to describe, but it appears to be a fairly straight distal edge. In general, the metatarsals seem to become larger moving from digits I to IV.

Phalanges

The right middle phalanx of metatarsal I (**R.Mid.P.Mt**I) is fused with and directly distal to Metatarsal I. It appears to be proximo-distally flattened and is shorter than Metatarsal I. Its lateral edge is narrow and convex, while its medial edge is slightly concave. Its proximal borders is straight although the lateral corner is skewed downwards. The dorsal surface of the bone is slightly horizontally concave due to the raised proximal and distal margins. The distal edge is convex and is fused to the terminal phalanx. **R.Dist.P.MtI** is distinct from all the other phalanges in that it is elongated and claw-shaped. Its proximal end is slightly convex and narrow. Its medial end is long and convex, while its lateral end is long and slightly concave with some rugosity on the surface. The medial and lateral sides narrow towards a strong distal point. The dorsal surface of the phalanx has some light longitudinal scarring and is a bit more rugose towards the distal point.

R.Prox.P.MtII is directly distal to and fused with metatarsal II. It has an irregular trapezoidal shape with a straight proximal edge, skewed at an angle similar to R.Mid.PMtI. Its medial and lateral sides are strongly concave, with a more convex distal edge which articulates with R.Mid.P.MtII. the dorsal surface of R.Prox.PMtII is smooth, and becomes more convex towards the medial edge. **R.Mid.P.MtII** is directly distal and is in an articulated position. The lateral corners of the proximal and distal border are more prominent than the medial. This phalanx is slightly larger and more square-shaped. The distal and proximal edges are fairly straight, and the lateral border is slightly convex in dorsal view. The centre of the dorsal surface is smooth and a bit concave. Directly distal to and fused with this phalanx is **R.Dist.P.MtII**. In comparison, it is more robust but less slender than the terminal phalanx of digit I. The lateral and medial sides are wider across the proximal expansion and taper to a narrow distal end, but the end is more convex and spatulate than that of R.Dist.P.MtI. The dorsal surface is rugose and the medial border is uneven.

R.Prox.P.MtIII is a broad, spool-like bone with a robust, wide proximal expansion that has a shallow concavity (in proximal view). The phalanx is narrow towards the middle and expands outward distally. The dorsal, medial and lateral edges are strongly concave, while the distal edge is straighter. **R.Mid.P.MtIII** is positioned directly distal to R.Prox.P.MtIII and is fused on both proximal and distal ends. It appears to be quite dorsoventrally compressed and generally deformed as a result of preservation. The proximal and distal borders are unclear, but the lateral and medial relatively straight with a small degree of concavity across the horizontal plane of the bone. The terminal

phalanx of digit III, **R.Dist.P.MtIII** also seems dorsoventrally compressed, but its medial and lateral edges are fairly straight. It is more rectangular than the other terminal phalanges and is lateromedially wide and proximo-distally short. The distal edge is slightly convex and rugose. The rugosity looks similar to breakage, and if a claw was present distally on the terminal phalanx, it possibly broke off.

On the fourth digit, an element fused distally to the metatarsal is identified as **R.Prox.P.MtIV** based on its position. However, this bone is also badly preserved and potentially has post-mortem damage. The proximal border is unclear, while the medial, lateral and distal ends seem relatively straight. The dorsal surface is convex but uneven. The last element of the tarsus is located distal and slightly lateral to R.Prox.P.MtIV, and it might be the R.Mid.P.MtIV or R.Dist.P.MtIV based on its position; however the breakage and rugosity at the distal border suggests that it could also be a terminal phalanx that had its claw broken off. This is a round, robust bone and is larger than the other phalanges.

v. *Left pes*

Most bones of the left hindlimb are exposed in ventral view. The left femur, tibia and fibula are beneath the left pelvic bones. The left pes is preserved in ventral view (Figure 16). By comparison to the well-preserved right pes, the fact that the left pes is ventrally exposed is supported by the shape of terminal phalanx of the most lateral digit, which is not elongate or claw-shaped as it would be if it belonged to digit I. Thus, it is most likely digit V. Furthermore, the positions of the astragalus and calcaneum relative to the tibia and fibula are swapped around (Figure 15). Approximately 22 pedal elements are preserved, and although the digits can be confidently identified by position, most of the individual elements are severely distorted, melded together and are thus only tentatively identified. Elements of digits III, IV and V are seen as follows:

The terminal phalanx of digit III is short and spatulate, and the middle and proximal phalanges are positioned proximal to it. They are also both short with wide proximal and distal ends. Metatarsal III is elongate and slightly oval-shaped. The terminal phalanx of digit IV is also spatulate and short but is more triangular in shape than that of digit III. The elements proximal to the terminal phalanx are identified as the middle and proximal phalanges, but only tentatively, due to the heavy deformation, particularly seen in the proximal phalanx. Proximal to this is metatarsal IV. The terminal phalanx of digit V is slightly wider than the other terminal phalanges, but it is also short and spatulate. The middle and proximal phalanges are block-like. Proximal to these are a distorted metatarsal V. One dislodged metatarsal is seen unattached to any of the digits present, and is distinctly hour-glass shaped. Both left and right pes are incomplete, but together they both provide the full complement of pedal digits in SAM-PK-K011271: the right pes has digits I–IV preserved and the left has digits III–V. The pedal phalangeal formula of SAM-PK-K011271 and thus of *E. bathystoma* is 2-3-3-3-3.

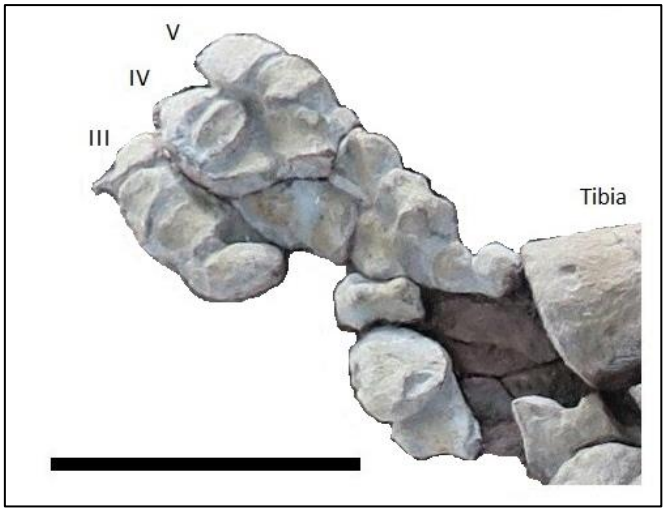

Figure 16. Photograph of left pes of *E. bathystoma*, SAM-PK-K011271, exposed in ventral view. Scale bar represents 100 mm.

3.1.2.5 Vertebral column and Ribs

i. *Cervical vertebrae*

The SAM-PK-K011271 skeleton has a similar cervical vertebral count as those reported in other dicynodont studies (Table 9). Most dicynodonts have between five and seven cervical vertebrae, and SAM-PK-K011271 has five. The atlas and axis vertebrae of SAM-PK-K011271 are compressed and fused to the occipital region of the skull and displaced from the rest of the vertebral column. Three more isolated cervical vertebrae that have been displaced and fragmented are seen on the rock base near the neck region.

ii. *Dorsal vertebrae*

The series of dorsal vertebrae is estimated to start at the first element of the articulated column (just past the left scapula). Although none of the dorsal vertebrae in the series will be identical, an estimation of approximate size and morphology of the rest of the dorsals can be taken from the description of the isolated dorsal vertebra. There are 17 dorsals exposed along the gently curved vertebral column. Along the dorsal series, neural spine height (mm) and width was measured as far as possible. Dorsal vertebra 1 (DV1) had a neural spine height of 58.14 mm and a neural spine width of 11.01 mm. From DV1 to DV6, neural spine height seems to generally decrease slightly to 46.29 mm

(DV6); and neural spine width increases along the series to 26.29 mm (DV6). Contrary patterns are displayed after DV7. Neural spine heights from DV7 to DV17 are inconsistent and do not conform to any trend to increase or decrease. However, there is a general pattern of a decrease in neural spine width from DV8 to DV11, and from DV13 to DV16; while DV7, DV12 and DV17 can be considered outliers. The compression of the vertebral column around DV13 to DV16 give the appearance of short, robust neural spines. The tilt of all neural spines is slightly posteriorly directed, and there does not seem to be any significant differences in tilt along the series, if the curvature of the spine as a whole is taken into consideration.

A very well-preserved, single, isolated vertebra (Figure 17) protrudes out of the vertebral column such that all its structures can be seen clearly. It is located near the pelvis of the skeleton and sits between the end of the series of dorsal vertebrae and the start of sacral vertebrae. However, it is not certain that this is the exact position to which it belongs, due to how well-preserved it is out of articulation. Although all vertebrae in a single vertebral column are not identical to one another, the following description of the isolated element provides, at the very least, new information on the generalized structure of an *Endothiodon* vertebra. The neural spine of the isolated element is long and slender, the apex of which is slightly more bulbous than its length, and in ventral view is tilted slightly posteriorly (to the left in lateral view). The neural spine has a length of 48.90 mm and widths of 9.56 mm and 17.67 mm in anterior view and right lateral view respectively. The bone surface at the apex of the neural spine is quite rugose. The width of the vertebra across the transverse processes is 75.02 mm. The neural canal has a length of 16.52 mm and a width of 12.81 mm, and is deep and oval. The centrum is amphicoelous (concave anterior and posterior surfaces) although the posterior side may not be completely prepared out of the rock. The centrum has widths of 38.88 mm and 21.53 mm in anterior and lateral view, respectively. The postzygapophysis is slightly bulbous but does not protrude more than 10.06 mm from the base of the neural spine. The bone surface between the transverse processes and pedicles show slight scarring.

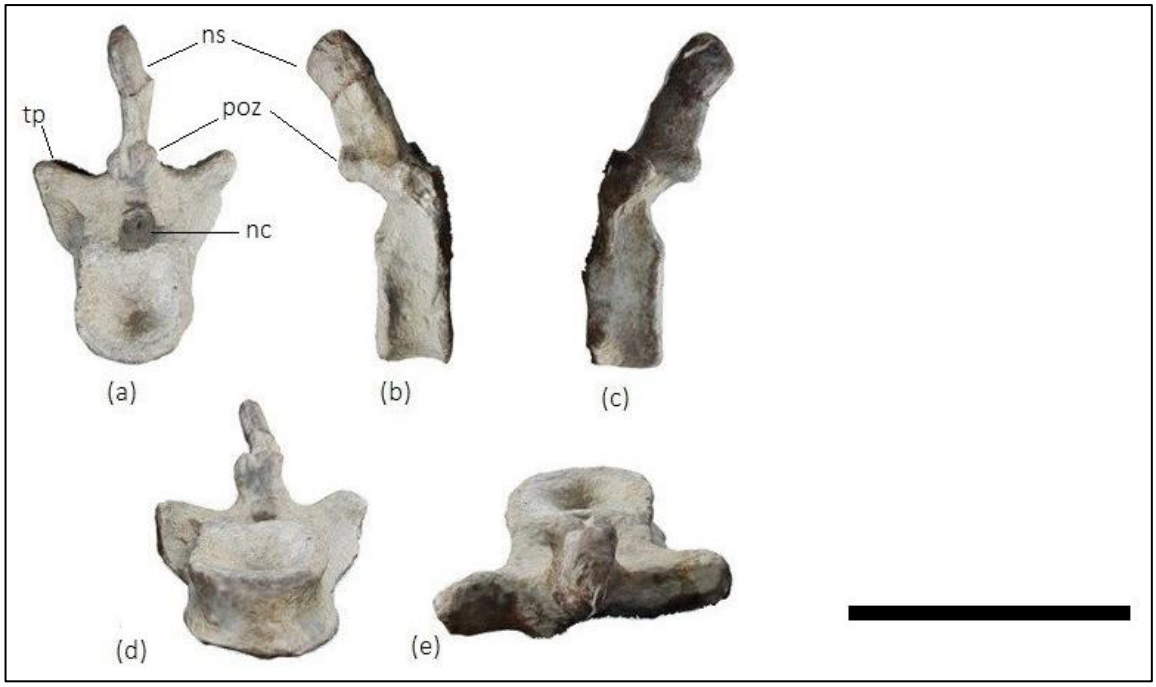

Figure 17. Isolated dorsal vertebra of SAM-PK-K011271 in (a) anterior; (b) right lateral; (c) left lateral; (d) ventral and (e) dorsal views. Scale bar represents 100 mm.

iii. *Sacral and caudal vertebrae*

The sacrum of SAM-PK-K011271 is preserved but shows a fair amount of lateral compression, as indicated by the flattening of the spines of the sacral vertebrae. There are five sacral vertebrae but no sacral ribs seen. It is also difficult to distinguish the end of the sacral series from the start of the caudal series. There are 10 caudal vertebrae that curl towards the tail end, making them difficult to describe.

iv. *Ribs*

The right ribs of the skeleton are exposed in lateral view, and most of them seem to be well articulated. Longitudinal costal grooves are seen on dorsal ribs 2–14 which run down the lateral surface following the curvature of the rib itself. A total of 18 ribs are partially to fully exposed. Only four rib heads were preserved out of articulation. The lengths of these rib heads appear to decrease caudally. The rib heads are expanded and flattened at their articulating end but become slender along the shaft. The ribs increase in length from rib 1 to rib 7, and thereafter decrease in length. The rib heads become increasingly articulated into the vertebral column, whilst the distal ends of the ribs

appear fairly rounded, with not much rugosity on the surface, although it is an expected site for cartilaginous attachment to the sternum. Compression on the left side of the skeleton has caused approximately 10 left ribs to bundle-up together beneath the vertebral column. There are also three rib fragments seen on the rock base near the skull. The first of these fragments is about 189.62 mm long and has a width of 19.08 mm. Its shaft is round and less flattened than the articulated ribs of the skeleton. The second fragment is an isolated rib head that has a width of 26.24 mm, and the third is a longer shaft fragment that is 19 mm in width. Both the second and third fragments are flatter than the first.

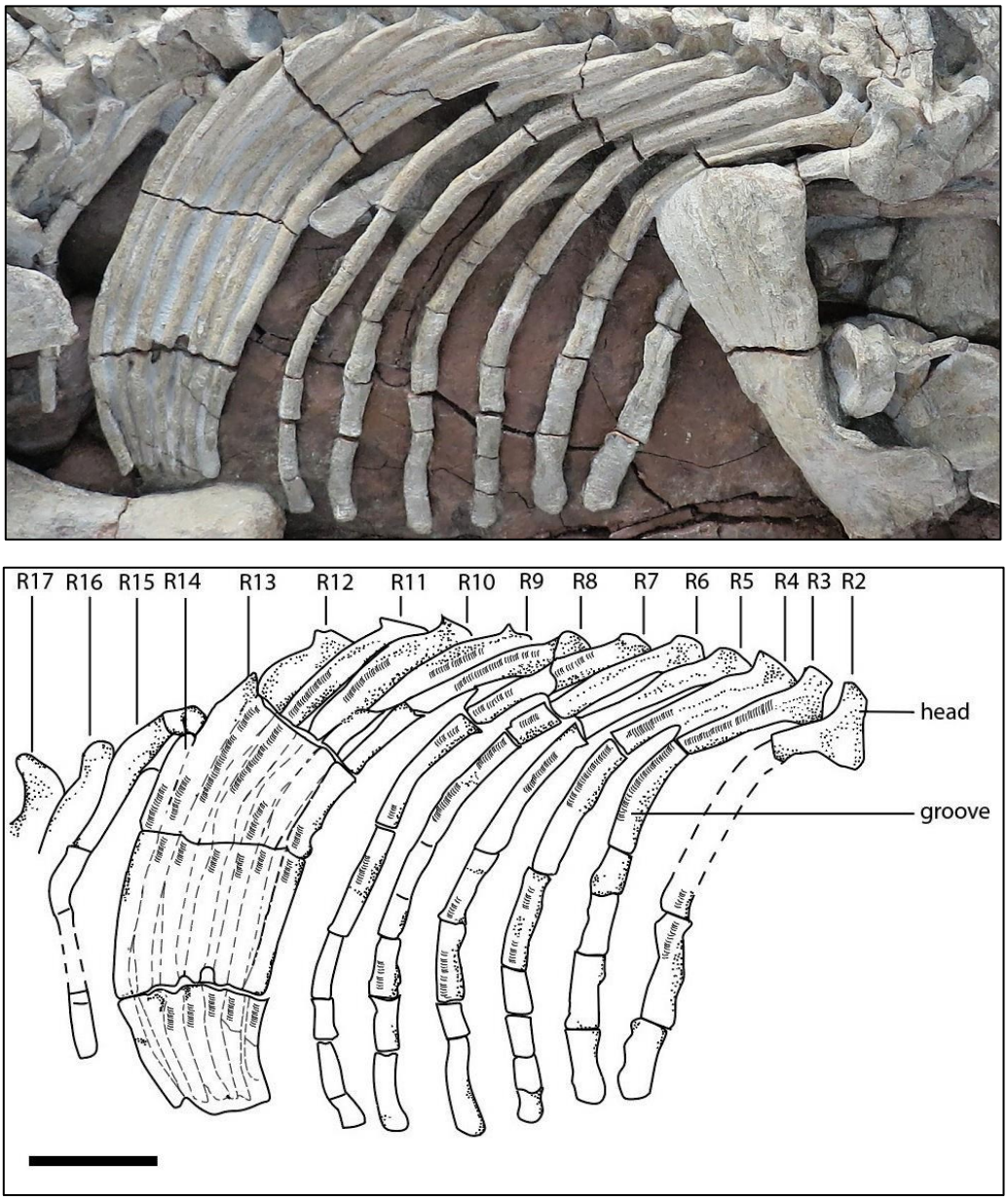

Figure 18. Visible ribs of the *E. bathystoma* skeleton, SAM-PK-K011271 in lateral view. Broken lines show estimated rib shape in areas that are unclear. NB. R2–17 indicate ribs 2–17. Scale bar represents 100 mm.

Table 7. Lengths of ribs of *E. bathystoma*, SAM-PK-K011271 (numbered from anterior to caudal). Note that the distal ends of ribs 10–15 were distorted.

Rib	Length (mm)	Width (mm)	
		Middle	Distal
1	205.1	-	-
2	349.3	18.71	20.8
3	406.7	18.92	27.32
4	425.2	24.13	20.43
5	451.9	20.8	24.28
6	466.25	22.36	20.06
7	466.25	18.96	18.50
8	447.9	19.02	20.7
9	441.25	16.53	18.7
10	413.3	12.35	7.9
11	399.6	12.35	8.03
12	382.6	14.49	7.54
13	353.9	10.69	9.39
14	299.7	11.27	8.03
15	257.4	13.7	11.07
16	-	-	-
17	-	-	-
18	-	-	-

3.2 SPECIES IDENTIFICATION

Out of all *Endothiodon* cranial and postcranial elements studied from South African collections, 17 were previously identified as *E. bathystoma*, nine were previously identified as *E. uniseries*, one was previously identified as *E. whaitsi* and 19 were unidentifiable on a species level (as per collection databases).

Since the first description of *E. bathystoma* (Owen, 1876), there has been discussion about which cranial features are diagnostic for the species. The following features are considered indicative of the species (Broom, 1905; Cox and Angielczyk, 2015; Owen, 1876; Ray, 2000): a large skull size, a robust dentary symphysis, three longitudinal ridges on the snout, a wide interorbital and swollen prefrontals, a narrow intertemporal bar, postorbitals overlapping parietals, parietal crest raised above frontal plate, a circular pineal foramen on a high boss, boss positioned on the anterior end of the intertemporal bar.

SAM-PK-K011271 was assessed for diagnostic features present in the comparable skull specimens, shown in Table B (Appendix). The assessment of all South African *Endothiodon* specimens was narrowed down to only those cranial elements with comparable features. Not all these features were useful in differentiating species clearly enough, due to factors like poor preservation. The present study tentatively accepts the revision that Cox and Angielczyk (2015) suggest, which limits the species of *Endothiodon* to *E. bathystoma*, *E. mahalanobisi* and *E. tolani*. Under this assumption, all *Endothiodon* specimens examined in South Africa, including SAM-PK-K011271, can only belong to the species *E. bathystoma*. This is supported by the large skull size, robust pineal boss and the presence of three longitudinal ridges in SAM-PK-K011271, all of which are clearly not similar to *E. mahalanobisi* or *E. tolani*. A thorough taxonomical review must be done to clarify this in future, but for now there is sufficient evidence that SAM-PK-K011271 belongs to the species *E. bathystoma*.

3.3 ONTOGENETIC CONTEXT OF SAM-PK-K011271

Postcrania and crania are roughly equally represented in the *Endothiodon* material within the South African collections. Approximately 49% of all *Endothiodon* elements were cranial, while 51% were postcranial. However, most of the postcranial elements were fragmented and not attributable to any known individuals or species, and could not therefore be used in this ontogenetic study. The ontogenetic status of SAM-PK-K011271 was deduced by examining skull size only. Out of 45 cranial elements studied, only a few were comparable in terms of skull size. This is due to the presence or absence of notable morphological cranial features among the specimens *viz*. squamosal wings, dorsal midline, orbital and dentary symphysis. See Appendix Table B for skull size measurements pertaining to each of the above-mentioned cranial features.

The largest skull is specimen CGP/1/708, having skull lengths of 452.89 mm (dorsal midline) and 511.8 mm (across the squamosals) (Figure 19). These are the highest recorded values in both skull length categories. This skull was previously identified as belonging to an individual of *E. bathystoma* from the Teekloof formation (*Tropidostoma* Assemblage Zone) of the Murraysburg District in the Western Cape. It is laterally compressed and has a notably dark yellow to brown bone surface colour which is likely due to a coating of Glyptal.

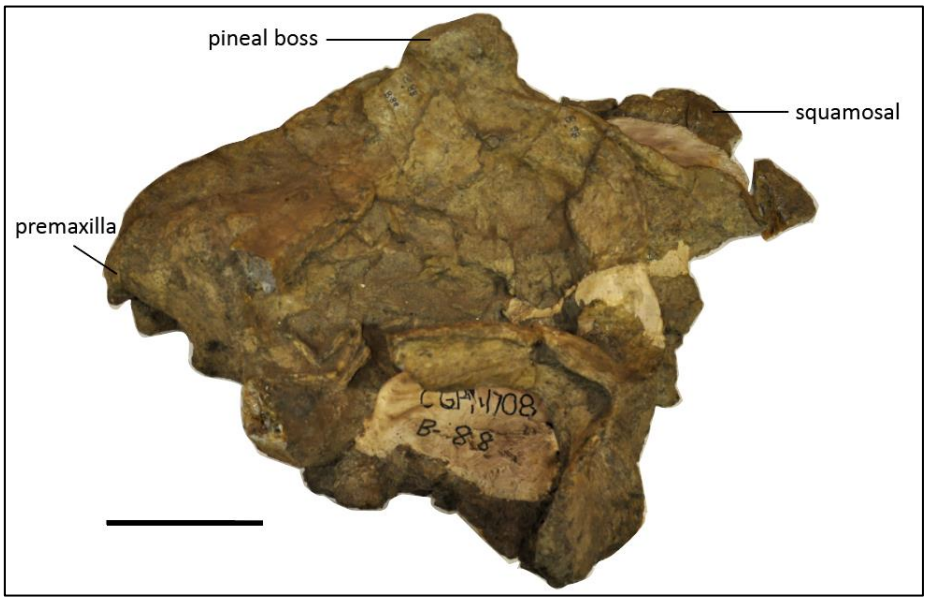

Figure 19. Skull of *E. bathystoma*, CGP/1/708 in left lateral view. Scale bar represents 100 mm.

Although SAM-PK-K011271 has the most complete cranial and postcranial elements compared to all other South African *Endothiodon* specimens, it has a skull length of only 447 mm across the

squamosal wings, which is 87% the length of the largest skull, CGP/1/708 (see Table 8). However, due to the heavy compression and distortion of squamosal wings in many of the *Endothiodon* skulls, skull length measured across the dorsal midline was a more accurate indicator of skull size and was used by Ray (2000) in differentiating skull sizes among species. In this case, the skull length of SAM-PK-K011271 is 433.69 mm, which is about 96% the length of the largest skull, CGP/1/708. Based on skull size alone, SAM-PK-K011271 is the second largest skull in the collections, as depicted in Table 8. It must be noted that the degree of lateral compression on the studied skulls needs to be considered when assessing skull size. Furthermore, for the skulls to be comparable, an ontogenetic assessment of each skull needs to be done to obtain clarity regarding which cranial features are taxonomically significant among species. The autapomorphic features of each species need to be clearly established in future studies, as there is still much uncertainty regarding *Endothiodon* taxonomy.

Table 8. Skull length comparison of *E. bathystoma* SAM-PK-K011271 (highlighted) with other South African *Endothiodon* skulls in ascending order.

***Endothiodon* Specimen**	**Skull length**
SAM-PK-2676	220.76 mm
SAM-PK-629	351.64 mm
CGP/1/689	377.5 mm
CGP/1/709	382.59 mm
SAM-PK-K11131	420.22 mm
SAM-PK-K011271	433.69 mm
CGP/1/708	452.89 mm

CHAPTER 4

DISCUSSION

4.1 OVERVIEW

To date, there has been no other study that describes the complete postcranial skeleton of *Endothiodon*. Thus, the anatomical assessment of this almost complete *Endothiodon*, SAM-PK-K011271 is important in filling in the gaps in our understanding of this enigmatic genus. This chapter discusses the significance of the anatomy and morphology of SAM-PK-K011271 (described in Chapter 3) and provides an indication of its ontogenetic stage as compared to all known South African *Endothiodon* specimens. Furthermore, the presently accepted taxonomy of *Endothiodon* and the issues surrounding this are discussed.

Some dicynodont functional morphology studies include work on disarticulated kannemeyeriid dicynodont remains from the Middle Triassic of India, *Dicynodon huenei* postcrania from the Permian of Zambia and *Diictodon* postcrania from the Permian of South Africa, (Bandyopadhyay, 1988; King, 1981; Ray and Chinsamy, 2003). Descriptions of semi- or mostly-complete articulated skeletons, such as *Diictodon* (Smith, 1987) and *Eosimops newtonii* (Angielczyk and Rubidge, 2013) have been even more beneficial in understanding how features of the skeleton, particularly the articulation of limb girdles hind and forelimbs, the curvature of the vertebral column as well as the morphology of the vertebrae, would have functioned in the animal's life, by indicating limb movements and stride. Postcranial material of *Endothiodon* is relatively rare in Karoo vertebrate collections, and hence there has been rather limited research on their functional morphology and locomotion. This might be due to the manner in which therapsid material was excavated in the late 18th and early 19th century, when most of the *Endothiodon* material was first found and described (pers. comm., W. J. de Klerk, 2017); whereby preference was given for the collection of cranial material rather than postcranial.

Apart from the present study, the only other account of *Endothiodon* postcrania is a description of *E. bathystoma* (SAM-PK-629) by Broom (1905), but unfortunately some of this material is missing from the Iziko Museum collections. Broom (1905) used his description of a partial skull, vertebrae, scapula, humerus, sacrum and femur to produce a tentative reconstruction of *E. bathystoma* (See Appendix, Figure A). However, in recent years, closer inspection of the bones has revealed that most of the bones were fragmented and rebuilt with plaster thus rendering the reconstruction as unreliable. Nevertheless, where applicable, Broom's *E. bathystoma* elements are compared to SAM-PK-K011271.

The proximal end of the humerus of SAM-PK-629 was preserved, and shares the general shape of SAM-PK-K011271 (Figure 20 a). It has a width of 97.86 mm while SAM-PK-K011271 has a width of 124.30 mm on the proximal end. The femur of SAM-PK-629 appears slightly more slender than that of SAM-PK-K011271 in the drawing by Broom (1905) (Figure 20 b), but the missing shaft of SAM-PK-629 has been merely estimated by Broom (1905) and thus, the precise length of the bone is not known. However, the femur of SAM-PK-K011271 is preserved and its length is 229.81 mm (Figure 20 b). The pelvic bones of SAM-PK-K011271 are slightly laterally compressed, and the shape of the acetabulum is distorted. In the description of a partial pelvis by Broom (1905), the acetabulum of SAM-PK-629 was fairly circular (Figure 20 c). SAM-PK-629 seemed to have had a wider iliac neck than that of SAM-PK-K011271. This may be because SAM-PK-K011271 has a more well-developed, fan-shaped iliac blade than SAM-PK-629, and this could be an ontogenetic feature, which is supported by the fact that SAM-PK-629 has a smaller skull length than SAM-PK-K011271 (Table 8).

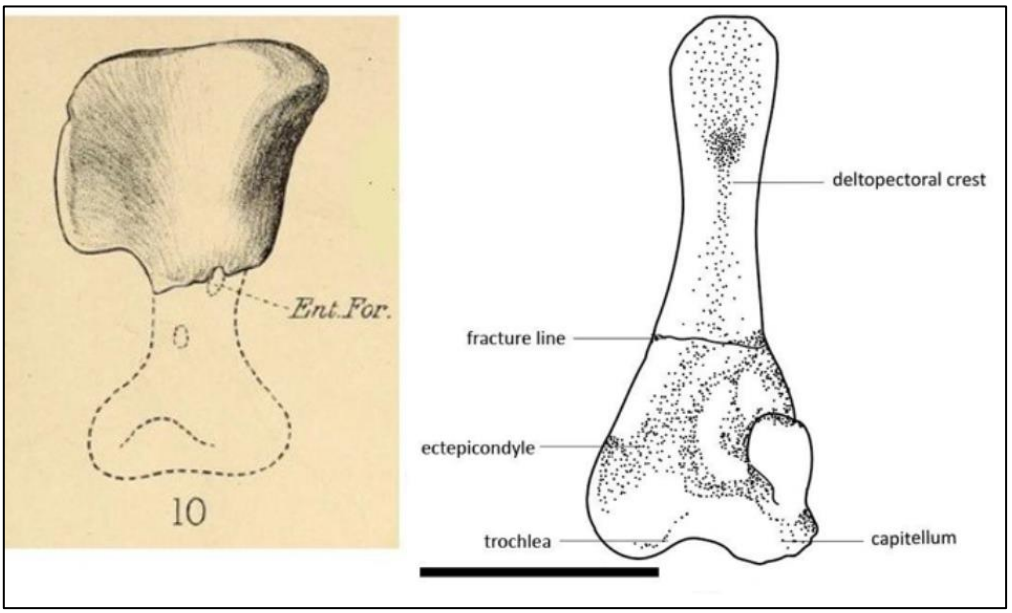

Figure 20. **(a)** LEFT: Right humerus of *E. bathystoma*, SAM-PK-629 in front view. Broken lines indicate areas rebuilt with plaster. Image from Broom (1905). RIGHT: Right humerus of *E. bathystoma*, SAM-PK-K011271 in dorsal view. Scale bar represents 100 mm.

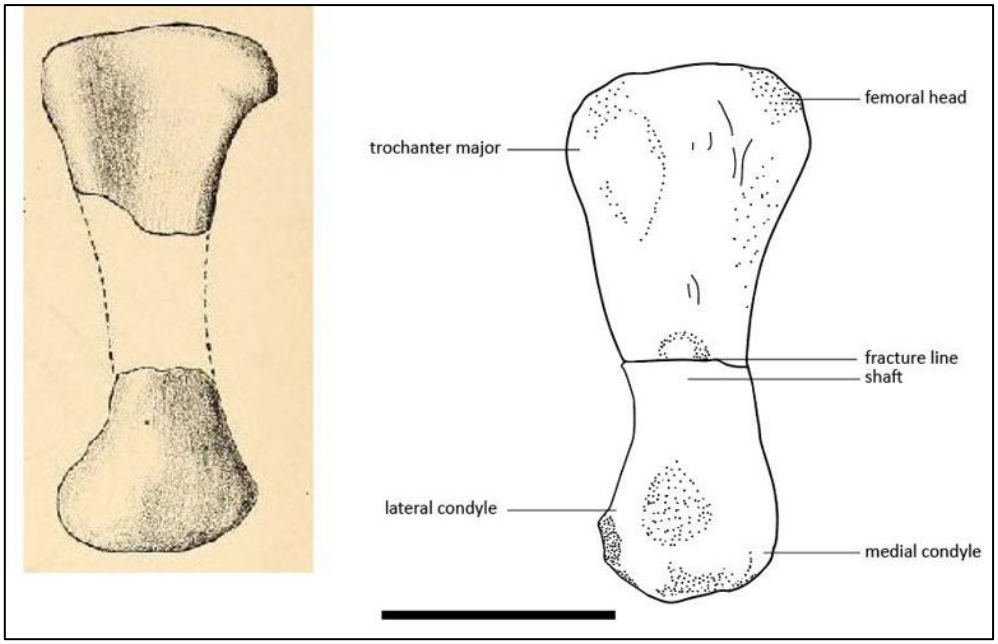

Figure 20. **(b)** LEFT: Right femur of *E. bathystoma*, SAM-PK-629 in front view. Broken lines indicate areas rebuilt with plaster. Image from Broom (1905). RIGHT: Right femur of *E. bathystoma*, SAM-PK-K011271 in dorsal view. Scale bar represents 100 mm.

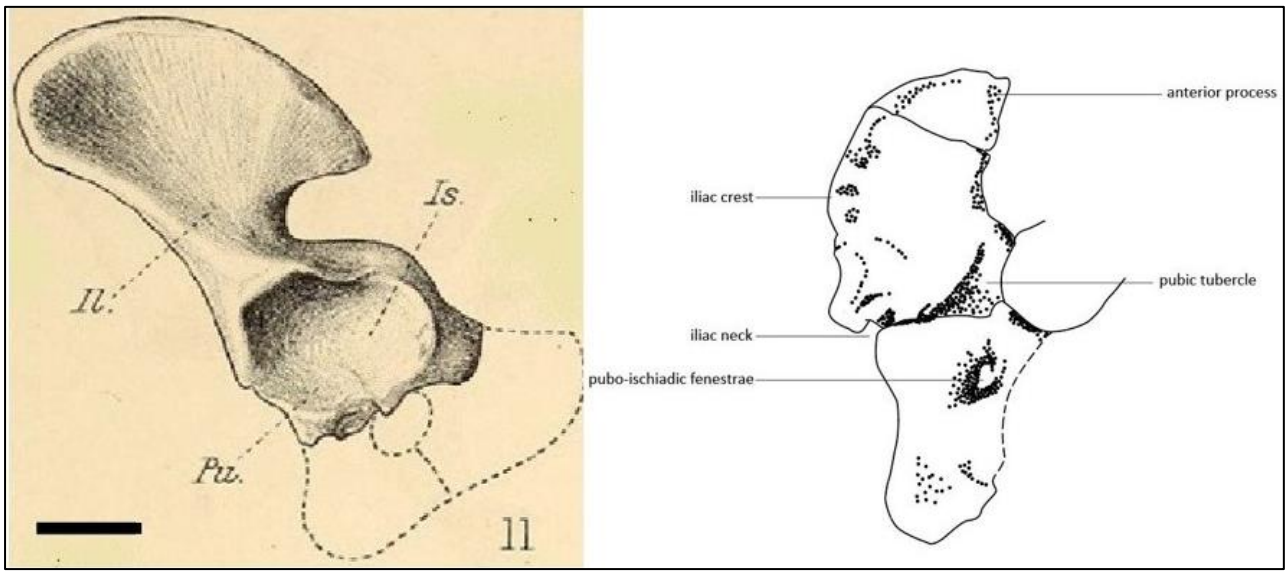

Figure 20. **(c)** LEFT: Pelvis of *E. bathystoma*, SAM-PK-629 in lateral view. Broken lines indicate areas rebuilt with plaster. Image from Broom (1905). RIGHT: Right pelvis of *E. bathystoma*, SAM-PK-K011271 in lateral view. Scale bar represents 100 mm.

4.2 *ENDOTHIODON* MORPHOLOGY

4.2.1 Crania

Upon close inspection of all South African *Endothiodon* skull material, and of the descriptions in published literature (Boos *et al.*, 2013; Cox and Angielczyk, 2015; Ray, 2000), it is clear that SAM-PK-K011271 has the most complete *Endothiodon* skull found to date. The favourable preservation of the skull in articulation with the rest of the axial skeleton showed deformation only on the left and ventral sides, allowing for a comparison with previous descriptions. A comparison of *Endothiodon* species in Ray (2000) notes that the Indian form *E. mahalanobisi* was the only species to have a single medial ridge, while all other species including *E. bathystoma* had three ridges. The angle of inclination from the frontals to the pineal boss is significantly larger than that of *E. mahalanobisi* from India (Ray, 2000) such that the entire pineal crest is very raised in lateral view. In keeping with Ray (2000), the present study shows that SAM-PK-K011271 has three ridges on the snout, and this in addition to the robust skull size and raised pineal boss can therefore be used to confidently assign SAM-PK-K011271 to *E. bathystoma*.

4.2.1.1 Lower jaw and "upturned beak"

Members of Dicynodontia are known to have evolved a keratinous covering of the jaws and a "turtle-like" beak, rather than incisor teeth for feeding (Kemp, 2012). In addition, some species display the presence of maxillary tusks and/or postcanine teeth (e.g., Kemp, 2012; King, 1990). SAM-PK-K011271 lacks tusks but it does have teeth arranged in replacement waves (which could not be examined in this study), and the premaxilla, maxilla and dentary bones display rugose patterns on the surface, suggesting that they were both directly overlain by keratin. Furthermore, SAM-PK-K011271 has a clearly upturned beak-like shape of the anterior part of the dentary, fitting into a notched premaxilla (Figure 21). This notch was also prominent in other complete *E. bathystoma* skulls *viz.* CGP/1/708 and CGP/1/709. Jasinoski and Chinsamy-Turan (2012) described the microstructure of dicynodont crania and reported the presence of Sharpey's fibers in the snout and mandibular regions of *Lystrosaurus* and *Oudenodon*. Sharpey's fibers are associated with soft tissue attachment, and thus indicated the attachment of a keratinous beak in these specimens. In the current study, similarities in terms of the roughness of bone surface of the jaws, as well as the shape of the anterior lower jaw were also noted in many of the other South African *E. bathystoma* specimens, although the extent and thickness of the keratinous beak in life is uncertain.

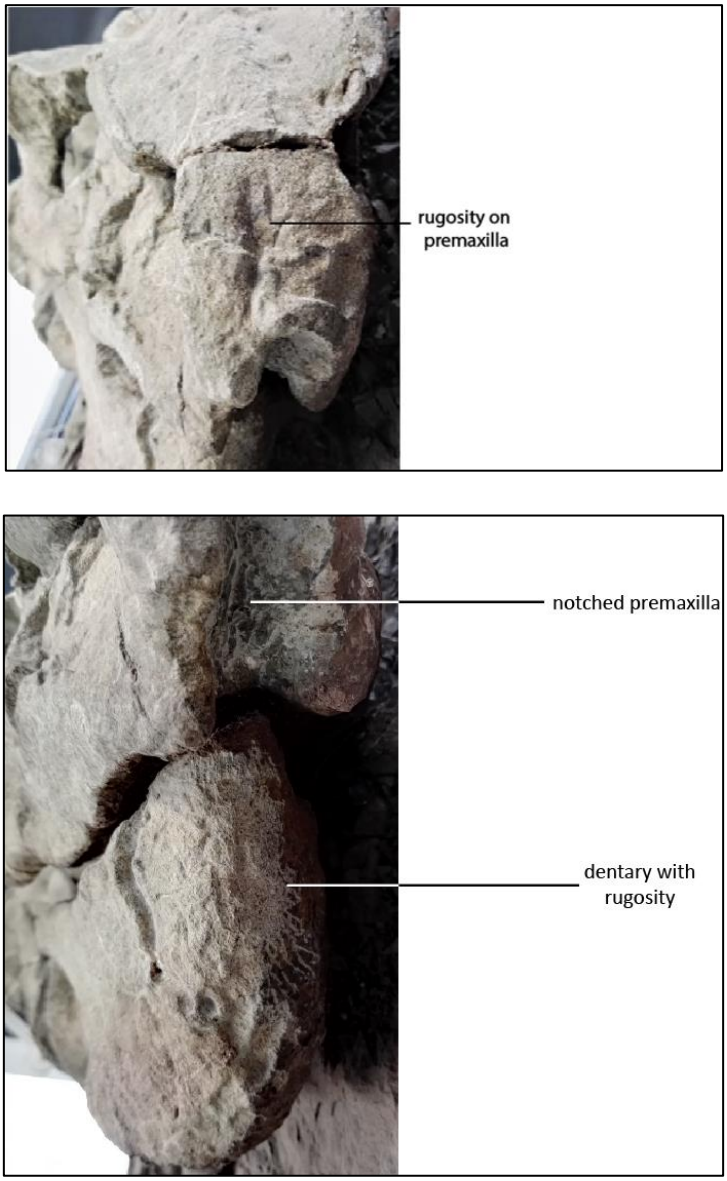

Figure 21. Photographs of anterior views of the *E. bathystoma* skull, SAM-PK-K011271 showing rugosity on the bone surface of the (TOP) premaxilla and (BOTTOM) dentary.

4.2.1.2 Pineal boss and foramen

The variation in the descriptions of pineal bosses in various *Endothiodon* specimens provides an interesting perspective on the differentiation of the different species within the genus. In the Indian species, *E. mahalanobisi*, the pineal boss is very low, and contains a sagittally elongated pineal

foramen (Ray, 2000). In the Tanzanian species, *E. tolani*, the pineal boss is absent, and instead there is only a thin, raised collar of bone within which an elliptical foramen lies (Cox and Angielczyk, 2015). However, prominently bulbous or raised pineal bosses have been reported in many descriptions of *E. bathystoma*, including those previously named *E. uniseries* and *E. whaitsi* (Boos *et al*., 2013; Cox and Angielczyk, 2015; Ray, 2000). Furthermore, in the current study, pineal bosses were seen in a few complete South African *Endothiodon* skulls: Specimen CGP/1/709 displayed a raised boss with a length of 33.04 mm, containing a pineal foramen 14.44 mm wide and 19.10 mm long. CGP/1/708 has a pineal boss 62.04 mm long and 50.09 mm wide; while the boss of CGP/1/689 is 43.77 mm long, containing a pineal foramen 17.04 mm long and 15.54 mm wide. Boos *et al*. (2013) also reported a prominent boss in a Brazilian *Endothiodon* skull that could only be identified to genus level. However, the description of the type specimen of *E. bathystoma* by Owen (1876) did not mention the presence or absence of any such pineal boss, and it was not seen in the drawings of the skull, because that part of the skull was not preserved. The skull of *E. bathystoma* (SAM-PK-629) first described by Broom (1905) shows that no pineal boss was preserved either, and it is likely that it broke off, given the fragmented nature of the bones.

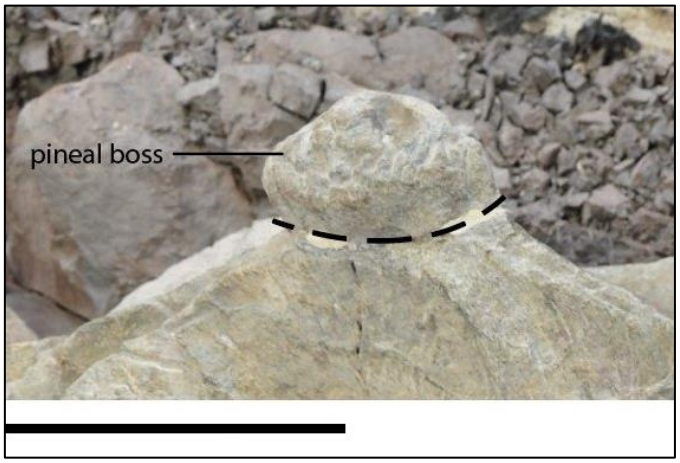

Figure 22. Raised pineal boss of *E. bathystoma*, SAM-PK-K011271. Broken lines indicate where the boss was broken off. Scale bar represents 100 mm.

As mentioned in Chapter 3 (section 3.1.1.2), the pineal boss of SAM-PK-K011271 was found broken off the skull upon discovery, and was re-attached, along with several other skull elements, during preparation (Figure 22). The fact that it was detached raises interesting questions about the pineal boss. The distinct rugosity on the bone surface suggests that the pineal boss provided the attachment for a keratinous structure. This may have been a type of armament or even a sexually dimorphic character in *Endothiodon*. However, considering that the pineal foramen housed a light-sensitive

organ, the keratinous covering would be similar to the shape of the underlying boss rather than being a horn-like structure. The pineal boss of the Brazilian *Endothiodon* skull was broken anteriorly, in the region of the preparietal suture, and an *E. bathystoma* skull previously called *P. stockleyi* also had a broken boss, which was evident by the thickening of bones surrounding its foramen, as well as by the extensive weathering of the skull (Boos *et al*., 2013; Cox and Angielczyk, 2015). These findings pertaining to the boss could explain the lack of bosses preserved in a few skulls of *E. bathystoma* that should have been there originally. Nevertheless, it is clear that *E. bathystoma* skulls would have had bulbous, high bosses, in contrast to *E. mahalanobisi* which has a low boss, and *E. tolani* which has no boss at all. This is discussed as a diagnostic feature in section 4.4 of this chapter.

Sullivan *et al*. (2002) proposed that the function of the pineal boss in the smaller dicynodont *Diictodon* was a means of protecting the pineal foramen during aggressive intraspecific conflict, such as head-butting. The association between the pineal bosses and tusks in *Diictodon* may have been sexually dimorphic (Sullivan *et al*., 2002), and it is quite possible that the extent of the pineal boss structure in *E. bathystoma*, may have had a similar role.

4.2.2 Postcrania

4.2.2.1 Pectoral girdle and forelimb

The Kannemeyeriid *Wadiasaurus* is considered to be a heavily-built dicynodont and is thought to have kept its body raised off the ground. This is deduced from the length of the scapular blade which has a large enough area for the origin of the deltoid muscle, M. deltoideus, permitting the elevation of the proximal humerus (Ray, 2006). A wider scapular blade in *Lystrosaurus* suggested a more humerus-dominated style of digging, similar to that of *Diictodon* (Ray and Chinsamy, 2003; Ray, 2006). Since both *Endothiodon* scapulae in SAM-PK-K011271 are visible to some extent, it is possible to locate muscle attachment and humeral articulation sites. The long, gently curved scapula of *Endothiodon* has a large area of rugosity on its medial side from the dorsal edge to the centre of the blade, likely for M. deltoideus insertion, which suggests that *Endothiodon* may also have elevated its body well above the ground (Figure 23).

A few rib heads fused to the ventral part of the left scapula suggest that the scapular angle relative to the horizontal axis was preserved as it was in life. The rugose surface of the distal right scapula and proximal humerus suggest that cartilage was present at the articulation of these two elements in life. The rugosity on the surface of the humeral head of *Endothiodon* would have been the site for articulating cartilage (Govender and Yates, 2009). This could also indicate that the humerus was not

completely developed and that the individual was still growing at the time of death. This is further supported by the fact that the present study found the *Endothiodon* skull SAM-PK-K011271 to be 96% the size of the largest known South African *Endothiodon* skull, suggesting that this was still a growing individual.

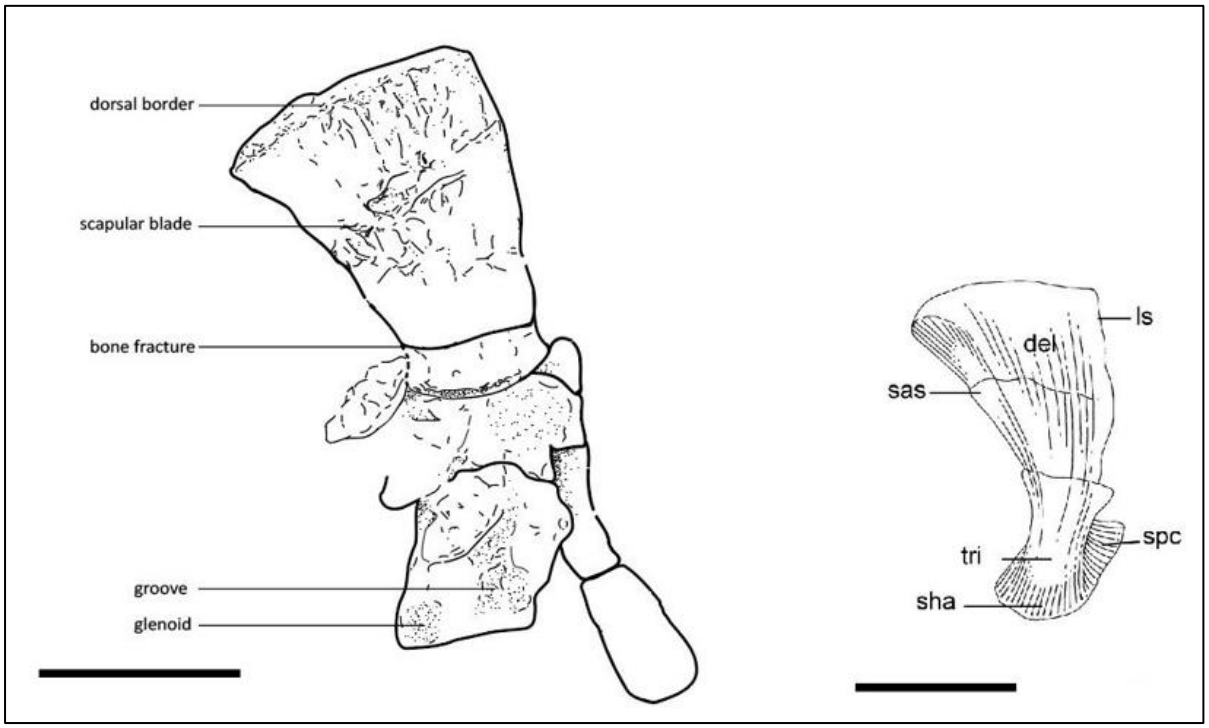

Figure 23. LEFT: Left scapula of *E. bathystoma*, SAM-PK-K011271 in medial view. RIGHT: Right scapula of *L. murrayi*, SAM-PK-K8 in lateral view with muscle insertion areas. Image from Ray (2006). Scale bars represent 100 mm.

The robustness of the *Endothiodon* humerus can be compared to other dicynodonts having varying lifestyles. Among the smaller dicynodonts, *Pristerodon* has an abducted humerus that is orientated more laterally than in *Diictodon*, whose humerus articulates almost horizontally (Ray and Chinsamy, 2003; Ray, 2006). Another fossorial dicynodont, *Cistecephalus* displays a robust humerus, having proximal and distal ends as wide as the length of the humerus itself, as well as a strong olecranon and a long radius that nearly matches the humerus in length (Cluver, 1978; Nasterlack *et al*, 2012). In the larger-bodied dicynodonts *Lystrosaurus* and *Wadiasaurus*, an area of concavity on the ventral surface of the proximal humeral end is suggested to facilitate the humerus rolling over the coracoid region of the glenoid fossa, similar to a movement displayed in the forelimb of the cynodont, *Luangwa* (Ray, 2006). *Dicynodon* also had an abducted forelimb, which allowed protraction-retraction and humeral rotation, which supported its posture and movement (King, 1981).

Wadiasaurus may have had stronger flexors and extensors than *Lystrosaurus*, as suggested by a well-developed entepicondyle and ectepicondyle which provide large muscle origin and insertion sites (Ray, 2006). The combined swimming and digging lifestyle of *Lystrosaurus* is further explained by a "paddle-like" distal forelimb. This consists of a radius and ulna that expand lateromedially, as well as a broad, robust manus (Ray, 2006). The humerus of *Endothiodon* is not as wide at its proximal and distal ends as the smaller fossorial *Diictodon*, but has a well-defined entepicondyle and ectepicondyle, suggesting that flexor and extensor sites were also large, as in *Wadiasaurus*.

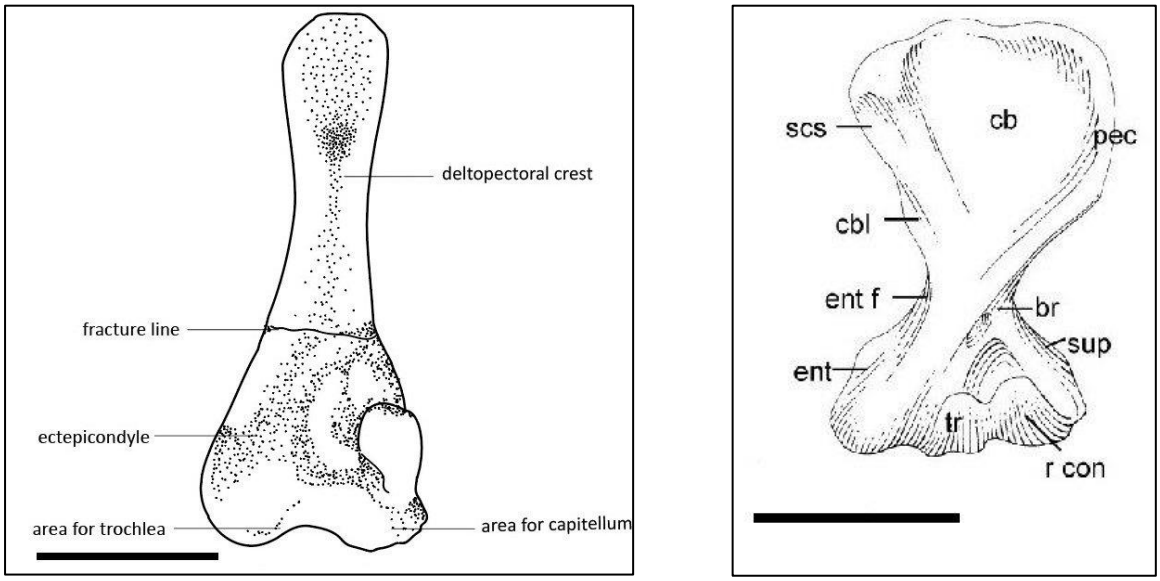

Figure 24. LEFT: Right humerus of *E. bathystoma*, SAM-PK-K011271 in ventral view. RIGHT: Left humerus of *Wadiasaurus indicus*, ISIR175/16 in ventral view. Image from Ray (2006). Scale bar represents 100 mm.

Although the manus of *Endothiodon* is not completely preserved, the elongated nature of the digits suggests that the manus was not as broad and robust as the metacarpals of *Lystrosaurus* (Ray, 2006). As in most anomodonts, *Endothiodon* has the phalangeal formula 2-3-3-3-3 (Angielczyk and Rubidge, 2013; Ray, 2006). The terminal phalanges of *Endothiodon* are blunt and broad as in *Wadiasaurus*. Bandyopadhyay (1988) suggested the presence of keratinous claws on the rounded, short terminal manual phalanges of *Wadiasaurus*, which is likely the case in SAM-PK-K011271.

4.2.2.2 Vertebral column and ribs

A study by Ray and Chinsamy (2003) of the postcranial elements of the digging dicynodont *Diictodon* makes note of the differences in cervical vertebrae between *Diictodon* and *Kingoria*. It is noted that high caudally-oriented neural spines in cervical vertebrae create a large area for neck muscle attachment. A similar conclusion was determined from observation of the long neural spines of *Wadiasaurus* (Ray, 2006), and the attachment of these muscles assists in the elevation, support and movement of a large head.

Dicynodonts such as *Pristerodon* and *Robertia* used lateral undulating of the vertebral column for locomotion (Ray, 2006). The pre- and postzygapophyses of *Diictodon* have high angles relative to the horizontal axis, but this implied a restriction in lateral movement (Ray and Chinsamy, 2003). This was also noted in the vertebrae towards the sacrum of *Wadiasaurus*, implying constrained lateral undulation in this region (Ray, 2006). The vertebrae of *Cistecephalus* also display zygapophyses with high angles, but this is throughout the vertebral column and indicates a great reduction in lateral undulation, with the possibility of dorsoventral flexion and axial rotation instead (Ray, 2006). Lateral undulation is also reduced in *Dicynodon*, instead the animal had long axis rotation in the proximal limbs (King, 1981; Ray, 2006). In a functional morphology study of *Wadiasaurus* and *Lystrosaurus*, Ray (2006) attributed lateral undulation in *Lystrosaurus* to the wide, flat zygapophyses in the presacral vertebrae, differing from the digging *Diictodon*.

Table 9. Comparison of vertebral count of among various dicynodonts, including *E. bathystoma*, SAM-PK-K011271 (highlighted). Displaced vertebra of SAM-PK-K011271 included.

Dicynodont	Total	Presacrals	Cervicals	Dorsals	Sacrals	Caudals	Reference
E. newtoni	47	29	6	23	3	15	Angielczyk and Rubidge (2013)
Diictodon	45	-	6	21	3 or 4	14	Ray and Chinsamy (2003)
Wadiasaurus	-	-	7	18	5 or 6	?	Bandyopadhyay (1988)
Lystrosaurus	41–42	-	6	20	6	10	Ray (2006)
Dinodontosaurus	-	23–24	5	18–19	5	15	Cox (1965)
D. trigonocephalus	45	-	7	20	5	13	King (1981)
E. bathystoma	37	-	5	17	5	10	Current study
Endothiodon	-	28	-	-	-	-	Broom (1905)
Robertia	-	-	-	-	3	-	Angielczyk (2001)
Parakannemeyeria	44	-	-	20	-	-	Sun (1963)
Placerias	45	-	-	-	-	-	Camp and Welles (1956)
Dicynodontoides	-	-	-	21	-	-	Cox (1959)
Pristerodon	-	-	-	24	-	-	Sushkin (1926)
D. amalitzkii	-	-	-	24	-	-	Watson (1960)
Cistecephalus	-	-	-	25	-	-	Cluver (1978)

Close inspection of an isolated dorsal vertebra of *Endothiodon* indicates the height of the neural spines and zygapophyses of the rest of the dorsal vertebrae in the series, even though no two vertebrae will be identical. The dorsal vertebra has a slender neural spine with an apex that is bulbous and rugose in texture, indicating a site for muscle attachment. In *Endothiodon*, the shorter neural spines of the caudal vertebrae may be attributed to the spines having a caudal slope, as in *Wadiasaurus*, which also suggests an abrupt downturning of the tail. In *Wadiasaurus*, this downturning is allowed by the mid-caudal centra being caudoventrally inclined, with the neural spines having a caudal slope; the dorsal edge of the iliac blade and the 45° angle of its caudal end to the horizontal; as well as the orientation of the sacral rib facets. There is also a decrease in centra length caudally.

This could also be further evidenced by the preserved curl of the caudal end of SAM-PK-K011271. The postzygapophyses become slightly flatter towards dorsal series. It is not certain whether this indicates any lateral undulation in the caudal half of the skeleton, since flat zygapophyses in only the presacral vertebrae of *Lystrosaurus* suggest lateral undulation (Ray, 2006). A break in the natural curve of the dorsal vertebrae series with more caudally tilted neural spines and zygapophyses could suggest limited lateral flexibility of the spine in this area, as seen in the small dicynodont *Eosimops* (Angielczyk and Rubidge, 2013). The vertebral centra of *Endothiodon* are amphicoelous, which is a typical feature in dicynodonts (Bandyopadhyay, 1988). Table 9 depicts the number of vertebrae known among dicynodonts.

Apart from breakage in some of the ribs of the *Endothiodon* specimen SAM-PK-K011271, the angle at which they are preserved appears fairly undistorted. The heavy curvature of the proximal rib heads articulating to the vertebral column, and the relatively straighter distal ends indicate that the outward curves of the ribs would have formed a rather barrel-shaped body. This is also suggested in other large dicynodonts such as *Lystrosaurus* and *Wadiasaurus* (Ray, 2006). The thick distal ends of the dorsal ribs may indicate a cartilaginous attachment to the sternum, as seen in *Wadiasaurus* ribs (Bandyopadhyay, 1988). The distal ends of the ribs differ from those of *Eosimops newtoni* which displayed a strong medial curvature, likely for attachment to the sternum (Angielczyk and Rubidge, 2013). However, unlike in *Wadiasaurus*, the proximal ends of the *Endothiodon* ribs do not arch upwards, which could suggest that the spine of *Endothiodon* may have been straighter with less dorso-ventral curvature than *Wadiasaurus*.

The three isolated rib fragments seen near the skull of SAM-PK-K011271 are described in Chapter 3 (Section 3.1.2.5 a), and bring forward the question of whether they came from the *E. bathystoma* individual SAM-PK-K011271 or not. The bone surface of these rib fragments has the same colour and texture of the articulated ribs of SAM-PK-K011271. Although it is not possible to tell which parts of the fragments are proximal, middle or distal, the width measurements taken fall in the range of the ribs of SAM-PK-K011271 (Table 7). The rib head of the second fragment is very similar in shape to the rib heads that articulate with the vertebral column of SAM-PK-K011271. Furthermore, the position of the fragments on the rock base are near the skull and in close proximity to three displaced cervical vertebrae. Therefore, it is likely that these rib fragments belong to the *E. bathystoma* individual SAM-PK-K011271 and were broken off and displaced. It is also possible that these fragments were part of the cervical ribs, based on their position.

4.2.2.3 Pelvic girdle and hindlimb

In most dicynodonts, the acetabulum is circular, but the compression in this area of the *Endothiodon* skeleton makes this difficult to confirm. There is a significant amount of rugosity on the femoral head and the acetabular region of the pelvis. The broad fan-shaped ilium has longitudinal striations towards the dorsal border, which are an indication of strong muscle attachments. The fan-shaped blade is common in all dicynodonts except *Eodicynodon* which is rectangular, and the narrowing of the iliac blade toward the acetabulum is very similar to that of the large Permian dicynodont *Aulacephalodon* (Govender, 2008). A description of *Eosimops* discusses the possibility of contact between the left and right side of the pelvis in dicynodonts and suggests that *Eosimops* would have had a small gap between left and right puboischiaic plates along the ventral midline (Angielczyk and Rubidge, 2013). The pelvic blades of the studied *Endothiodon* specimen have fallen apart which makes this hypothesis

difficult to test, unless the pelvic elements were lifted and separated to expose the ventral elements (this was not permissible in this study).

The articulation of the femur and acetabulum in the smaller dicynodonts *Diictodon* and *Pristerodon* allow for a hindlimb gait that is said to be similar to the semi-erect gait of crocodilians (Ray and Chinsamy, 2003; Ray, 2006). In *Kingoria*, the ischium extends caudoventrally and its acetabular-femoral articulation indicates adduction of the hindlimb, turning the femur towards its body, which allowed retraction by femoral head rotation. In the dicynodont *Dicynodon*, the hindlimb was semi-erect during its stride, causing a slower movement (King, 1981). The acetabulum of *Lystrosaurus* and *Wadiasaurus* shows that the femur could rotate medially on its longitudinal axis in order for the head to lay in the acetabulum (Ray, 2006). Since the limb bones are still partially embedded in the rock matrix, it cannot be determined if the hindlimb of *Endothiodon* was adducted toward the body as in *Kingoria*.

A comparison of hindlimb and forelimb length was made for SAM-PK-K011271. On the right-hand side, the length from the proximal head of the femur to the distal edge of the tibia is 381.43 mm, while the length from the proximal humeral head to the distal edge of the ulna is 402.89 mm (both are a sum of lengths of the individual elements). Thus, the forelimb of *Endothiodon* is slightly longer than the hindlimb. In addition to this, the large areas for muscle attachment on the forelimb suggest that there may have been greater stability for the anterior body, as is in *Dicynodon* (King, 1981). The naturally lower position of the posterior body could indicate that the hindlimb was not as elevated as the forelimb, and *Endothiodon* could have displayed the same powerful, slow stride as seen in *Dicynodon*.

The pes in *Endothiodon* and many dicynodonts is usually slightly smaller than the manus, as shown in *Wadiasaurus*, *Lystrosaurus* and *Diictodon* (Ray and Chinsamy, 2003; Ray, 2006), and also has a phalangeal formula of 2-3-3-3-3. The terminal pedal phalanges appear more elongated and claw-shaped than those of the manus. However, the round, down-turned edges of terminal phalanges could suggest the presence of claws as seen in *Wadiasaurus* (Bandyopadhyay, 1988), and therefore the manus of *Endothiodon* may have had claws as well. Spatulate claws have been suggested to assist the digging action of *Diictodon* (Ray, 2006).

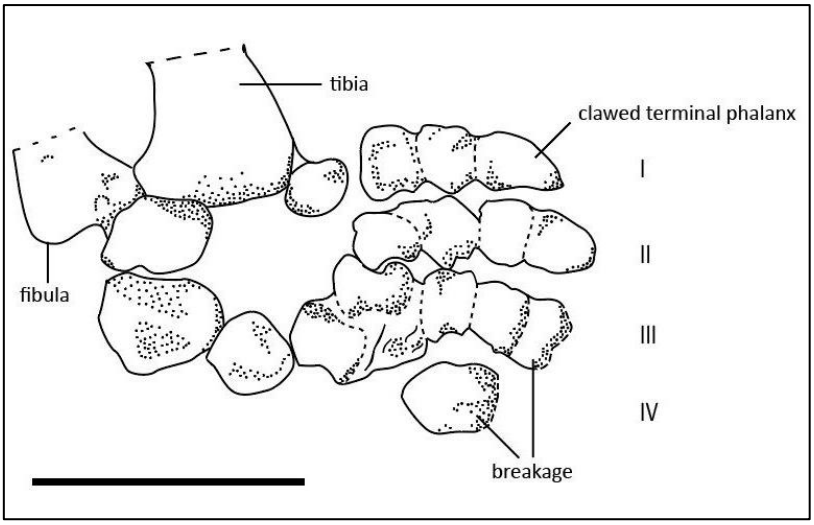

Figure 25. Right pes of *E. bathystoma*, SAM-PK-K011271 in dorsal view showing the claw-shaped terminal phalanx of digit I. I–IV indicate digits. Scale bar represents 100 mm.

4.2.2.4 General posture, locomotion and lifestyle

The following discussion highlights suggested lifestyles inferred from various dicynodont postcrania, and attempts to speculate about the type of posture and lifestyle *Endothiodon* may have had in life:

The smaller dicynodonts, particularly those adapted for digging lifestyles such as *Diictodon* and *Cistecephalus* had forelimbs that facilitated a rotation-thrust digging method using humeral excursion. Limbs of *Diictodon* were short with a long manus and for digging, and the pes had short, blunt claws for soil removal (Ray, 2006). *Cistecephalus* displayed postural dichotomy whereby the humerus was abducted and in a lateral position, while the femur was adducted, causing the knee to be nearer to the body (Cluver, 1978; Ray, 2006).

The heavy-bodied *Wadiasaurus* was a generalized terrestrial herbivore and is known to have had a semi-sprawling gait. It most likely exhibited herding behaviour as shown in a taphonomical analysis of the postcranial remains of several individuals found together (Bandyopadhyay, 1988). Similarities exist in the skeletal structure of *Wadiasaurus* and *Lystrosaurus*, such as scapular blade angle and rib curvature which indicate the barrel-like body shape of these two genera (Ray, 2006). However, essential differences in the scapula, forelimb and hindlimb of *Lystrosaurus*, as well as the presence of articulated skeletons in preserved burrows, suggest both semi-aquatic and digging lifestyles (Botha-Brink, 2017; Ray, 2006). These differences are noted by Ray (2006) as a “paddle-like” distal forelimb, a broad scapular blade and muscle insertion sites that imply the closeness of the hindlimb to its body. The semi-aquatic habit is further evidenced by bone microstructure studies showing thick

dorsal rib cortices and trabecular infilling of the medullary region (Ray, 2006). The distal forelimb of *Endothiodon* has a morphology more similar to that of *Wadiasaurus* than *Lystrosaurus*, with a more slender ulna and radius; as well as a thinner, longer scapular blade. The anatomy of *E. bathystoma* suggests that it was also a large, barrel-bodied, slow moving terrestrial herbivore, with the forelimbs being longer and thus holding the fore part of the body higher. Although there is no evidence for fossoriality, the similarity of the manus and pes to other known fossorial dicynodont taxa suggest that it may have had the ability to dig or remove soil.

4.3 ONTOGENETIC STATUS OF SAM-PK-K011271

Collection visits to South African museums showed that although *Endothiodon* postcrania were occasionally represented, they were often fragmented and incomplete, thus rendering them ineffective for comparisons with SAM-PK-K011271; nor did they allow for a full ontogenetic study of the skeletal *Endothiodon* elements. As mentioned previously, the lack of more complete postcranial *Endothiodon* material (compared to skull material) may be due to excavation methods used in the past. Thus, only when more complete *Endothiodon* skeletons are recovered will a more comprehensive ontogenetic assessment be possible. Nevertheless, given the current the limitations outlined above the current study used other *Endothiodon* crania to deduce the ontogenetic context of SAM-PK-K011271.

It should however be noted that skull size is not the only factor that dictates the ontogenetic status of an animal. Ray (2000) argued against the notion that *E. mahalanobisi* skulls were small because they were juveniles, by noting the presence of well-developed dentition and sutures between bones, which suggested that they were mature individuals. The current study suggests that South African *Endothiodon* specimens are considered to all represent *E. bathystoma* but cautions that the substantial deformation and compression of the studied skulls should be considered when assessing skull size.

Comparisons were made between SAM-PK-K011271 and six reasonably well-preserved *E. bathystoma* skulls in the collections. It was determined that the largest *E. bathystoma* skull in the collections was CGP/1/708 and that SAM-PK-K011271 was about 96% of its size, and therefore the second largest *E. bathystoma* skull known among the South African specimens. The smallest specimen SAM-PK-2676 has a skull length about 51% of that of SAM-PK-K011271 (and about 49% of the largest skull in the collections).

Specimen CGP/1/709 is only the fourth largest skull in the collection, but is the smallest, most complete skull with features comparable to the other skulls in the collections. It is about 88% the size of SAM-PK-K011271 and about 84% the size of the largest skull. Despite not being as well-preserved, CGP/1/709 clearly has a different bone surface texture over the dentary and snout up to the pineal boss to SAM-PK-K011271, having a far smoother and less rugose texture. The anterior tip of the dentary and premaxilla is slightly rugose but not nearly as much as SAM-PK-K011271. Since rugosity in this area indicates attachment of a keratinous beak-like structure, a smoother bone surface in this specimen could indicate that the attachment was still forming and that the individual was not a fully-grown adult. The dentary itself, however, seems already quite robust, having a height of 69.22 mm, a width of 34.98 mm and a length of 158.37 mm, and the pointedness of its anterior “up-turned beak” is as prominent as in SAM-PK-K011271. Finally, a pineal boss is present on CGP/1/709 surrounding a circular foramen, but is not as raised as SAM-PK-K011271, nor is it rugose. The lack

of rugosity on the pineal boss could also indicate the keratinous structure and its attachment is still in the process of being formed in this younger individual.

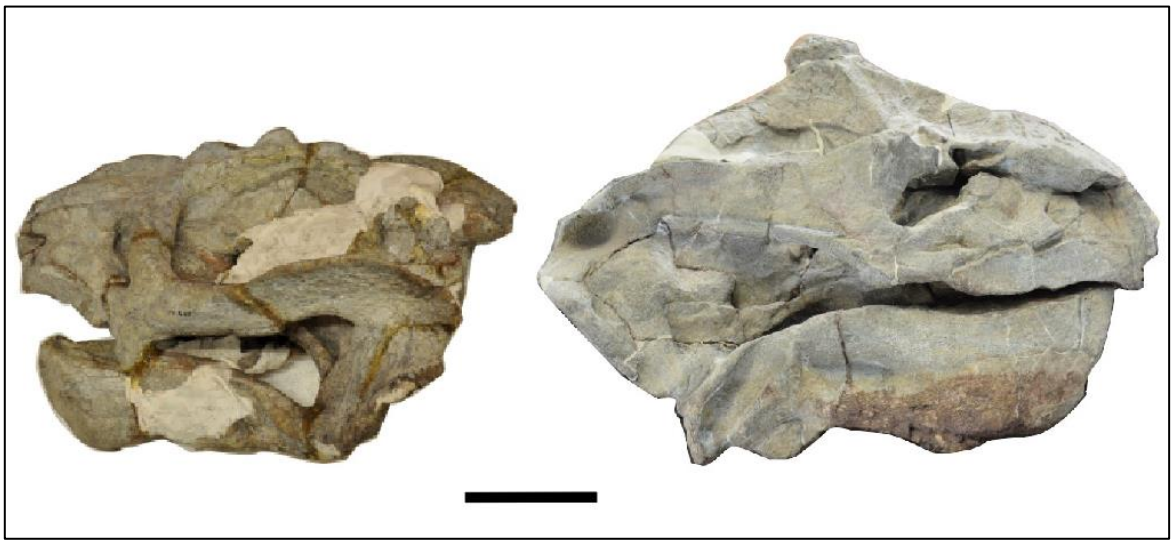

Figure 26. Skulls of *E. bathystoma*, CGP/1/709 (LEFT) and SAM-PK-K011271 (RIGHT) in left and right lateral views, respectively. Scale bar represents 100 mm.

4.4 *ENDOTHIODON* TAXONOMY

4.4.1 Diagnostic features among *Endothiodon* species

E. tolani from Tanzania (Figure 29) has two main species-defining charachters: small caniniform tusks and a thin collar of bone surrounding the pineal foramen (Cox and Angielczyk, 2015). It is interesting to note that *E. tolani* has both tusks and tooth rows on the upper jaw, since tusks are not present in any other *Endothiodon* species. Cox and Angielczyk (2015) state that phylogenetically, *E. tolani* is basal for the presence of tusks and pineal boss morphology, and suggests that *E. mahalanobisi* and *E. bathystoma* could have lost their tusks and increased the development of boss-like bone around the pineal foramen.

E. tolani can be clearly distinguished from *E. bathystoma* and *E. mahalanobisi*, but there has been debate about the differences between *E. bathystoma* and *E. mahalanobisi*. Ray (2000) suggested that although *E. mahalanobisi* is a smaller form (Figure 28), the highly interdigitated skull sutures and well-developed teeth show that it may not be a juvenile. However, Botha-Brink and Angielczyk (2010) note similarities in bone histology between subadult *E. bathystoma* specimens and *E. mahalanobisi*. A comparison of *Endothiodon* species in Ray (2000) notes that the Indian form *E. mahalanobisi* was the only species to have a single medial ridge, while all other species including *E. bathystoma* has three ridges (Cox, 1964; Ray, 2000). The current study notes the presence of three longitudinal ridges in *E. bathystoma*, SAM-PK-K011271 (Figure 27), although the slight compression of the skull has caused them to appear less distinct than the prominent, single ridge in *E. mahalanobisi*. However, the South African *E. bathystoma* skull CGP/1/709 has three very distinct ridges on its snout, and it is accepted that three longitudinal ridges are a suitable diagnostic feature to further distinguish *E. bathystoma* from *E. mahalanobisi*.

The angle of inclination from the frontals to the pineal boss in *E. bathystoma*, SAM-PK-K011271 is significantly larger than that of *E. mahalanobisi* from India (Ray, 2000) such that the entire pineal crest is highly raised in lateral view. The current study considers a robust pineal boss to be another diagnostic feature of *E. bathystoma*, as supported by (Ray, 2000). This is because *E. mahalanobisi* has a very low boss surrounding an elliptical foramen, and *E. tolani* only has a thin collar of bone surrounding the pineal foramen (Cox and Angielczyk, 2015; Ray, 2000) as explained in section 4.2.1.2 of this chapter.

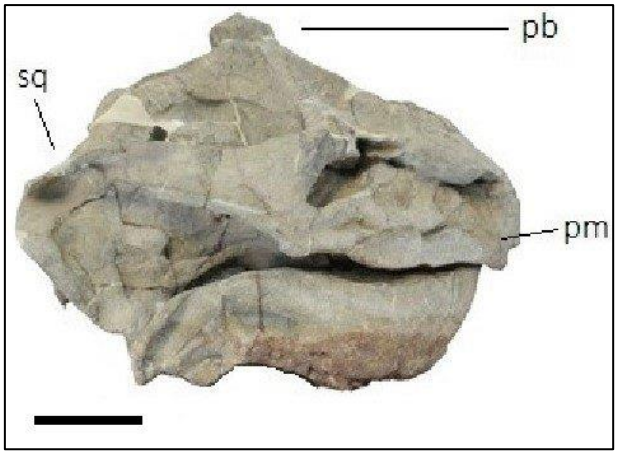

Figure 27. *E. bathystoma* skull SAM-PK-K011271 in right lateral view. Scale bar represents 100 mm.

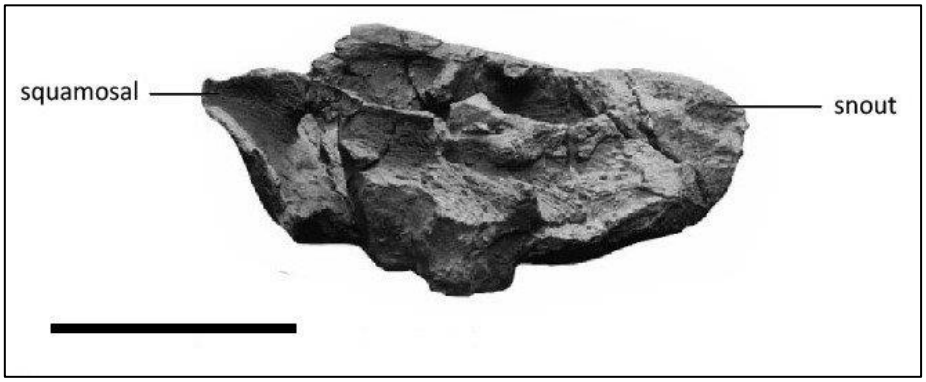

Figure 28. *E. mahalanobisi* skull ISI R201 in lateral view. Image from Ray (2000). Scale bar represents 100 mm.

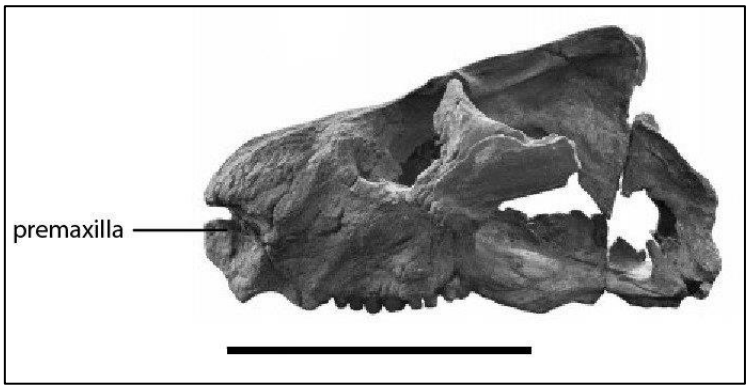

Figure 29. *E. tolani* skull NHMUK PV R12443 in lateral view. Image from Cox and Angielczyk (2015). Scale bar represents 100 mm.

4.4.2 Currently accepted *Endothiodon* taxonomy

An overview of *Endothiodon* taxonomy was outlined in Chapter 1, where it was noted that *Endothiodon* was categorized as only one of four genera belonging to the Endothiodontidae (Lydekker, 1890). A review paper on the validity of therapsid holotypes described by Robert Broom was written by Wyllie (2003). He reported that only 57% of all Broom's holotypes stood the test of time and remained valid. With regard to the taxonomy of *Endothiodon*, Wyllie (2003) noted that the holotypes *Prodicynodon pearstonensis* (1904) and *P. beaufortensis* (1912) were reassigned to *Endothiodon sp*. (King 1988). *Esoterodon whaitsi* (1904) was reassigned to *Endothiodon* (Owen) by Cox (1964). *Emydochampsa platyceps* (1912) was reassigned to *E. uniseries* (King 1988), as was *Endothiodon seeleyi* (1915), *Esoterodon paucidens* (1915), *Esoterodon augusticeps* (1915) and *Endogomphodon minor* (1921). *Endogomphodon crassus* (1932) was reassigned to *E. whaitsi*. Cox (1964) stated that *Endothiodon* was the only valid genus containing *E. bathystoma*, *E. uniseries* and *E. whaitsi*. This review was accepted until Cox and Angielczyk (2015) synonymised *E. uniseries* and *E. whaitsi* with *E. bathystoma*, and noted the addition of *E. mahalanobisi* from India and *E. tolani* from Tanzania to the genus *Endothiodon*. Cox and Angielczyk (2015) stated that this was however tentative, and called for a more thorough review of taxonomy.

Boos *et al*. (2013) cautioned against using the robustness of a dentary symphysis as a taxonomic feature, which was previously used by Ray (2000), because it could vary throughout the animal's ontogeny. The current study agrees with this, as there was significant variation in the robustness of the different dentary fragments studied in the South African collections. Upon closer inspection of South African *Endothiodon* specimens, it can be stated that at this very early point in the taxonomic investigation, all South African specimens are *E. bathystoma* and there are no significant morphological differences among the specimens to indicate otherwise. This supports the reassignment of many South African skulls as *E. bathystoma* by Christian Kammerer (pers. comm., C. Kammerer, 2016). Furthermore, the current study accepts that the three species *E. bathystoma*, *E. mahalanobisi* and *E. tolani* are significantly distinct enough from each other, but concurs with Cox and Angielczyk (2015) regarding the need for a more in-depth investigation in order to confirm this.

CHAPTER 5

CONCLUSION

5.1 OUTCOMES OF THE CURRENT STUDY

5.1.1 Hypotheses

The findings of the current study support the first hypothesis that the *Endothiodon* specimen SAM-PK-K011271 is *E. bathystoma*. This is known from studying the cranial anatomy of SAM-PK-K011271, as well as noting its size relative to that of all other South African *Endothiodon* specimens known thus far. The large skull size, the three longitudinal grooves on the snout and the robustness of the pineal boss are the species-defining features of *E. bathystoma*.

The second hypothesis, which states that SAM-PK-K011271 is the largest known individual, is rejected, since on the basis of skull length SAM-PK-K011271 was found to be the second largest known individual among all South African *Endothiodon* specimens. The postcrania cannot be compared in an ontogenetic perspective until other well represented *E. bathystoma* skeletons are found in the future. SAM-PK-K011271 is the most well-preserved skull of *E. bathystoma* in South Africa, and the most complete skeleton of any known *Endothiodon* individual.

5.1.2 *E. bathystoma* anatomy

The current study provides the most up to date description of postcrania of *E. bathystoma* since the early study by Broom (1905). The completeness of SAM-PK-K011271 in articulation along with the current description of the skeleton makes this specimen an ideal reference skeleton for *E. bathystoma*.

The anatomy of SAM-PK-K011271 suggests that it may have been a large, slow-moving, barrel-bodied herbivore. Its forelimb may have allowed an elevation of its body above the ground. *E. bathystoma* has a phalangeal formula of 2-3-3-3-3 and there is evidence to indicate that the pes was clawed. The spine of *E. bathystoma* may not have arched as much as that of the large dicynodont, *Wadiasaurus*, and it may have displayed an abrupt down-turning of its tail. Although *E. bathystoma* shows no signs of fossoriality, it may have been able to dig and remove soil.

5.1.3 Ontogenetic context

SAM-PK-K011271 has the second largest skull of *E. bathystoma* known in South Africa, and is approximately 96% the size of the largest skull, CGP/1/708. Comparisons with other *E. bathystoma* skulls show certain cranial features (such as rugosity on the pineal boss) indicate that there are younger individuals in the collections, such as specimen CGP/1/709.

5.1.4 Taxonomy

The current study agrees that the previously described species *E. uniseries* and *E. whaitsi* are in fact both *E. bathystoma*. It also tentatively accepts that only three species of *Endothiodon* are known, *viz*., *E. bathystoma* (South Africa), *E. mahalanobisi* (India) and *E. tolani* (Tanzania). They each have the following autapomorphies: *E. bathystoma* has a large skull size, three longitudinal grooves on the snout and a robust, raised pineal boss; *E. mahalanobisi* has a small skull size, one longitudinal groove on the snout and a very low pineal boss; and *E. tolani* has small caniniform tusks and a pineal foramen surrounded by a thin collar of bone. The current study emphasises the need for a more thorough taxonomic review of *Endothiodon* in the future.

5.2 FUTURE INSIGHTS

This study provides the most complete skeletal description of *E. bathystoma*, and although it finally sheds light on the previously unknown postcranial skeleton of this animal, there are still many gaps in our knowledge of *Endothiodon* taxonomy, palaeobiology as well as posture and locomotion. A detailed taxonomic study needs to be carried out to determine if the genus *Endothiodon* does indeed consist of only *E. bathystoma*, *E. mahalanobisi* and *E. tolani*. A thorough comparative investigation of *E. mahalanobisi* and *E. bathystoma* needs to be undertaken to determine whether it is a juvenile of *E. bathystoma*, or a separate species. This can be done by comparing the cranial anatomy of SAM-PK-K011271 with specimens of *E. mahalanobisi* and other South African *E. bathystoma* specimens, as well as by undertaking comparative histological studies. It will also be interesting to investigate the presence and function of the tusks in *E. tolani*, and to compare its dentition with that of both *E. bathystoma* and *E. mahalanobisi*.

As a reference specimen, SAM-PK-K011271 can be used to infer the type of posture and locomotion *E. bathystoma* might have displayed in life. This can be achieved by a detailed functional morphology analysis of the skeletal elements, estimating musculature and body size in order to produce a reconstruction of the animal. The unusual dentition of *Endothiodon* can be investigated further using micro-CT scanning, isotope analysis and by histological examination. Such analyses will permit a detailed description of the structure and function of *Endothiodon*'s unusual dentition.

It is abundantly clear that SAM-PK-K011271 and comparative studies of other skeletal material in the collections, as well as new specimens that are still to be collected have potential to shed even more light on our understanding of the palaeobiology of the enigmatic *Endothiodon bathystoma*.

APPENDIX

Table A. List of all *Endothiodon* specimens[1] housed in South African collections that were examined for this study. Specimens assigned to *Endothiodon* according to collection catalogues.

Collection	Accession No.	Genus/Species	Fragment type
Albany Museum	AM3874	*E. whaitsi*	Anterior lower jaw
	AM298	*E. bathystoma*	3 vertebrae
	AM296	*E. bathystoma*	5 dorsal vertebrae and scapula frag
	AM293	*E. bathystoma*	Part of pelvis
	AM292	*E. bathystoma*	2 pieces of pelvis
	AM297	*E. bathystoma*	Vertebrae
	AM303 (1)	*E. bathystoma*	Occiput and vertebrae
	AM303 (2)	*E. bathystoma*	Vertebrae fragment
	AM299	*E. bathystoma*	2 vertebrae
CGS	CGP/1/709	*E. bathystoma*	Complete skull
	CGP/1/782	*E. bathystoma*	Anterior lower jaw
	CGP/1/784	*E. bathystoma*	Jaw fragment
	CM86790	*E. bathystoma*	Anterior lower jaw
	AK8359	*E. bathystoma*	Jaw fragment
	CGP/1/700	*Endothiodon*	Anterior lower jaw
	CGP/1/689	*E. bathystoma*	Skull and upper jaw
	CGP/1/708	*E. bathystoma*	Complete skull
ESI	BP/1/7376 a	*Endothiodon*	Anterior portion of lower jaw
	BP/1/7376 b	*Endothiodon*	Postcrania (PC) fragment
	BP/1/7376 c	*Endothiodon*	Jaw fragment
	BP/1/7267	*Endothiodon*	Anterior portion of lower jaw
	BP/1/7267 a	*Endothiodon*	PC fragment
	BP/1/7267c	*Endothiodon*	PC fragment
	BP/1/7067	*Endothiodon*	Posterior skull fragment
	BP/1/7279 a	*Endothiodon*	Anterior portion of lower jaw
	BP/1/7279 b	*Endothiodon*	PC fragment
	BP/1/7349	*Endothiodon*	Ant portion of med sized skull
	BP/1/5509	*Endothiodon*	Jaw and PC fragments
	BP/1/5470 a	*Endothiodon*	Lower jaw
	BP/1/5470 b	*Endothiodon*	Humerus fragment
	BP/1/5470 c	*Endothiodon*	Jaw fragment
	BP/1/5470 d	*Endothiodon*	Anterior lower dentary

	BP/1/5470 e	*Endothiodon*	PC fragment
	BP/1/5471	*Endothiodon*	PC fragment
	BP/1/5502	*Endothiodon*	Palatal fragment of premaxilla
	BP/1/5505	*Endothiodon*	Large snout
	BP/1/5504	*Endothiodon*	Right maxilla
	BP/1/7460	*Endothiodon*	PC fragments
Iziko Museum	SAM-PK-3443	*Endothiodon*	Right dentary fragment
	SAM-PK-10642	*E. bathystoma*	Maxilla fragment
	SAM-PK-10638	*E. bathystoma*	Dentary fragment
	SAM-PK-10643	*E. bathystoma*	Jaw fragment
	SAM-PK-7876	*Endothiodon*	Skull fragment
	SAM-PK-3442	*Endothiodon*	Skull and PC fragments
	SAM-PK-3420	*Endothiodon*	Upper jaw and PC fragments
	SAM-PK-2676	*E. uniseries*	Upper jaw
	SAM-PK-628	*E. bathystoma*	Skull fragment
	SAM-PK-581	*E. uniseries*	Occiput
	SAM-PK-588	*Endothiodon*	Lower jaw fragment
	SAM-PK-629	*E. bathystoma*	Skull and PC
	SAM-PK-6406	*Endothiodon*	Vertebra
	SAM-PK-K6727	*Endothiodon*	Jaw fragment
	SAM-PK-K6051	*Endothiodon*	Anterior upper jaw
	SAM-PK-1682	*Endothiodon*	Anterior dentary fragment
	SAM-PK-5605	*Endothiodon*	Lower jaw and PC fragments
	SAM-PK-K6618	*Endothiodon*	Long bone fragments
	SAM-PK-K7005	*Endothiodon*	Dentary and posterior skull
	SAM-PK-K11131	*Endothiodon*	Large skull fragment
	SAM-PK-K11221	*E. bathystoma*	Dentary
	SAM-PK-K11134	*Endothiodon*	Lower jaw and PC fragments

[1] Postcranial elements listed here need to be examined closely in further work to determine whether or not they truly represent *Endothiodon*.

Table B. Skull data on various *Endothiodon* elements from South African collections.

Accession No.	Species	Fragment	SL (sq)	SL (dors. mid)	SW (orb)	SW (sq)	Dentary H
SAM-PK-2676b	*E. uniseries*	Squamosal wing fragments	229.04	N/A	N/A	N/A	N/A
SAM-PK-2676a	*E. uniseries*	Large anterior upper jaw	N/A	220.76	183.02	N/A	N/A
SAM-PK-K11131	*E. bathystoma*	Right part of skull and anterior lower jaw	414.95	420.22	N/A	97.20	92.72
CGP/1/689	*E. bathystoma*	Medium sized skull	417.61	377.5	N/A	45.07	N/A
CGP/1/709	*E. bathystoma*	Complete skull	423.87	382.59	N/A	272.72	69.22
SAM-PK-K011271	*E. bathystoma*	Complete skull	447	433.69	156.65	281.22	97.0
SAM-PK-629	*E. bathystoma*	Skull, lower jaw, partially plaster (Broom, 1905)	448.51	351.64	175.68	N/A	87.5
CGP/1/708	*E. bathystoma*	Complete skull	511.8	452.89	N/A	267.44	N/A
SAM-PK-3420	*Endothiodon*	Large anterior skull with upper jaw and teeth	N/A	N/A	146.64	N/A	N/A
BP/1/7349	*Endothiodon*	Anterior portion of medium sized skull	N/A	N/A	N/A	N/A	55.72
AM3874	*E. whaitsi*	Slightly fragmented lower jaw	N/A	N/A	N/A	N/A	93.35

Table C. Field data for comparable *Endothiodon* skulls from South African collections.

Accession No.	Collection	Species	Group	Locality / District	Assemblage Zone	Date found
AM3874	Albany Museum	*E. whaitsi*	-	Beaufort West commonage	-	1913
CGP/1/709	CGS	*E. bathystoma*	-	Beaufort West	*Tropidostoma*	2005
CGP/1/689		*E. bathystoma*		Beaufort West		2005
CGP/1/708		*E. bathystoma*		Murraysburg		2005
BP/1/7349	ESI	*Endothiodon*	Beaufort	Weltevrede Wes	*Pristerognathus*	2013
SAM-PK-629	Iziko Museum	*E. bathystoma*	Beaufort	Beaufort West	*Tapinocephalus*	1904
SAM-PK-K11131		*Endothiodon sp.*	Beaufort	Reiersvlei, Fraserburg District	*Pristerognathus*	2012
SAM-PK-3420		*Endothiodon sp.*	Beaufort	Beaufort West	*Tropidostoma*	1913
SAM-PK-2676		*E. uniseries*	Beaufort	Beaufort West	*Tapinocephalus*	
SAM-PK-K011271		*E. bathystoma*	Beaufort		Upper *Pristerognathus*	2013

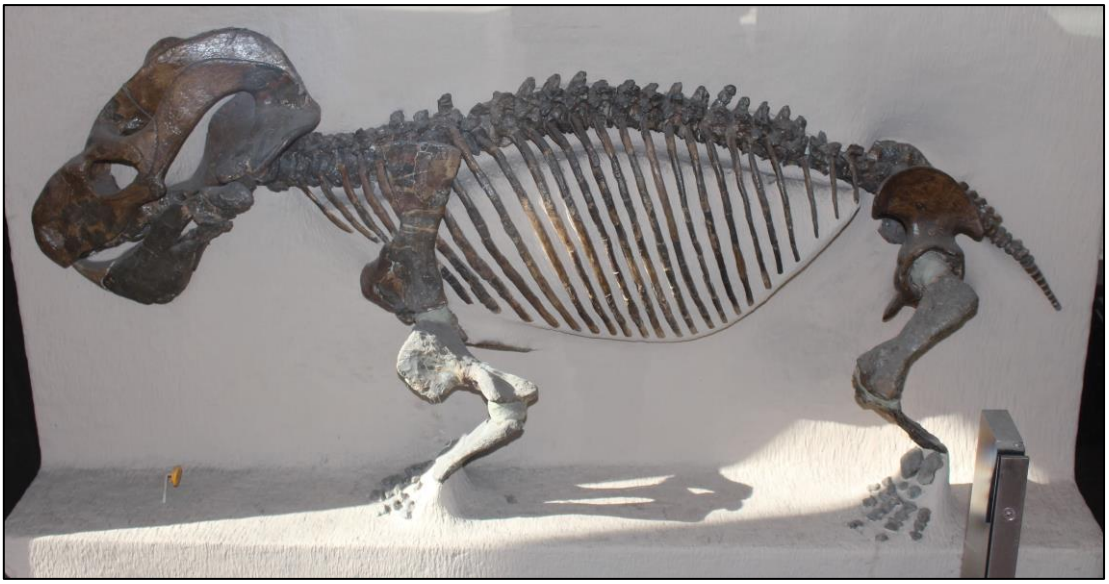

Figure A. Photograph of mounted reconstruction of *Endothiodon* (Broom, 1905) at the American Museum of Natural History.

REFERENCES

Angielczyk, K. D. 2001. Preliminary phylogenetic analysis and stratigraphic congruence of the Dicynodont Anomodonts (Synapsida: Therapsida). *Palaeontologia africana*. 37:53–79.

Angielczyk, K. D. and Kurkin, A. A. 2003. Phylogenetic analysis of Russian Permian dicynodonts (Therapsida: Anomodontia): implications for Permian biostratigraphy and Pangaean biogeography. *Zoological Journal of the Linnean Society*. 139:157-212.

Angielczyk, K. D. and Sullivan, C. 2008. *Diictodon feliceps* (Owen, 1876), a dicynodont (Therapsida, Anomodontia) species with a Pangaean distribution. *Journal of Vertebrate Paleontology*. 28:788-802.

Angielczyk, K. D. and Rubidge, B. S. 2013. Skeletal morphology, phylogenetic relationships and stratigraphic range of *Eosimops newtoni* Broom, 1921, a pylaecephalid dicynodont (Therapsida, Anomodontia) from the Middle Permian of South Africa. *Journal of Systematic Palaeontology*. 11(2):191–231.

Angielczyk, K. D., Steyer, J.-S., Sidor, C. A., Smith, R. M. H., Whatley, R. L. and Tolan, S. 2014. Permian and Triassic Dicynodont (Therapsida: Anomodontia) faunas of the Luangwa Basin, Zambia: taxonomic update and implications for dicynodont biogeography and biostratigraphy p 93–138. In Kammerer, C. F., Angielczyk, K. D. and Fröbisch, J., *Early Evolutionary History of the Synapsida*: *Vertebrate Paleobiology and Paleoanthropology Series*. Springer, Dordrecht, Heidelberg, New York and London.

Bajdek, P., Owocki, K. and Niedźwiedzki, G. 2014. Putative dicynodont coprolites from the Upper Triassic of Poland. *Palaeogeography, Palaeoclimatology, Palaeoecology*. 411:1–17.

Bandyopadhyay, S. 1988. A kannemeyeriid dicynodont from the Middle Triassic Yerrapalli formation. *Philosophical Transactions of the Royal Society of London.* 320:185–233.

Basu, C., Falkingham, P. L. and Hutchinson, J. R. 2015. The extinct, giant giraffid *Sivatherium giganteum*: skeletal reconstruction and body mass estimation. *Biology Letters*. DOI: 10.1098/rsbl.2015.0940

Boos, A. D. S., Schultz, C. L., Vega, C. S. and Aumond, J. J. 2013. On the presence of the Late Permian dicynodont *Endothiodon* in Brazil. *Palaeontology*. 56(4):837–848.

Boos, A. D. S., Kammerer, C. F., Schultz, C. L., Soares, M. B. and Ilha, A. L. R. 2016. A New Dicynodont (Therapsida: Anomodontia) from the Permian of Southern Brazil and Its Implications for Bidentalian Origins. *PLOS One*. DOI: 10.1371/journal.pone.0155000.

Botha, J. 2003. Biological aspects of the Permian dicynodont *Oudenodon* (Therapsida: Dicynodontia) deduced from bone histology and cross-sectional geometry. *Palaeontologia africana.* 39:37–44.

Botha-Brink, J. 2017. Burrowing in *Lystrosaurus*: preadaptation to a postextinction environment? *Journal of Vertebrate Paleontology*. DOI:10.1080/02724634.2017.1365080.

Botha-Brink, J. and Angielczyk, K. D. 2010. Do extraordinarily high growth rates in Permo-Triassic dicynodonts (Therapsida, Anomodontia) explain their success before and after the end-Permian extinction? *Zoological Journal of the Linnean Society.* 160:341–365.

Botha, J. and Smith, R. M. H. 2007. *Lystrosaurus* species composition across the Permo-Triassic boundary in the Karoo Basin of South Africa. *Lethaia*. 40:125–137.

Broili, F. and Schröder, J. 1936. Beobachtungen an Wirbeltieren der Karrooformation XXIV. Über Theriodontier-Reste aus der Karrooformation Ostafrikas. *Sitzungsberichte der Mathematisch-naturwissenschaftlichen Abteilung der Bayerischen Akademie der Wissenschaften zu München*. 1936:311–355.Broom, R. 1905. On the structure and affinities of the Endothiodont reptiles. *Transactions of the South African Philosophical Society.* 15:259–282.

Camp, C. L. and Welles, S. P. 1956. Triassic dicynodont reptiles: part I, The North American genus *Placerias*. *Memoirs of the University of California*. 13:255–304.

Castanhinha, R., Araújo, R., Júnior, L. C., Angielczyk, K. D., Martins, G. G., Martins, R. M. S., Chaouiya, C., Beckmann, F. and Wilde, F. 2013. Bringing Dicynodonts Back to Life: Paleobiology and Anatomy of a New Emydopoid Genus from the Upper Permian of Mozambique. *PLOS One*. 8(12): e80974. DOI: 10.1371/journal.pone.0080974.

Chinsamy, A. and Rubidge, B. S. 1993. Dicynodont (Therapsida) bone histology: phylogenetic and physiological implications. *Palaeontologia africana.* 30:97–102.

Cluver, M. A. 1978. The skeleton of the mammal-like reptile *Cistecephalus* with evidence for a fossorial mode of life. *South African Museum*. 76:213–246.

Cox, C. B. 1959. On the anatomy of a new dicynodont genus with evidence of the position of the tympanum. *Journal of Zoology.* 132(3):321–367.

Cox, C. B. 1964. On the Palate, Dentition, and Classification of the Fossil Reptile *Endothiodon* and Related Genera. *American Museum Novitates*. 2171:1–24.

Cox, C. B. 1965. New Triassic dicynodonts from South America, their origins and relationships. *Philosophical Transactions of the Royal Society of London*. 248(753):457–516.

Cox, C. B. 1972. A new digging dicynodont from the Upper Permian of Tanzania p 173-189. In Joysey, K. A. and Kemp, T. S. *Studies in Vertebrate Evolution*. Oliver & B., New York.

Cox, C. B. and Angielczyk, K. D. 2015. A new endothiodont dicynodont (Therapsida, Anomodontia) from the Permian Ruhuhu Formation (Songea Group) of Tanzania and its feeding system. *Journal of Vertebrate Paleontology*. DOI: 10.1080/02724634.2014.935388.

Cruickshank A. R. I., Clark, N. D. L. and Adams, C. 2005. A new specimen of *Dicynodon traquairi* (Newton) (Synapsida: Anomodontia) from the Late Permian (Tartarian) of northern Scotland. *Palaeontologia africana.* 41:35-43.

Day, M. 2013. Charting the fossils of the Great Karoo: a history of tetrapod biostratigraphy in the Lower Beaufort Group, South Africa. *Palaeontologia africana.* 48:41-47.

Fiorelli L. E., Ezcurra, M. D., Hechenleitner, E. M., Arganaraz, E., Taborda, J. R. A., Trotteyn, M. J., von Baczko, M. B. and Desojo, J. B. 2013. The oldest known communal latrines provide evidence of gregarism in Triassic megaherbivores. *Scientific Reports*. 3(3348): doi:10.1038/srep03348.

Frobisch, J. 2009. Composition and similarity of global anomodont-bearing tetrapod faunas. *Earth-Science Reviews*. 95:119-157.

Govender, R. 2008. Description of the postcranial anatomy of *Aulacephalodon baini* and its possible relationship with '*Aulacephalodon peavoti*'. *South African Journal of Science*. 104:479–486.

Govender, R. and Yates, A. 2009. Dicynodont postcrania from the Triassic of Namibia and their implication for the systematics of Kannemeyeriiforme dicynodonts. *Palaeontologia africana*. 44:41–57.

Hancox, P. J. and Rubidge, B. S. The role of fossils in interpreting the development of the Karoo Basin. *Palaeontologia africana.* 33:41–54.

Haughton, S. H. 1932. On a collection of Karroo Vertebrates from Tanganyika Territory. *Quarterly Journal of the Geological Society*. 88:634–671.

Hotton III, N. 1984. Dicynodonts and Their Role as Primary Consumers p 71–82. In Hotton III, N., MacLean, P. D., Roth, J. J. and Roth, E. C., *The Ecology and Biology of Mammal-like Reptiles*. Smithsonian Institution Press, Washington and London.

Jasinoski, S. C., Rayfield, E. J. and Chinsamy, A. 2009. Comparative feeding biomechanics of *Lystrosaurus* and the generalized dicynodont *Oudenodon*. *The Anatomical Record*. 292:862–874.

Jasinoski, S. C. and Chinsamy-Turan, A. 2012. Biological inferences of the cranial microstructure of the dicynodonts *Oudenodon* and *Lystrosaurus* p 149-176. In Chinsamy-Turan, A., *Forerunners of Mammals.* Indiana University Press, Bloomington and Indianapolis.

Kammerer, C. F., Angielczyk, K. D. and Fröbisch, J. 2011. Comprehensive taxonomic revision of *Dicynodon* (Therapsida, Anomodontia) and its implications for dicynodont phylogeny, biogeography and biostratigraphy. *Journal of Vertebrate Paleontology*. 31(6):1–158.

Kammerer, C. F., Fröbisch, J. and Angielczyk, K. D. 2013. On the Validity and Phylogenetic Position of *Eubrachiosaurus browni*, a Kannemeyeriiform Dicynodont (Anomodontia) from Triassic North America. *PLOS One*. 8(5):e64203. DOI: 10.1371/journal.pone.0064203.

Kemp, T. S. 2012. The Origin and Radiation of Therapsids p 3–28. In Chinsamy-Turan, A., *Forerunners of Mammals.* Indiana University Press, Bloomington and Indianapolis.

King, G. M. 1981. The functional anatomy of a Permian dicynodont. *Philosophical Transactions of the Royal Society of London, B.* 291(1050):243–322.

King, G. M. 1990. Introducing dicynodonts p 1–20. In King, G., *The Dicynodonts, A study in palaeobiology*. Chapman and Hall Ltd, London and New York.

King, G. M., 1993. Species longevity and generic diversity in dicynodont mammal-like reptiles. *Palaeogeography, Palaeoclimatology, Palaeoecology*. 102(3–4):321–332.

King, G. M., Oelofsen, B. W. and Rubidge, B. S. 1989. The evolution of the dicynodont feeding system. *Zoological Journal of the Linnean Society*. 96(2):185–211.

Kitching, J. W. 1977. The distribution of the Karoo vertebrate fauna, with special reference to certain genera and the bearing of this distribution on the zoning of the Beaufort beds. *Memoirs of the Bernard Price Institute.* 1:1–131.

Latimer, E. M., Gow, C. E. and Rubidge, B. S. 1995. Dentition and Feeding Niche of *Endothiodon* (Synapsida; Anomodontia). *Palaeontologia africana*. 32:75–82.

Lucas, S. G. 2005. *Dicynodon* (Reptilia: Therapsida) from the Upper Permian of Russia: Biochronologic significance. p 192. In Lucas, S. G. and Zeigler, K. E. *The Nonmarine Permian: Bulletin 30*. New Mexico Museum of Natural History & Science.

Lydekker, R. 1890. Family Endothiodontidae. *Catalogue of Fossil Reptilia and Amphibia*. 4:64–66.

Nasterlack, T., Canoville, A. and Chinsamy, A. 2012. New insights into the biology of the Permian genus *Cistecephalus* (Therapsida, Dicynodontia). *Journal of Vertebrate Paleontology*. 32(6):1396–1410.

Owen, R. 1876. Endothiodontia. *Descriptive and illustrative catalogue of the fossil Reptilia of South Africa in the collection of British Museum (Natural History)*. Taylor and Francis, London. 66–88.

Owen, R. 1879. On the endothiodont Reptilia with evidence of the species *Endothiodon uniseries*. *Quarterly Journal of the Geological Society, London*. 35:557–564.

Ray, S. 2000. Endothiodont Dicynodonts from the Late Permian Kundaram Formation, India. *Palaeontology*. 43(2):375–404.

Ray, S. 2006. Functional and evolutionary aspects of the postcranial anatomy of dicynodonts (Synapsida, Therapsida). *Palaeontology*. 49(6):1263–1286.

Ray, S. and Chinsamy, A. 2003. Functional aspects of the postcranial anatomy of the Permian dicynodont *Diictodon* and their ecological implications. *Palaeontology*. 46(1):151–183.

Romer, A. S. 1956. The Limb Girdles p 298–330. In Romer, A. S., *Osteology of the Reptiles*. Chicago, University of Chicago Press.

Smith, R. M. H. 1987. Helical burrow casts of therapsid origin from the Beaufort Group (Permian) of South Africa. *Palaeogeography, Palaeoclimatology, Palaeoecology*. 60:155–170.

Smith, R. M. H. 1993. Vertebrate taphonomy of Late Permian floodplain deposits in the Southwestern Karoo Basin of South Africa. *PALAOIS*. 8(1):45–67.

Smith, R., Rubidge, B. S. and van der Walt, M. 2012. Therapsid Biodiversity Patterns and Paleoenvironments of the Karoo Basin, South Africa p 31–62. In Chinsamy-Turan, A., *Forerunners of Mammals.* Indiana University Press, Bloomington and Indianapolis.

Sullivan, C., Reisz, R. R. and Smith, R. M. H. 2002. The Permian mammal-like herbivore *Diictodon*, the oldest known example of sexually dimorphic armament. *Proceedings of the Royal Society of London*. 270:173–178.

Sun, A. -L. 1963. The Chinese kannemeyeriids. *Palaeontologia Sinica New Series C*. 17:1–109.

Sushkin, P. P. 1926. Notes on the pre-Jurassic Tetrapods from Russia II: contributions to the morphology and ethology of the Anomodontia. *Palaeontologia Hungarica*. 1:328–336.

Watson, D. M. S. 1960. The anomodont skeleton. *Journal of Zoology*. 29(3):131–209.

Wyllie, A. 2003. A review of Robert Broom's therapsid holotypes: have they survived the test of time? *Palaeontologia africana.* 39:1–19.